NARSIS

New Approach to Reactor Safety ImprovementS

WP3: Integration and safety analysis

Del 3.11 - Constraining the uncertainties in the components modelling (causes and consequences) – Application to Station Blackout event

This project has received funding from the Euratom research and training programme 2014-2018 under Grant Agreement No. 755439.

Project Acronym:	NARSIS
Project Title:	New Approach to Reactor Safety Improvements
Deliverable:	Del 3.11 - Constraining the uncertainties in the components modelling (causes and consequences) – Application to Station Blackout event
Month due:	42 **Month delivered:** 40
Leading Partner:	Jožef Stefan Institute (JSI)
Version:	Final
Primary Authors:	Andrej PROŠEK, Andrija VOLKANOVSKI (JSI)

Deliverable Review:

- **Reviewer #1:** Rohmer Jeremy (BRGM) **Date:** 06/01/2021
- **Reviewer #2:** Varenya K. Duvvuru Mohan (TU Delft) **Date:** 14/01/2021

Dissemination Level		
PU	Public	**X**
PP	Restricted to other programme participants (including the Commission Services)	
RE	Restricted to a group specified by the consortium (including the Commission Services)	
CO	Confidential, only for members of the consortium (including the Commission Services)	

Table of contents

List of Figures

List of Tables

List of Abbreviations

AA	average amplitude
AC	alternate current
BAT	battery
BBN	Bayesian Belief Network
BEPU	Best Estimate Plus Uncertainty
BWR	Boiling Water Reactor
CCF	common-cause failure
CDF	core damage frequency
CSNI	Committee on the Safety of Nuclear Installations
DC	direct current
DG	diesel generator
EDG	Emergency Diesel Generator
FFTBM	fast Fourier transform based method
FFTBM-SM	fast Fourier transform based method by signal mirroring
IAEA	International Atomic Energy Agency
I&C	instrumentation and control
IEEE	Institute of Electrical and Electronics Engineers
LBS	load break switch
LOCA	loss of coolant accident
LOOP	Loss Of Offsite Power
MG	main generator
MHI	Mitsubishi Heavy Industries
NARSIS	New Approach to Reactor Safety ImprovementS
NPP	nuclear power plant
NRC	Nuclear Regulatory Commission
OSE	Optimal Statistical Estimator
PRT	pressurizer relief tank
PRZ	pressurizer
PSA	Probabilistic Safety Assessment
PWR	pressurized water reactor
RCP	reactor coolant pump
RCS	reactor coolant system
SBO	Station Blackout
SBO-L	SBO longer
SBO-S	SBO shorter
SG	steam generator
SPE4	Standard Problem Exercise no. 4
TD-AFW	turbine driven – auxiliary feedwater
VA	variable accuracy
WR	wide range

1 Executive Summary

This deliverable presents the results from Sub-Task 3.2.2: Constraining the uncertainties in the components modelling (causes and consequences).

The specific goal of the deliverable is to identify, classify and analyse the main sources of uncertainties of the parameters that affect the progression and consequences of one selected event for the nuclear power plant.

The selected event for the purposes of this study is Station Blackout (SBO) event resulting in loss of all alternate current power sources in the nuclear power plant. This event was selected as one of the most demanding events for the light water reactors.

The identification of the most important parameters was done on basis of results of the previous parametric studies, sensitivity study of deterministic calculations as well as their potential utilization in other studies planned in NARSIS project.

Those parameters and corresponding uncertainties were classified in two categories: external and internal. The internal parameters were defined as those parameters that indicate the state of the primary coolant system of the nuclear power plant (and secondary system in case of pressurized water reactors). All other parameters were classified as external.

The analysis of the uncertainties of the selected parameters shows that dominant contribution to the progression of the event and final consequences, for SBO event, have operator actions (especially recovery of system functions). The remaining parameters have small/negligible impact on the event progression so they can be omitted in further analyses.

The most important uncertainties can be decreased with deterministic sensitivity calculations. Sensitivity calculations with variation one parameter at a time have been used to study the influence of different parameters upon the predicted SBO transient evolution. This study does not constitute an uncertainty evaluation for the analysis of SBO event but shall be used as guidance for constraining uncertainties, when deriving uncertainty from PSA calculations. Sensitivity study shows that external parameters, like start and operational time of emergency power sources, have large impact on SBO event progression.

Based on the above sensitivity study the SBO event progression tree developed with main events and operator actions can be included in the Bayesian belief network for extended SBO in the frame of NARSIS Task 3.2.3 dealing with integrating risk sub-networks.

2 Introduction

The main purpose of nuclear safety is the prevention of release of radioactive materials, ensuring that the operation of nuclear power plants (NPPs) does not contribute significantly to individual and societal health risk (Volkanovski and Prošek, 2013). The main specific issue of nuclear safety is the need for removing the decay heat, necessary even for a reactor in shutdown.

The NPP power systems are divided into safety related Class 1E and Non-1E power systems (IEEE, 2002). Fig. 1 shows an example NPP electrical energy distribution system with main constituting elements. The Class 1E power system of the NPP is marked with dashed rectangles on Fig. 1.

Main elements of the Non-1E power system include the main generator (MG on Fig. 1), generator step-up transformers (GT1 and GT2 on Fig. 1), unit (T1 and T2 on Fig. 1) and auxiliary transformer (T3 on Fig. 1) with the corresponding buses. The unit transformers T1 and T2 are connected to the generator bus and serve as the normal source of power for non-safety buses. The unit transformers also serve as the preferred source for start up of the plant through the generator step-up transformers and with the generator load break switch (LBS on Fig. 1) open. The station auxiliary transformer, marked T3 on Fig. 1, is an alternate source of power when main sources are not available.

Main elements of the Class 1E power system include safety buses, emergency diesel generators (DG1 and DG2) and plant batteries (Bat A and Bat B on Fig. 1).

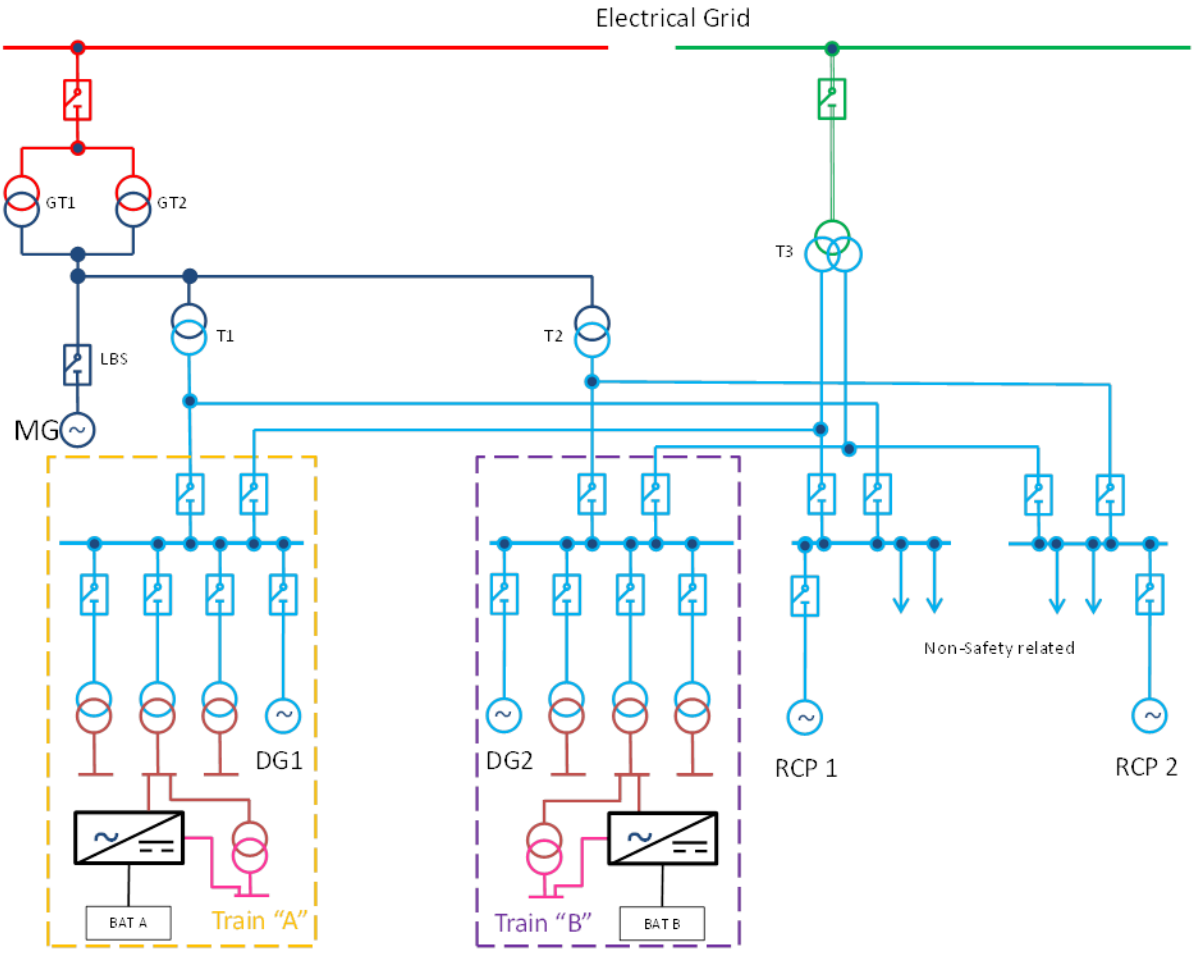

Fig. 1: Example NPP electrical energy distribution system

The loss of offsite power (LOOP) initiating event occurs when all electrical power to the plant from external sources is lost (red and green lines on Fig. 1). Loss of alternating current (AC) as a result of complete failure of both offsite and on-site AC power sources is referred to as a

station blackout (SBO) (U.S. NRC, 1988). The NPPs are equipped with batteries (BAT A and BAT B on Fig. 1) that provide electrical power for the essential safety systems (Essential I&C) for limited time known as station blackout coping time. Typical stations blackout coping times for existing NPPs range from 2 to 8 hours.

The results of the Probabilistic Safety Assessment (PSA) show that initiating events LOOP and SBO are the most important contributors to the core damage frequency (CDF) including the shutdown CDF (Nishio and Fujimoto, 2011).

Fig. 2 shows the percentage share of SBO and LOOP in the obtained CDF for four nuclear power plants (Bertucio et al., 1990; Kolaczkowski et al., 1989; Bertucio and Brown, 1990) and two advanced designs (AREVA, 2007; MHI, 2008; Eide et al., 2005). The SBO-S and SBO-L are designations for the SBO shorter and longer than station blackout coping time. During an extended SBO functional failure would occur for nearly all instrumentation, control and electric driven safety systems leading ultimately to core damage, if no other equipment would be available (e.g. mobile).

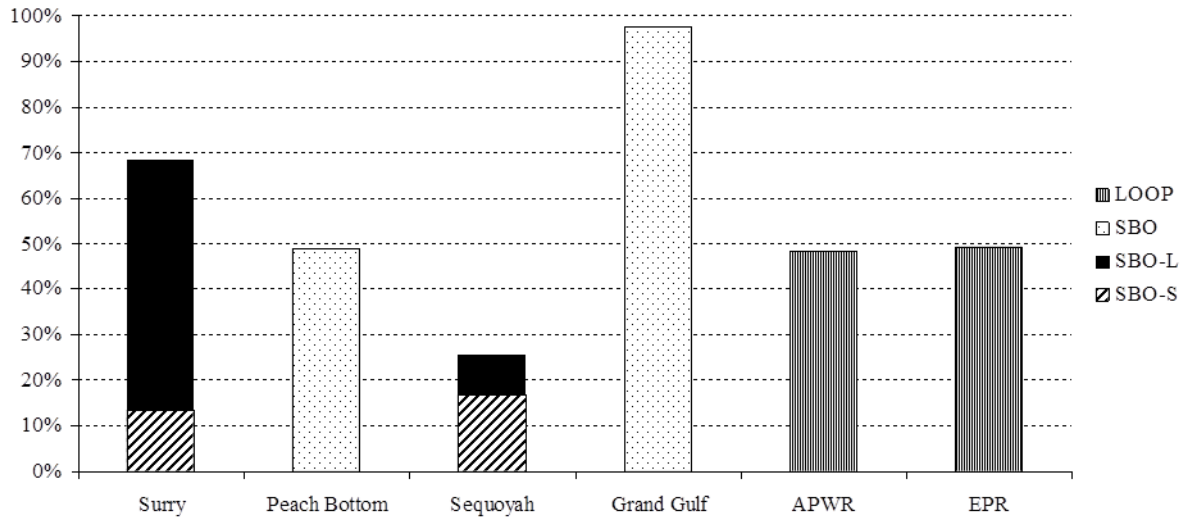

Fig. 2: Percentage contribution of LOOP and SBO to CDF

The accident at the Fukushima Dai-ichi NPP (U.S. NRC, 2011) supports the PSA results obtained by Nishio and Fujimoto, 2011. On March 11, 2011, the Tohoku-Taiheiyou-Oki Earthquake occurred near the east coast of Honshu, Japan (USGS, 2011). The earthquake and the subsequent tsunami caused significant damage to at least four of the six units of the Fukushima Daiichi NPP as the result of a sustained loss of both offsite and on-site power systems (U.S. NRC, 2011). Units 1 through 3, which had been operating at the time of the earthquake, scrammed automatically. Following the loss of electric power to normal and emergency core cooling systems and the subsequent failure of back-up decay heat removal systems, water injection into the cores of all three reactors was compromised resulting in core damage. The Fukushima Dai-ichi NPPs are Boiling Water Reactors (BWRs) that require injection of water/coolant directly in the reactor pressure vessel in order to remove the decay heat. Efforts to restore power to emergency equipment have been hampered or impeded by damage to the surrounding areas due to the tsunami and earthquake (TEPCO, 2011) including common-cause failure (CCF) of NPP on-site distribution system due to the flooding and ground motion. The timescale of the accident sequence development, following tsunami in Fukushima Dai-ichi NPP, is given in Table 1.

Table 1: Accident sequence following tsunami in Fukushima Dai-ichi NPP (Volkanovski and Cizelj, 2018)

	Unit 1	**Unit 2**	**Unit 3**
Loss of AC power	+ 51 min	+ 55 min	+ 52 min
Loss of cooling	+ 1 hour	+ 71 hours	+ 36 hours
Water level down to top of fuel	+ 3 hours	+ 74 hours	+ 37 hours
Core damage starts	+ 5 hours	+ 87 hours	+ 62 hours
Fire pumps with fresh water	+ 15 hours	-	+ 42 hours
Hydrogen explosion	+ 24 hours service floor	+87 hours suppression chamber	+ 68 hours service floor
Fire pumps with seawater	+ 28 hours	+ 78 hours	+ 46 hours
Off-site electrical supply	+ 9-10 days		
Fresh water cooling	+ 12-14 days		

The modelling and analysis of the SBO event requires consideration of the uncertainties characterizing the development of the event. In Section 0 the main parameters affecting progression of SBO event and corresponding uncertainties are identified and classified.

3 Uncertainties classification and qualification

The uncertainties of nuclear safety analyses, probabilistic and deterministic, can be classified in the following three main categories (Volkanovski and Čepin, 2011): parameter, model and completeness uncertainties.

Parameter uncertainty relates to the uncertainty in the computation of the input parameter values used to quantify the models in the corresponding analyses. For example, in the PSA, the parameter uncertainty relates to the values used for the probabilities of failures of the events. The parameter uncertainties result from their interdependence with modelling assumptions, lack of statistically significant data due to rarity of modelled events and subjectivity of expert opinion.

Model uncertainty arises because different models can be used for same systems and processes. Uncertainty exists with regard to which model appropriately represents that aspect of the nuclear power plant (NPP) being modelled.

Completeness uncertainties are uncertainties due to the portion of risk that is not explicitly included in the PSA.

Some of the uncertainties can be resulting from several sources. For example, earthquake as an external event can result in different consequences/failures in the plant. The uncertainty lies in which failures will be considered and how to model those failures into the safety analyses.

For the purposes of this study the parameters and corresponding uncertainties are divided in two main categories. The external parameters are all those parameters characterizing/affecting the progression of the event that are not related to the status of the primary coolant system of the NPP. The primary coolant system of the NPP includes the reactor core and all the vessels and pipes where the reactor coolant flows.

For example, the external parameters include time when LOOP and/or SBO event happened, the availability/reliability of external power sources etc.

The internal parameters include all parameters that characterise the state of the primary coolant system. For example, the temperature and pressure in the primary coolant system, if/what size is loss of coolant event within primary coolant system etc.

Study presented in publication (Prošek and Volkanovski, 2015a) shows that following external parameters are identified as most important for the development of the SBO event:

- Time delay between LOOP and extended SBO (what time the emergency diesel generator's (EDG's) are operational)
- Time delays between the extended SBO start and start of the pump injections to steam generator (SG)

The following internal parameters are identified (Prošek and Volkanovski, 2015a) as the most important for SBO scenario development:

- Types of reactor coolant system (RCS) coolant loss scenarios (existence of normal system leakage, seal and letdown loss, success of depressurization).
- Primary system depressurization strategy (depressurization using primary or secondary safety and relief valves, valves setpoints, time delays between the extended SBO and start of depressurization).

These parameters with corresponding uncertainties are discussed in the following sections.

3.1 External parameters uncertainties

Two external parameters are identified as the most important for the development of the SBO event (Prošek and Volkanovski, 2015a).

First parameter is the time interval between the loss of external power to the NPP (LOOP event) and the time when all electrical power in the plant is lost (extended SBO). This time

interval was considered in the study by Prošek and Volkanovski (2015a), in order to simulate the accident corresponding to the Fukushima Dai-ichi NPP accident scenario.

The earthquake resulted in LOOP at the Fukushima Dai-ichi NPP and consequential start of EDG's providing power to the operating safety systems. Approximately one hour after the earthquake, the subsequent tsunami hit the site resulting in loss of all electrical power sources (extended blackout) as shown in Table 1. Operation of the emergency diesel generator (EDG) for 1 h in pressurized water reactor (PWR), as shown in Prošek and Volkanovski (2015a), extends the available time for the start of pump injecting into steam generator to 4 h (reactor cooling through the steam generator). The operational interval has large uncertainties and depends on design of the plant (protection from hazards) and operational guidelines (if/what actions are planned for the operator).

Second important parameter identified by Prošek and Volkanovski (2015a) is the time interval between loss of cooling (because of loss of electricity) and restoration of cooling by alternate means. This time depends if/what type of restoration strategies exist in the plant, utilization of mobile and/or fixed equipment, consideration of these actions in operator training and guidelines etc.

The uniform distribution is recommended for characterization of the uncertainties of both parameters with minimal and maximal values given in Table 2. The maximum value was estimated based on previous studies and expected time when given system can effectively change the event progression.

Table 2: Description of external uncertainty parameters

Parameter	Distribution type	Unit	Min	Max
EDG operation time	Uniform	Time [hours]	0	8
Restoration of Cooling	Uniform	Time [hours]	0	4

3.2 Internal parameters uncertainties

The analysis of the SBO event (Prošek and Volkanovski, 2015a) shows that the most important parameter impacting progression of the event is existence and type of loss of coolant accident (LOCA) scenario causing RCS inventory loss, leading to core uncovery and later core heatup. For example, the failure to isolate letdown results in core damage before 24 h in all analysed scenarios. Alternative strategy to isolate letdown loss is to depressurize the primary system pressure below opening setpoint of letdown relief valve (4.24 MPa) to pressurizer relief tank (PRT). The consideration of the normal system leakage (allowed leakage for normal operation, not considering LOCA) has small impact on the results. The existence and size of the reactor coolant pump (RCP) seal loss (called seal LOCA) is identified as important for the development of the event. Another important aspect of primary system depressurization is accumulator injection of coolant into primary system below 48.9 MPa.

The primary system pressure is assessed as important for scenarios where seal loss is not existent or is small, and depends on success of depressurization actions on the secondary side of the reactor coolant system. The parameters intervals are assessed from Prošek and Volkanovski (2015a) and are given in Table 3.

Table 3: Description of internal uncertainty parameters

Parameter	Distribution type	Unit	Min	Max
Normal system leakage	Uniform	Flow [l/s]	0	0.6
Seal LOCA	Uniform	Flow [l/s]	0	1.3
Letdown leakage	Uniform	Flow [l/s]	0	5.2
Start of depressurization	Uniform	Time [hours]	0	1

4 Constraining uncertainties

The uncertainties of the external parameters identified in Table 2 and internal parameters identified in Table 3 affect the progression of the event. They are not related to the model uncertainties or parameter uncertainties (i.e. initial and boundary conditions) of the deterministic code. Deterministic code uncertainties are assessed (based on previous studies, e.g. Prošek and Mavko, 1999) to have smaller impact on the scenario progression and obtained results than external parameters identified in Table 2 and internal parameters identified in Table 3. Therefore only assessment of the external and internal parameters uncertainties influence on the scenario progression is done.

The assessment of the impact of the main internal parameters uncertainties on the scenario progression is done with the utilization of sensitivity study on dependence of the output upon one at a time parameter variation (Saltelli et al. 2019 stated that an analysis of the dependence of the output upon just one factor does not constitute a sensitivity analysis, therefore the term "quantitative assessment of sensitivity" is used in this report). A comprehensive overview of different methods for sensitivity analysis is given in NARSIS D3.3. In this study the Fast Fourier transform based method by signal mirroring (FFTBM-SM) is used to quantify the influence of different parameters on scenario progression, based on calculations (Prošek and Leskovar, 2015), in which the calculated results of scenario with input parameter variation(s) (i.e. sensitivity calculation) is compared to calculated results of reference scenario in which base values of input parameters are used (i.e. reference calculation). The nature of this approach is comparable to local sensitivity analysis according to terminology in deliverable D3.3 (except that only one parameter is varied). Its figure of merit can be further used to judge the similarity of two scenarios (Prošek and Leskovar, 2015). In such a way different groups of similar scenarios can be defined and reference scenario for that group. The reference scenarios can be later refined regarding their uncertainties by performing BEPU analysis to quantify the calculation uncertainty due to model uncertainties and parameter uncertainties (uncertain initial and boundary conditions).

4.1 FFTBM-SM method for sensitivity study

The original fast Fourier transform based method (FFTBM) was developed to quantify the accuracy of thermalhydraulic code calculations (Ambrosini et al., 1990) versus results from the corresponding experiments. This was achieved through the evaluation between the calculated and the experimental trends of relevant variables (i.e. comparing the shapes of two signals, usually experimental and calculated signals, to judge the accuracy of thermal-hydraulic computer codes). The main figure of merit proposed for single variable was the average amplitude (AA), the sum of the amplitudes of the frequency spectrum of the difference signal (difference between the two compared signals) divided by the sum of the amplitudes of the frequency spectrum of the signal used for normalization (e.g. experimental signal). The figure of merit for code accuracy was total AA (AA_{tot}), which is the sum of AAs of variables, each multiplied by normalized weights.

An improved version of FFTBM by signal mirroring (FFTBM-SM), which is described in detail in (Prošek et al., 2008), has been also developed.

4.1.1 Calculation of AA

For the calculation of the differences between two signals, reference signal F_{ref} and the difference signal $\Delta F(t)$ are needed. The difference signal in the time domain is defined as $\Delta F(t) = F_{ref} - F_{com}$, where F_{com} is the compared signal. The similarity of the signals is based on the amplitudes of the discrete experimental and difference signals obtained by fast Fourier transform FFT (frequency domain) at frequencies f_n, where n=0,1,...,2^m and m is the exponent defining the number of points N=2^{m+1} (where m=8, 9, 10, 11; this gives minimum 512 and maximum 4096 point). The average amplitude AA_m is defined as:

$$AA = \sum_{n=0}^{2^m} |\tilde{\Delta}F(f_n)| / \sum_{n=0}^{2^m} \left|\tilde{F}_{ref}(f_n)\right| \quad (1)$$

where $|\tilde{\Delta}F(f_n)|$ is the difference signal amplitude at frequency f_n and $\left|\tilde{F}_{ref}(f_n)\right|$ is the reference signal amplitude at frequency f_n. The AA factor can be considered a sort of average fractional difference and the closer the AA value is to zero, the larger is the similarity of the signals. In our specific application, the larger the sensitivity, larger is the difference between the signals, normally resulting in a larger AA value.

4.1.2 Calculation of AA_m

For the calculation of the average amplitude by signal mirroring AA_m the Eq. (1) is used like in the calculation of AA, except that, instead of the original signal, the symmetrized signal is used. This may be efficiently done by signal mirroring, where the investigated signal is mirrored before original FFTBM is applied. By composing the original signal and its mirrored signal (signal mirroring), a symmetric signal (also called symmetrized signal) with the same characteristics is obtained, but without introducing the edge when viewed as an infinite periodic signal (for details refer to Refs. (Prošek and Leskovar, 2007¸ Prošek et al., 2008). FFTBM using the symmetrized signals is called FFTBM-SM.

As already mentioned, the difference between FFTBM and FFTBM-SM is that in the latter the signals are symmetrized to eliminate the edge effect in calculating the average amplitude by signal mirroring (AA_m). However, the time shift between the signals can be determined only by FFTBM.

4.1.3 Calculation of total $AA_{m\text{-}tot}$

The overall picture of the sensitivity influence (using FFTBM-SM) for a given code calculation is obtained by defining average performance indices that is the total average amplitude $AA_{m\text{-}tot}$ (total sensitivity):

$$AA_{m-tot} = \sum_{i=1}^{N_{var}} (AA_m)_i (w_f)_i \quad (2)$$

with

$$\sum_{i=1}^{N_{var}} (w_f)_i = 1 \quad (3)$$

where N_{var} is the number of the variables analysed, and $(AA_m)_i$, and $(w_f)_i$ are the average amplitude and the weighting factors for the *i*-th analysed variable, respectively. Each $(w_f)_i$ accounts for the experimental accuracy (not applicable when calculated signals are used), the safety relevance of particular variables and its relevance with respect to primary pressure. The weights must remain unchanged during each comparison between compared calculation results and reference calculation data concerning the same class of a transient.

Experimental accuracy $(w_{exp})_i$: Experimental trends of thermalhydraulic variables are characterized by uncertainty due to intrinsic characteristics of instruments, the measurement method and different evaluation procedures used to compare experimental measures and the code predictions. As in our application only code calculations are used, the experimental accuracy weighting factor component is not considered.

Safety relevance $(w_{saf})_i$: Higher importance is attributed to the accuracy of those calculated variables, which are relevant for safety and design (such as pressure, peak clad temperature, etc.).

Primary pressure normalization $(w_{norm})_i$: This contribution is given by a factor, which normalizes the AA value calculated for the selected variables with respect to the AA value calculated for the primary pressure. This factor has been introduced in order to consider the physical relations existing between different quantities (i.e. fluid temperature and pressure in case of saturated blowdown must be characterized by the same order of error).

The weighting factor for the *i*-th variable is therefore defined as:

$$(w_f)_i = \frac{(w_{exp})_i (w_{saf})_i (w_{norm})_i}{\sum_{i=1}^{Nvar} (w_{exp})_i (w_{saf})_i (w_{norm})_i} \quad (4)$$

where w_{exp} is the contribution related to the experimental accuracy, w_{saf} is the contribution, which expresses the safety relevance, and w_{norm} the contribution of primary pressure normalization. The weighting factors are shown in Table 4.

Table 4: Weighting factor components for the analysed quantities (D'Auria et al., 1994)

Quantity	w_{exp}	w_{saf}	w_{norm}
Pressure drops	0.7	0.7	0.5
Mass inventories	0.8	0.9	0.9
Flowrates	0.5	0.8	0.5
Primary pressure	1.0	1.0	1.0
Secondary pressure	1.0	0.6	1.1
Fluid temperatures	0.8	0.8	2.4
Clad temperatures	0.9	1.0	1.2
Collapsed levels	0.8	0.9	0.6
Core power	0.8	0.8	0.5

4.1.4 Calculation of variable accuracy (VA_m)

Another accuracy measure, not considered in original FFTBM has also been proposed (Prošek, 2002) and tested on IAEA SPE-4 data. Let VA_i be the i-th variable accuracy:

$$VA_i = AA_i (w_f)_i N_{var} \quad (5)$$

which tells what would be total accuracy if all variables contribute to AA_{tot} as i-th variable. By this definition the criteria for AA_{tot} (see Section 4.1.5) are also applicable to VA, even more than for AA because for VA weights are taken into account. Same is true for $AA_{m\text{-}tot,}$ when AA_m is used in above Eq. (5).

4.1.5 Methodology to quantifying code accuracy

Given qualified user and qualified nodalization scheme, code assessment process involves three steps (D'Auria, 1994):

- selection of an experiment from validation matrices (or a plant transient),
- qualitative assessment, and
- quantitative assessment.

Step 1 involves subdivision of the scenario into "phenomenological windows" and for each phenomenological window methodology requires specification of key phenomena that are distinctive for this class of transients.

Step 2, qualitative assessment of obtained results, is done by comparison of the experimental and calculated variables trends. Qualitative assessment is done by evaluating and ranking the discrepancies between the measured and calculated variable trends. Assessment results can be verbally described as: excellent, reasonable, minimal and unqualified.

Step 3, the quantitative assessment, can be managed by applying method based on the Fast Fourier Transform base method (FFTBM). The most suitable factor for the definition of an acceptability criterion is the total average amplitude AA_{tot}. The original full FFTBM methodology

include 20 to 25 variables selected representing relevant thermal hydraulic aspects and standard weighting factors. It was noted (Ambrosini et al., 1990) that:

- $AA_{tot} \leq 0.3$ characterize very good code predictions,
- $0.3 < AA_{tot} \leq 0.5$ characterize good code predictions,
- $0.5 < AA_{tot} \leq 0.7$ characterize poor code predictions,
- $AA_{tot} > 0.7$ characterize very poor code predictions.

These values at the same time present similarity of sensitivity cases. As AA_m value is generally slightly larger than AA value, the above values can be used to judge (in stricter manner) also the results obtained by FFTBM-SM.

4.1.6 Figures of merit for quantitative assessment of sensitivity

The first figure of merit is AA_m, which tells how the single input parameter variation (or combination of input parameter variations) influences the output variable. For the sensitivity determination the reference calculation output variable (e.g. primary pressure or rod surface temperature) presents the “reference signal” and the sensitivity run variable presents the “compared signal”, of which spectra are used in Eq. (1). The variables from more calculations can be compared to the variable of reference calculation at the same time. The second figure of merit is $AA_{m\text{-}tot}$, which tells how the deterministic calculation (considering several output variables – flows, pressures, temperatures, levels) is sensitive to input parameter variation.

4.2 BEPU using optimal statistical estimator

In case of the thermalhydraulic code parameters, which also affect the progression and consequences of the selected event for the nuclear power plant, the best estimate plus uncertainty (BEPU) method could be used to quantify the uncertainties of deterministic code calculations. With respect to main internal uncertainties identified in section 3.2, these uncertainties are attributed to the code accuracy to simulate phenomena and are quantified once selected reference calculation is completed and qualitatively correct. These uncertainties could then be used in probabilistic assessment. The thermal hydraulic computer codes used are expected to be mature, validated and accurate enough to correctly predict the plant response. BEPU analysis is refinement of the reference calculation with providing the information on the uncertainty of calculation and pays off when margins to safety criteria are small. It seems meaningless to use BEPU, if reference (base) progression of event is not realistically predicted. Typically, for PSA calculations BEPU has not been used in the past.

It should be emphasized that just the use of more accurate system thermalhydraulic code (e.g. RELAP5) significantly reduces the uncertainties in calculated results comparing to best estimate severe accident codes (e.g. MELCOR, which have larger uncertainties comparing to system codes) for transient progression not resulting in core melt. To the authors knowledge in the literature there are no applications of uncertainty analysis to severe accident codes. Nevertheless, in principle the BEPU analysis could be performed when resources allows this. Therefore, in the following description is given how best estimate calculation could be further refined with considering the code calculation uncertainties.

Due to demanding calculation requirements the Monte Carlo method is currently not applicable for uncertainty evaluation of the complex thermalhydraulic codes (Prošek and Mavko, 1999a; Prošek and Mavko, 1999b; Prošek and Mavko, 2007; Prošek et al., 2016). In Monte Carlo analysis, a probability based sampling is used to develop a mapping from analysis inputs to analysis results. This mapping then provides a basis for both the evaluation of the probability (i.e. uncertainty analysis) and the evaluation of the effects of individual input parameters on output parameter (sensitivity analysis). Response surface method is similar to Monte Carlo analysis except that instead of thermalhydraulic computer code a response surface (i.e. surrogate model) is used (see some examples of NARSIS metamodeling developments in deliverable D4.2). However, for response surface generation the code calculations are

needed. The number of input uncertain parameters by such method is limited because of the required number of code calculations.

For BEPU analysis, surrogate modelling, based on the construction of the mathematical response function from the limited number of selected data points aiming to estimate the system response, can be used to replace thousands of complex computer code runs, which are needed to reach uncertainty statement (for example optimal statistical estimator (Grabec and Sachse, 1991; Mavko et al., 1993; Prošek and Mavko, 1999).

5 Application of FFTBM-SM to station blackout sensitivity study

5.1 Description of SBO event thermalhydraulic calculations

In the study by Prošek and Volkanovski (2015a) the extended station blackout mitigation strategy for a two-loop pressurized water reactor (PWR) has been studied using RELAP5/MOD3.3 best estimate thermalhydraulic system code. The simulations have been performed for 24 hours. Another study proposing a method for the assessment of portable pump flowrates for steam generator makeup has been also done by Prošek and Volkanovski (2015b), in which the considered SBO simulations have been extended to 72 hours.

Two cases have been considered. In the first case (C1) all alternate current (AC) electric driven safety systems are assumed to be unavailable after extended SBO start after 1 h (simulating the scenario of Fukushima Dai-ichi NPP). In the second case (C2) EDG start fails and extended SBO occurs concurrently with loss of offsite power. During extended SBO, the following passive systems are available: safety relief valves both on primary and secondary side of PWR, steam generator (SG) relief valves, which can be manually operated (it means that operator actions are needed) and accumulators for safety injection into RCS. Turbine-driven auxiliary feedwater (TD-AFW) system for feeding steam generators is also assumed to be unavailable after extended SBO start due to control and instrumentation loss (direct current (DC) electric loss), needed for TD-AFW valve control. Time needed for recovery of DC power and by this TD-AFW system depends on the operators (external parameter restoration of cooling).

After the reactor trip the heat sources on the primary side are core decay heat and stored energy in core and primary side (RCS) metal while possible heat removal ways are SG cooling, heat removed through the break and primary side relief valves, and heat removed to environment due to heat losses. SG cooling through relief valves is available only when there is sufficient SG water inventory. Efficient recovery procedure of SG water makeup is needed. In addition, it was shown in Prošek and Volkanovski (2015a) that depressurization strategy requiring operator action extends the time before the core uncovers.

The heat to be released through secondary side depends on the primary side heat balance, i.e. core decay heat and heat released directly from the primary side (e.g. through safety valves, primary system mass losses, environmental heat loses and initially also stored energy). The decay heat of the core is a function of the time after reactor trip and is largest in the initial period of reactor shutdown. The decrease of the RCS pressure through the secondary side depressurization results in accumulator injection resulting in makeup of RCS lost coolant and by this extends the heat release directly from the primary side.

The remaining heat should be released through the secondary side in order to prevent core damage. When SGs are boiled off, the RCS pressure starts to increase, resulting in the pressurizer safety valves opening, causing the RCS coolant discharge, which leads to core uncovery with heatup if feed flow to the steam generators is smaller than required or not available for the removal of the decay heat.

Three types of RCS coolant loss scenarios, shown in Table 5, were considered in the sensitivity study: the ‘S_LOSS’ with RCP seal loss starting one hour after the start of extended SBO, the ‘SL_LOSS’ with RCP seal loss and loss of coolant through the letdown relief valve when RCS pressure is greater than 4.24 MPa, and ‘SLD_LOSS’ with RCP seal and letdown loss (if RCS pressure is greater than 4.24 MPa) and depressurization of the primary side through the secondary side to 1.57 MPa, started 30 minutes after SBO occurrence.

Table 5: The types of RCS coolant loss scenarios

Scenario type	No loss	Normal loss	Seal loss	Letdown loss	Depressurization (terminating letdown loss)
NO_LOSS	yes	no	no	no	no
N_LOSS	no	yes	yes	no	no
S_LOSS	no	no	yes	no	no
SL_LOSS	no	no	yes	yes	no
SLD_LOSS	no	no	yes	yes	yes

In addition, delay on restoration of cooling was considered for EDG running for 1 hour after LOOP (case C1) and EDG not running after LOOP (case C2).

Table 6 shows labels for 37 scenarios used in the performed sensitivity study.

Table 6: Labels for scenarios used in sensitivity study

Delay (h)	RCS loss type scenario				
	NO_LOSS	N_LOSS	S_LOSS	SL_LOSS	SLD_LOSS
	EDG running for 1 hour after LOOP (case C1)				
0	N.A.	N.A.	S_LOSS_0 (C1)	SL_LOSS_0 (C1)	SLD_LOSS_0 (C1)
0.5	N.A.	N.A.	S_LOSS_05 (C1)	SL_LOSS_05 (C1)	SLD_LOSS_05 (C1)
1	N.A.	N.A.	S_LOSS_1 (C1)	SL_LOSS_1 (C1)	SLD_LOSS_1 (C1)
2	N.A.	N.A.	S_LOSS_2 (C1)	SL_LOSS_2 (C1)	SLD_LOSS_2 (C1)
3	NO_LOSS_3 (C1)	N_LOSS_3 (C1)	S_LOSS_3 (C1)	SL_LOSS_3 (C1)	SLD_LOSS_3 (C1)
4	N.A.	N.A.	S_LOSS_4 (C1)	SL_LOSS_4 (C1)	SLD_LOSS_4 (C1)
5	NO_LOSS_5 (C1)	N_LOSS_5 (C1)	S_LOSS_5 (C1)	SL_LOSS_5 (C1)	SLD_LOSS_5 (C1)
	EDG not running after LOOP (case C2)				
0	N.A.	N.A.	S_LOSS_0 (C2)	SL_LOSS_0 (C2)	SLD_LOSS_0 (C2)
0.5	N.A.	N.A.	S_LOSS_05 (C2)	SL_LOSS_05 (C2)	SLD_LOSS_05 (C2)
1	N.A.	N.A.	S_LOSS_1 (C2)	SL_LOSS_1 (C2)	SLD_LOSS_1 (C2)
2	N.A.	N.A.	S_LOSS_2 (C2)	SL_LOSS_2 (C2)	SLD_LOSS_2 (C2)

In demonstration cases the sensitivity to EDG operation time (external parameter), RCS loss type (internal parameter loss flow), the use of depressurization strategy for 'SL_LOSS' scenario – 'SLD_LOSS' scenario (internal parameter start of depressurization has not been studied as only calculation with delay time of 30 minutes was available) and delay of cooling has been studied.

The sensitivity cases studied are shown in Table 7. The sensitivity study consists of 10 sensitivity cases. Sensitivity case no. 1 studied the influence of emergency diesel generator (EDG) operation time on calculated SBO scenario progression. In sensitivity cases no. 2 and 3, the influence of RCS inventory loss type, when restoration of cooling is delayed by three (3) and five (5) hours, has been studied. In sensitivity case no. 4, the influence of using depressurization strategy has been studied. As the depressurization strategy is the most influential for 'SL_LOSS' type, only this scenario has been calculated by Prošek and Volkanovski (2015a). Namely, by depressurization below the letdown system relief valve setpoint, the letdown loss is eliminated. In addition, by reducing the primary pressure, the loss through RCP seals is smaller. Sensitivity cases no. 5 through no. 7 deal with the influence of delayed cooling restoration for 'S_LOSS', 'SL_LOSS' and 'SLD_LOSS' RCS loss types with EDG running one hour after LOOP initiation (case C1), respectively. Finally, sensitivity cases no. 8 through no. 10 deal with the influence of delayed cooling restoration for 'S_LOSS', 'SL_LOSS' and 'SLD_LOSS' RCS loss types with EDG not running after LOOP initiation (case C2), respectively.

Table 7: Sensitivity cases studied for SBO

ID	Uncertain parameter varied	Reference calculation	Compared calculation(s)
1	EDG operation time	S_LOSS_3 (C1)	S_LOSS_3 (C2)
2	RCS inventory loss type (delayed cooling for 5 h)	NO_LOSS_5 (C1)	N_LOSS_5 (C1), S_LOSS_5 (C1), SL_LOSS_5 (C1)
3	RCS inventory loss type (delayed cooling for 3 h)	NO_LOSS_3 (C1)	N_LOSS_3 (C1), S_LOSS_3 (C1), SL_LOSS_3 (C1)
4	Depressurization with 30 min. delay	SL_LOSS_5 (C1)	SLD_LOSS_5 (C1)
5	Delayed cooling restoration (loss type S_LOSS and EDG running 1 hour after LOOP)	S_LOSS_0 (C1)	S_LOSS_05 (C1), S_LOSS_1 (C1), S_LOSS_2 (C1), S_LOSS_3 (C1), S_LOSS_4 (C1)
6	Delayed restoration of cooling (loss type SL_LOSS and EDG running 1 hour after LOOP)	SL_LOSS_0 (C1)	SL_LOSS_05 (C1), SL_LOSS_1 (C1), SL_LOSS_2 (C1), SL_LOSS_3 (C1), SL_LOSS_4 (C1)
7	Delayed restoration of cooling (loss type SLD_LOSS and EDG running 1 hour after LOOP)	SLD_LOSS_0 (C1)	SLD_LOSS_05 (C1), SLD_LOSS_1 (C1), SLD_LOSS_2 (C1), SLD_LOSS_3 (C1), SLD_LOSS_4 (C1)
8	Delayed restoration of cooling (loss type S_LOSS and EDG not running after LOOP)	S_LOSS_0 (C2)	S_LOSS_05 (C1), S_LOSS_1 (C1), S_LOSS_2 (C1)
9	Delayed restoration of cooling (loss type SL_LOSS and EDG not running after LOOP)	SL_LOSS_0 (C2)	SL_LOSS_05 (C1), SL_LOSS_1 (C1), SL_LOSS_2 (C1)
10	Delayed restoration of cooling (loss type SLD_LOSS and EDG not running after LOOP)	SLD_LOSS_0 (C2)	SLD_LOSS_05 (C1), SLD_LOSS_1 (C1), SLD_LOSS_2 (C1)

The first step of sensitivity determination was qualitative analysis, based on visual observation of variables. For the above ten sensitivity cases the visual observation was done by comparing the reference calculation and the sensitivity calculations, in which an uncertain input parameter was varied (one parameter at a time) – see the last two columns in Table 7. The results of visual observation of variables are also shown in the frame of each sensitivity case study.

5.2 Selection of output variables for quantitative assessment of sensitivity

The selection of variables for FFTBM-SM quantitative assessment of sensitivity considered the study (Saghafi et al., 2016), dealing with application of FFTBM to station blackout scenario (calculations lasting a few hours). Some additional variables were also considered in this study. Namely, the calculations performed in the frame of study (Prošek and Volkanovski, 2015a) simulated extended station blackout lasting 72 hours, which differ from simulation lasting few hours. Therefore some new variables were required to describe the relevant thermalyhydraulic aspects. Finally, 21 output variables shown in Table 8 were selected to study the influence of external and internal parameters on total calculation. These variables are the representative of station blackout event simulation.

Besides the influence of uncertain parameters on total calculation, the influence of uncertain parameter variation on single output variables has also been studied.

Table 8: Representative variables for sensitivity study of code calculations

No.	Variable	Description
1	Primary pressure	Primary pressure is very important parameter, as it defines the sequence of events. Several system setpoints depends on the value of primary pressure like the pressurizer relief valves opening and closure, reactor trips on high and low pressure, safety injection signal, setpoints for starting injection of safety injection pumps and accumulators. Decreasing primary pressure indicated that all decay heat is removed and vice versa.
2	Core collapsed liquid level	The core collapsed liquid level is indication of core uncovery and subsequent core heatup.
3	Primary mass	Primary mass is indication if liquid inventory is decreasing or increasing. The mass typically decrease in case of leaks, breaks and open relief valves. The mass is increasing when charging flow and safety injection is larger than leak flows, break flow and mass discharged through the relief valves.
4	Steam generator no. 1 mass	Steam generator mass is important for heat transfer from primary to secondary side. When the steam generator mass boils off, the heat removal from primary to secondary side is interrupted (the steam generator mass is not measured in the plant – the indication is steam generator level).
5	Steam generator no. 2 mass	See variable 4.
6	Integrated PRZ discharge flow	The integrated PRZ discharge flow is indication of primary side mass and energy discharge through the pressurizer relief valve.
7	Integrated accumulator flow	Integrated accumulator flow is important for cooling the primary mass system and tells how much coolant is added to primary system.
8	Rod surface level 11 temperature	Rod surface temperature is indication of heat transfer in the core. It is indication if core is covered or partially uncovered.
9	Steam generator no. 1 pressure	Steam generator pressure is used as setpoint for steam generator relief valves. Increasing pressure is indication of decrease in the heat removal and vice versa.
10	Steam generator no. 1 wide range level	Steam generator (SG) level is an anticipatory indication of a loss of heat sink. The SG level must be sufficient that the heat transfer from primary to secondary side is not degraded and it provides information if steam generator is overfilled. It is also used to trip reactor on low level.
11	Steam generator no. 2 pressure	See variable 9
12	Steam generator no. 2 wide range level	See variable 10.
13	Steam generator no. 1 valves discharge	Steam generator valves discharge provides information on steam generator mass released.
14	Steam generator no. 2 valves discharge	See variable 13.
15	Cold leg no. 1 liquid temperature	Hot leg temperature and cold leg are representative of core delta temperature (which is their difference), the increase of coolant temperature due to heating in the core. The delta temperature is proportional to reactor power. The average hot and cold leg temperature is called average temperature. Higher it is, more heat can be transferred to steam generators, provided that secondary temperature is constant.
16	Cold leg no. 2 liquid temperature	See variable 15.
17	Hot leg no. 1 liquid temperature	See variable 15.
18	Hot leg no.2 liquid temperature	See variable 15.
19	Cold leg no. 1 flow	Cold leg flow is important for forced or natural convection.
20	Cold leg no. 2 flow	See variable 19.
21	Pressurizer level	Pressurizer level provides input to reactor protections systems for high pressurizer level trip, which protects from overfilling the pressurizer. The pressurizer level drop due to inventory loss cause primary pressure drop.

5.3 Sensitivity of SBO to EDG operation time

In the sensitivity case no. 1 (see Table 7) the EDG operation time influence was studied. In the reference scenario 'S_LOSS_3 (C1)' it was assumed, that EDGs start successfully at the time of LOOP and failed after one hour of operation (similar like in Fukushima Dai-ichi). Loss due to reactor coolant pumps (RCPs) seal leakage ('S_LOSS') and restoration of cooling after 3 h after SBO initiation ('_3' added to label) is assumed. In the sensitivity calculation (scenario 'S_LOSS_3 (C2)') the failure to start EDGs at LOOP initiation was assumed. All other assumptions and initial and boundary conditions were the same as for 'SL_LOSS_3 (C1)' scenario.

5.3.1 Visual observation of calculated parameters

The 21 variables shown in Table 8 were used for qualitative and quantitative assessment of SBO scenario sensitivity to assumed parameter variation. The qualitative analysis is done through visual observation of calculated reference and compared signals, shown in Figs. 3 through 8 (the variables are labelled (a1) through (a21)).

From Fig. 3(a1) showing primary pressure it can be seen that for scenario 'S_LOSS_3 (C2)' pressure starts to increase above pressurizer (PRZ) relief valves setpoint when the steam generator wide range (WR) levels (see Fig. 5(a10) and Fig. 5(a12)) drop below 5%, indicating that the steam generators water boils off resulting in termination of heat transfer from primary to secondary side at around 4100 s. The steam generators mass also decrease (see Fig. 3(4a) and Fig. 4(5a)). Shortly after the PRZ relief valves opening, discharging of RCS inventory occurred. Because it is assumed that seal loss of coolant occurs one hour after SBO initiation, some RCS mass is also lost from RCP seals, but mass lost is ten times smaller than that through PRZ relief valves. Due to discharged RCS inventory (see discharged mass in Fig. 4(6a)) the core starts to uncover (see Fig. 3(2a)) after 6500 s, resulting in the core heatup after 8000 s (see Fig. 4(8a)). Without any recovery action to restore injection into primary system the core damage is unavoidable. The steam generator pressures are oscillating (see Fig. 5(9a) and Fig. 5(11a)) due to opening and closing steam relief valves. The steam generator no. 1 and no. 2 discharged mass is shown in Fig. 6(13a) and Fig. 6(14a), respectively. Cold leg no. 1 and no. 2 temperatures are shown in Figs. 6(15a) and 6(16a), respectively. In scenario 'S_LOSS_3 (C2)' before 4000 s heatup is shown due to secondary side heat sink lost. Similar is the trend for the hot leg no. 1 and 2 temperatures shown in Fig. 7(17a) and Fig. 7(18a). Cold leg flow in loops no. 1 and 2 is shown in Fig. 7(19a) and Fig. 7(20a). After SBO start the reactor coolant pumps are stopped, resulting in the flow coastdown. Due to sufficient primary and secondary mass the natural circulation flow is established. However, when the core levels start to decrease in the 'S_LOSS_3 (C2)' scenario (see Fig. 3(2a)), also the cold leg flows are terminated for 'S_LOSS_3 (C2)' (see Fig. 7(19a) and Fig. 7(20a)). Finally, Fig. 7(21a) shows the pressurizer level. The pressurizer level at 100% in the case of 'S_LOSS_3 (C2)' scenario is the indication that pressurizer relief valve is discharging RCS inventory due to degraded cooling and heating up the primary system. When sufficient RCS mass is lost and core starts to uncover, the pressurizer level at around 7000 s start to decrease.

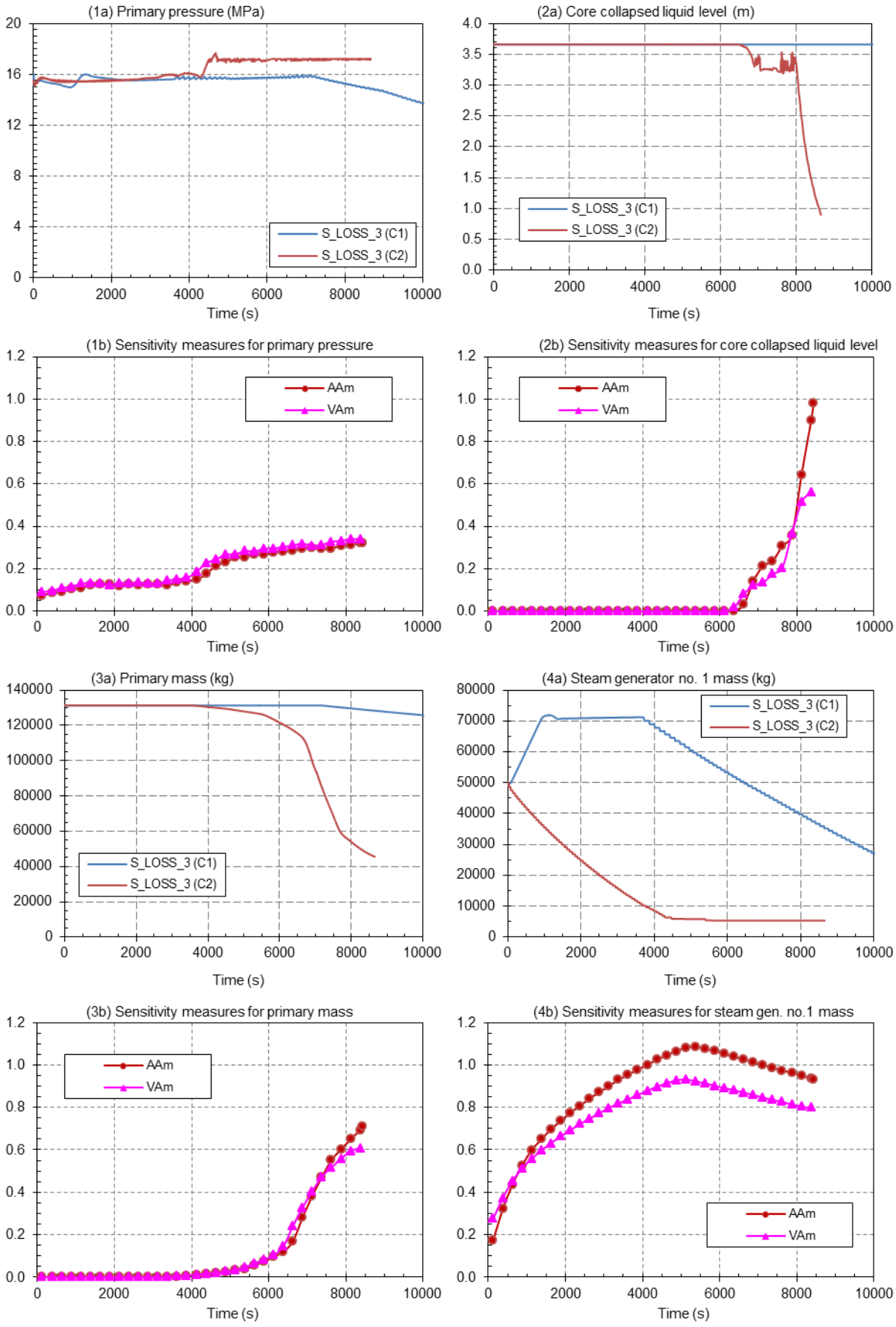

Fig. 3: (a) Time trends and (b) accuracy measures of important variables for scenario with different EDG operation time after LOOP occurrence and with 3 h operator action delay to recover cooling – Part 1 (note: the numbers in the parenthesis in the above graphs are the output variables as defined in Table 8)

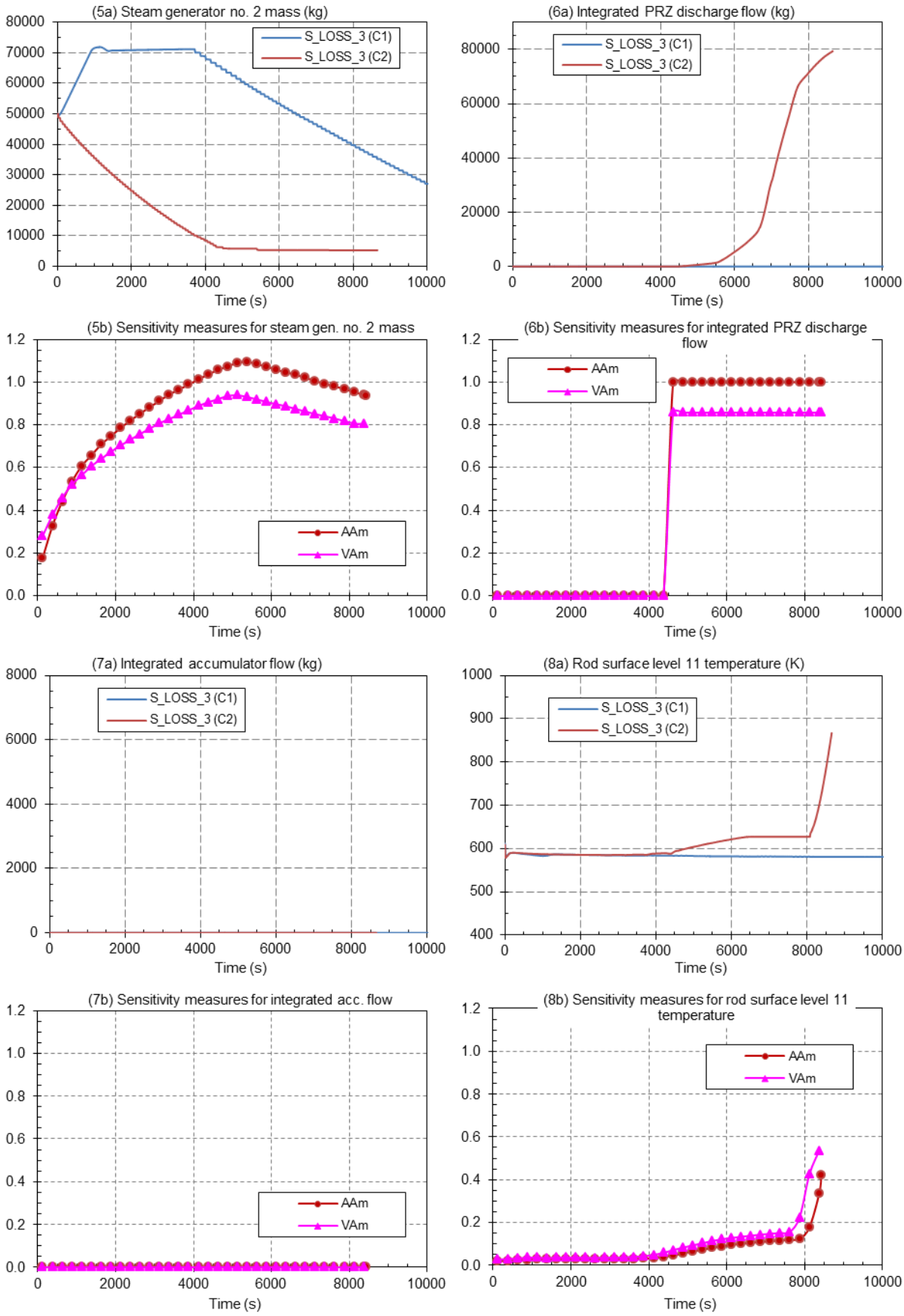

Fig. 4: (a) Time trends and (b) accuracy measures of important variables for scenario with different EDG operation time after LOOP occurrence and with 3 h operator action delay to recover cooling – Part 2 (note: the numbers in the parenthesis in the above graphs are the output variables as defined in Table 8)

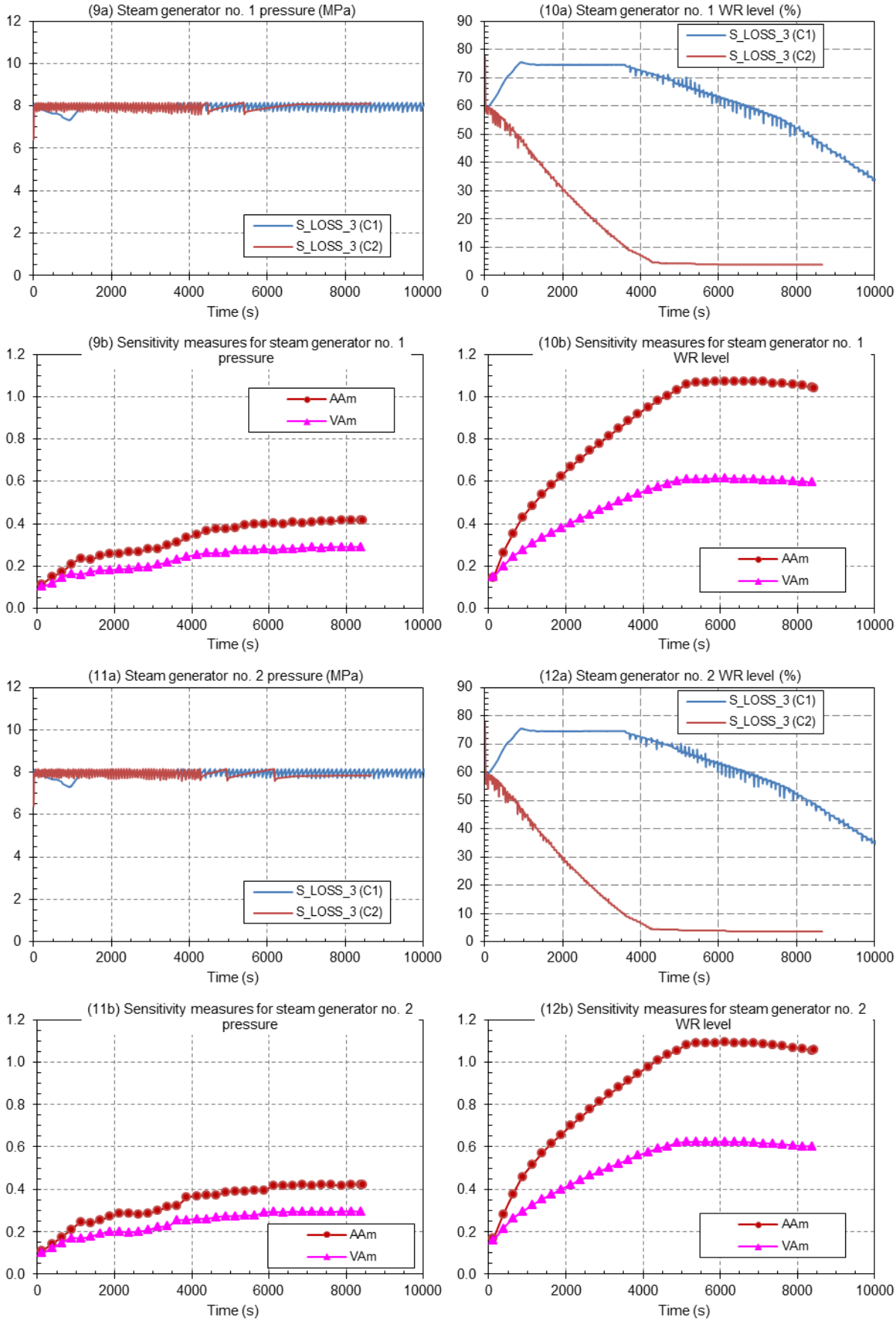

Fig. 5: (a) Time trends and (b) accuracy measures of important variables for scenario with different EDG operation time after LOOP occurrence and with 3 h operator action delay to recover cooling – Part 3 (note: the numbers in the parenthesis in the above graphs are the output variables as defined in Table 8)

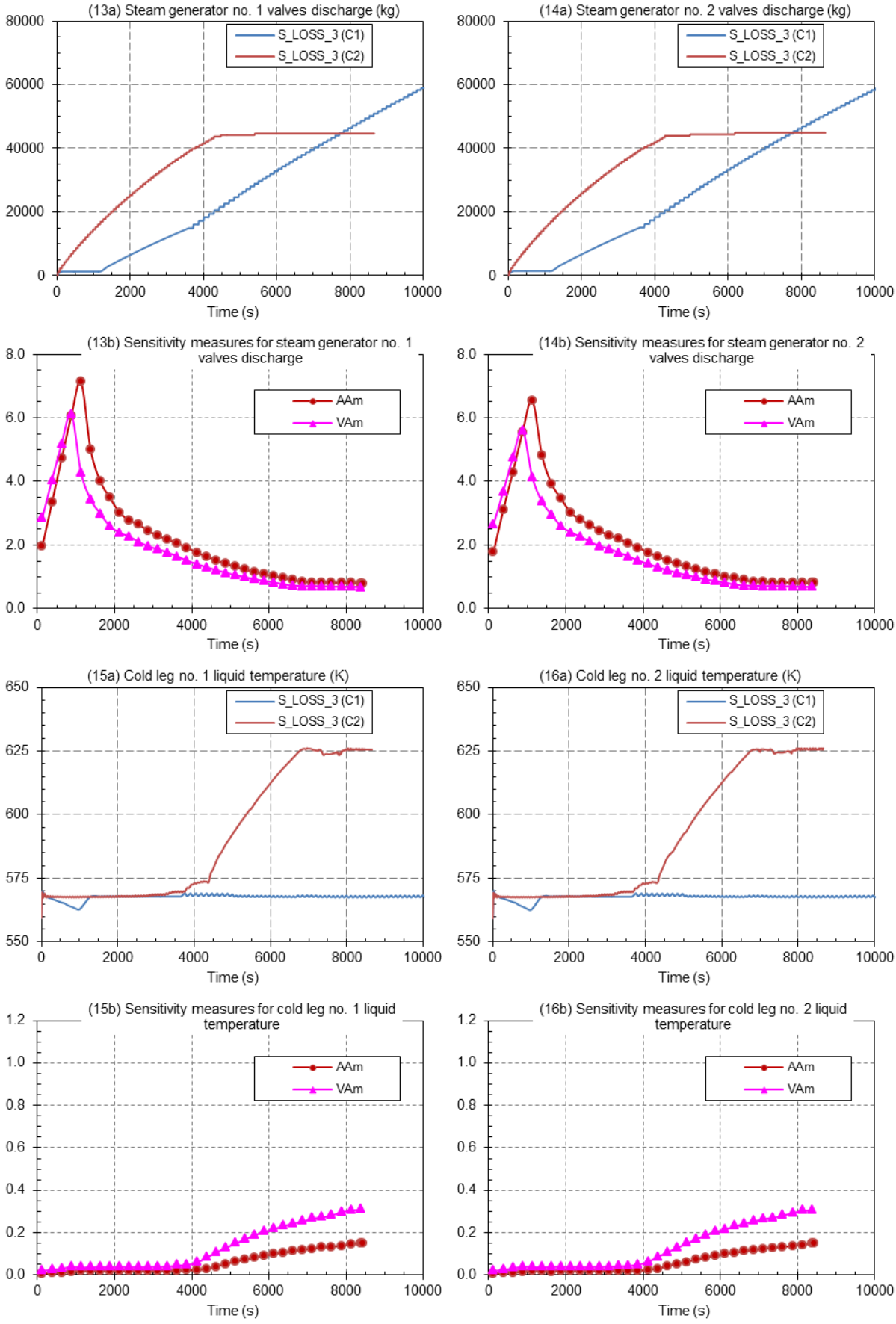

Fig. 6: (a) Time trends and (b) accuracy measures of important variables for scenario with different EDG operation time after LOOP occurrence and with 3 h operator action delay to recover cooling – Part 4 (note: the numbers in the parenthesis in the above graphs are the output variables as defined in Table 8)

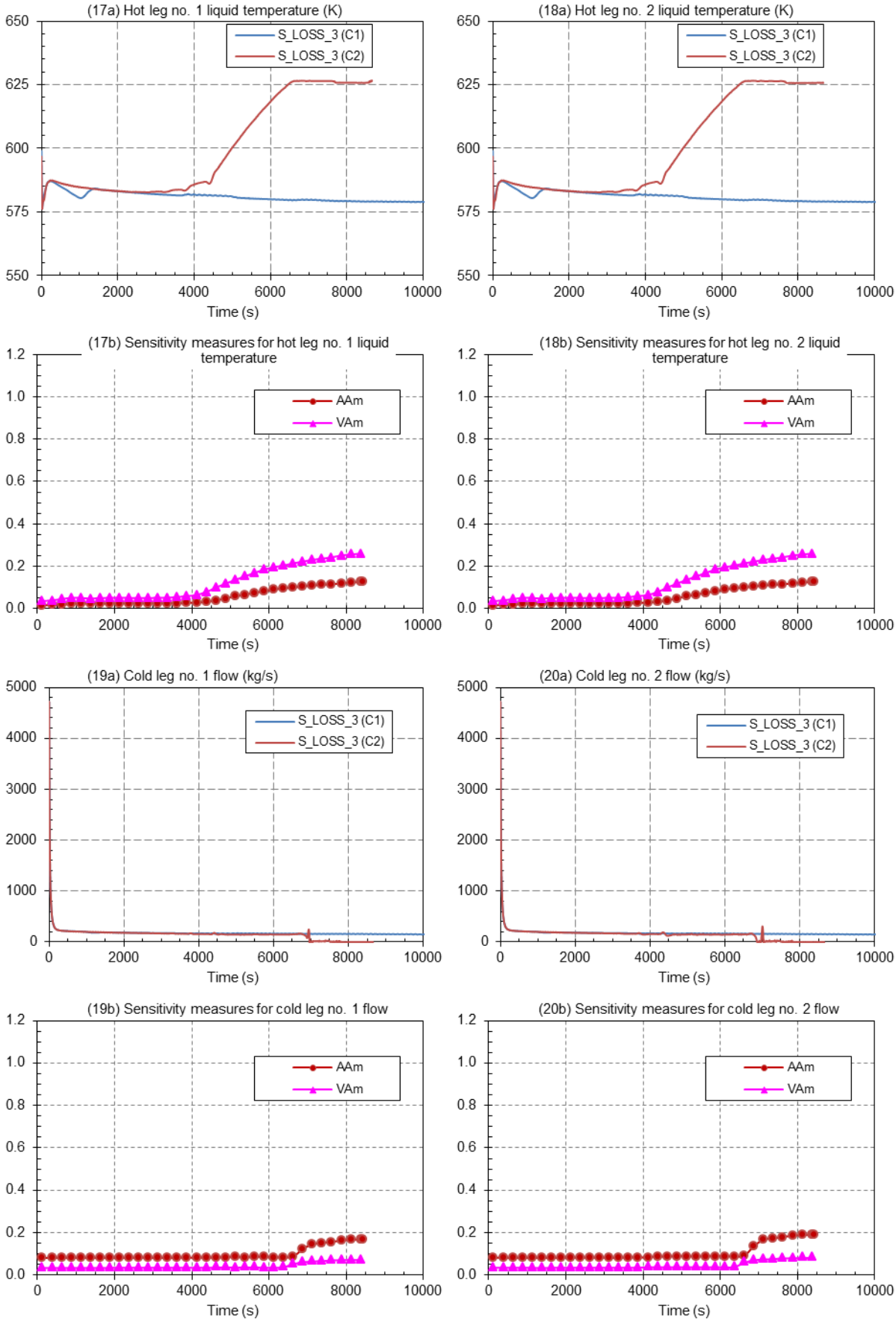

Fig. 7: (a) Time trends and (b) accuracy measures of important variables for scenario with different EDG operation time after LOOP occurrence and with 3 h operator action delay to recover cooling – Part 5 (note: the numbers in the parenthesis in the above graphs are the output variables as defined in Table 8)

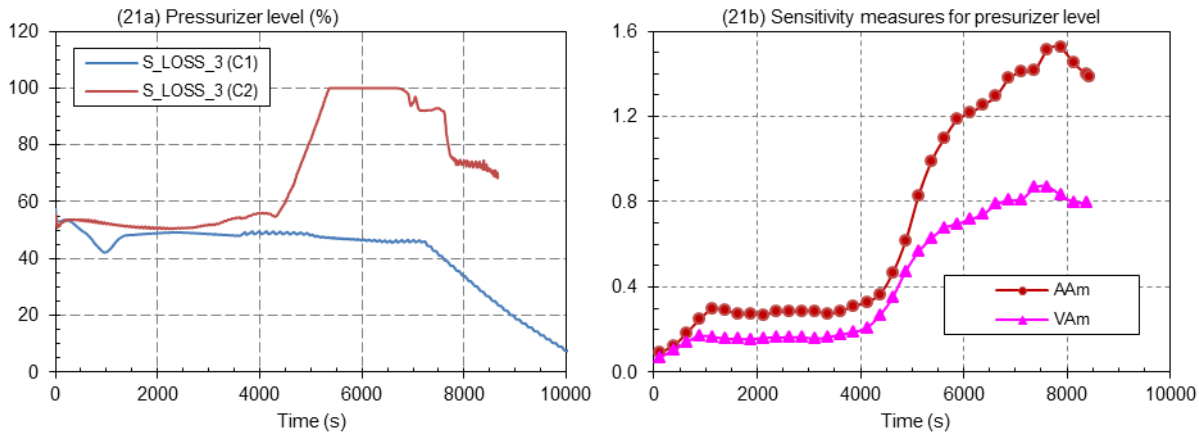

Fig. 8: (a) Time trends and (b) accuracy measures of important variables for scenario with different EDG operation time after LOOP occurrence and with 3 h operator action delay to recover cooling – Part 6 (note: the numbers in the parenthesis in the above graphs are the output variables as defined in Table 8)

5.3.2 Calculation of sensitivity measures

The results of sensitivity measures are shown in Table 9 and Figs. 3 through 8 (the parameters are labelled (b1) through (b21)). Table 9 shows that the calculated SBO scenario results are sensitive to the influence of external uncertain parameter EDG operation time (scenario 'S_LOSS_3 (C2)' with not running EDG is compared to the reference scenario 'S_LOSS_3 (C1)' in which EDG is running 1 h after LOOP). Quantitative analysis using FFTBM-SM showed that when EDG is not starting, this significantly influences the results of SBO scenario simulation. The parameters most contributing to the $AA_{m\text{-}tot}$ are masses, levels and rod surface temperature (see column for VA_m). The VA_m is calculated using Eq. (5), where N_{var} is equal to 21. The weights $(w_f)_i$ are calculated following Eq. 4 with using the weighting factors components shown in Table 4. The weights depend not only on the quantity, but also on the total number of variables considered (i.e. N_{var}). The weights are shown in the last column of Table 9. The variable accuracy shown in Table 9 is the product of AA_m for i-th variable, weight for i-th variable and the number of variables. This means that dividing the sum of variable accuracies with the number of variables gives the value of total sensitivity of calculation ($AA_{m\text{-}tot}$). In this way ranking could be done for variables contribution to the total sensitivity. From Table 9 it can be seen, that integrated loss flow through pressurizer relief valves is the most influential and cold leg flow the least influential (excluding accumulator integrated mass having no influence in this case). The second largest contributor to the total sensitivity is pressurizer level, which is related to variable integrated pressurizer relief valves flow. Namely, the pressurizer level increase is the indication of fluid flowing out of pressurizer through relief valves.

In principle comparison of calculated trends (qualitative analysis, see Figs. 3 through 8 – parameter trends labelled (a1) through (a21)) already shows the influence of failure to start EDG and quantitative assessment using FFTBM-SM confirms this finding. The time dependent sensitivity measures are shown in Figs. 3 through 8 (see sensitivity measures (b1) through (b21)). Here, it should be noted that for the absolute contribution to total sensitivity the trends of VA_m should be compared (see explanation in the previous paragraph). Also, the values of AA_m and VA_m for whole transient interval on Figs. 3 through 8 (from (b1) to (b21)) are presented in Table 9. Regarding results shown Fig. 4(6b), Fig. 6(13b) and Fig. 6(14b) for integrated masses it should be noted that the AA_m, until reference signal is non-zero (or not small constant comparing to compared signal), is not suitable for normalization. After, the results are meaningful. If reference signal all the time is zero, the AA_m is arbitrary set to 1 by FFTBM-SM software as is shown in Fig. 4(6b).

From Fig. 9 it can be seen that external parameter EDG operation time influences SBO progression from the very beginning due to difference on the secondary side (in case of 'S_LOSS_3 (C2)' steam generators are emptying, while in case of 'S_LOSS_3 (C1)' are filling).

When SGs are full at 1000 s, the filling is terminated and therefore $AA_{m\text{-}tot}$ decreases. When steam generators boil-off at around 4250 s, there is again increase of the sensitivity measure $AA_{m\text{-}tot}$ and the differences are present until the end time 8600 s, resulting in continuous slight increase of $AA_{m\text{-}tot}$ value.

Table 9: Sensitivity of whole transient to failure of EDG start at LOOP occurrence

No.	Variable	time interval 0 – 8600 s		weights	
		AA_m	VA_m	$(w_f)_i$	$(w_{saf})_i(w_{norm})_i$
1	Primary pressure	0.321	0.340	0.050	1.00
2	Core collapsed liquid level	0.981	0.561	0.027	0.54
3	Primary mass	0.708	0.608	0.041	0.81
4	Steam generator no. 1 mass	0.931	0.799	0.041	0.81
5	Steam generator no. 2 mass	0.937	0.804	0.041	0.81
6	Integrated pressurizer relief valves flow	1.000	0.858	0.041	0.81
7	Integrated accumulator flow	0.000	0.000	0.041	0.81
8	Rod surface level 11 temperature	0.420	0.534	0.061	1.20
9	Steam generator no. 1 pressure	0.416	0.291	0.033	0.66
10	Steam generator no. 1 wide range level	1.042	0.596	0.027	0.54
11	Steam generator no. 2 pressure	0.421	0.295	0.033	0.66
12	Steam generator no. 2 wide range level	1.057	0.604	0.027	0.54
13	Steam generator no. 1 valves discharge	0.803	0.689	0.041	0.81
14	Steam generator no. 2 valves discharge	0.810	0.695	0.041	0.81
15	Cold leg no. 1 liquid temperature	0.151	0.308	0.097	1.92
16	Cold leg no. 2 liquid temperature	0.150	0.305	0.097	1.92
17	Hot leg no. 1 liquid temperature	0.127	0.259	0.097	1.92
18	Hot leg no.2 liquid temperature	0.127	0.259	0.097	1.92
19	Cold leg no. 1 flow	0.168	0.071	0.020	0.40
20	Cold leg no. 2 flow	0.191	0.081	0.020	0.40
21	Pressurizer level	1.388	0.794	0.027	0.54
	Total	0.466			

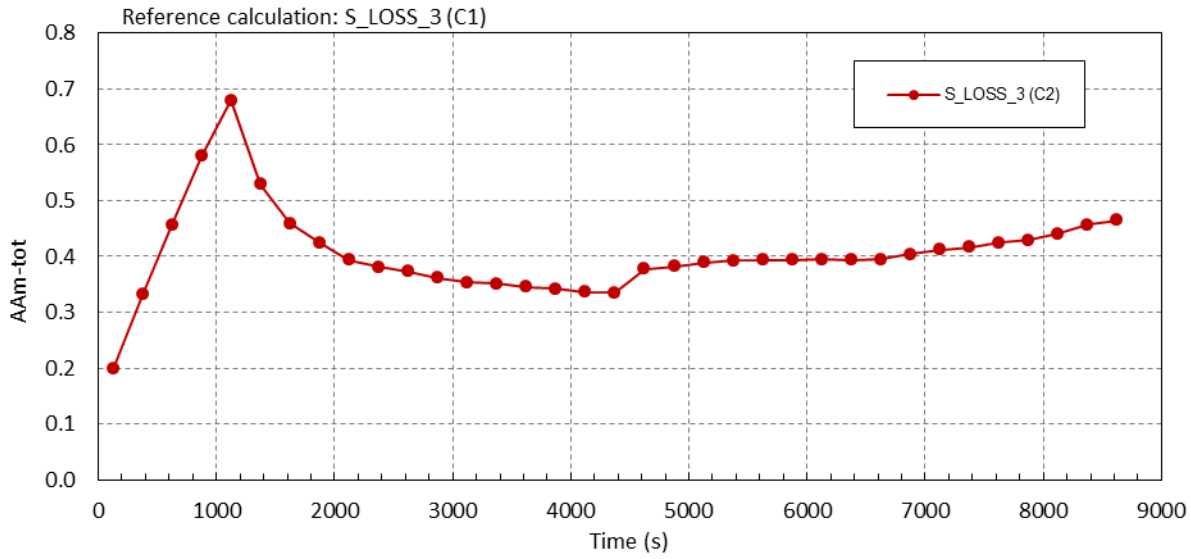

Fig. 9: Code calculation sensitivity (total average amplitude $AA_{m\text{-}tot}$) as a function of increasing time intervals starting at 0 s till 8600 s for scenario with failure of EGD start

5.4 Sensitivity of SBO to RCS inventory loss type

In the sensitivity cases no. 2 and 3 (see Table 7) the RCS inventory loss type influence has been studied, assuming the EDG running one hour after LOOP (Case C1). The sensitivity case using FFTBM-SM has been performed for three loss types during extended SBO defined in Table 5: normal system leakage ('N_LOSS'), loss due to RCPs seal leakage ('S_LOSS') and loss of RCS coolant through letdown relief valve unless automatically isolated or until isolation is procedurally directed ('SL_LOSS'). For more detailed description of RCS loss types the reader is referred to Prošek and Volkanovski (2015a). The reference calculation in that study shows that the maximum delay of the cooling start that prevents the core damage in the 'S_LOSS' type is 4 hours for Case 1 (C1) for simulations lasting 24 hours. Therefore, two cases are considered regarding delay time of restoration of cooling (external parameter), 5 h and 3 h, respectively. Restoration of cooling in the calculated scenarios means that makeup water to steam generators was provided after 5 h and 3 h of SBO initiation, respectively.

5.4.1 Sensitivity of SBO to RCS inventory loss type – restoration of cooling after 5 h

In the sensitivity case no. 2 (see Table 7) the RCS inventory loss types influence has been studied assuming the restoration of cooling with 5 h delay. The calculated results of scenarios used for visual observation are shown in Fig. 10. For brevity, only the most important variables are shown in Fig. 10. Primary pressure is shown in Fig. 10(a) and it is important because it directs the transient progression (safety valves opening/closing, accumulator injection, etc.). It depends on the decay heat removal and the RCS mass discharge (see Fig. 10(e)). The RCS mass depends on the mass lost through the breaks (studied loss types), the accumulator injection into RCS and the mass discharged through pressurizer relief valve (see Fig. 10(f)).

One hour after SBO initiation the steam generator no. 1 pressure starts to oscillate (similarly steam generator no. 2 pressure, which is not shown), indicating that the steam generator relief valves are opening and closing periodically (see Fig. 10(b)). This also gives information that decay heat removal through the secondary side to the heat sink is established. The RCS starts to heatup, after the steam generator inventory boils off, resulting in the empty steam generators (see steam generator no. 1 level in Fig. 10(h)). To remind, steam generator level is an anticipatory indication of a loss of heat sink. RCS heating up causes pressure increase and when pressure is reaching the pressurizer relief valve opening setpoint, the steam is discharged first. The pressurizer level gradually increases and when 100% level is reached (see Fig. 10(g)), the discharge is solid liquid, causing significant RCS mass decrease. This further resulted in the core uncovery (see core collapsed liquid level in Fig. 10(c)), leading to core heatup as shown in Fig. 10(d).

For all considered loss type scenarios the cooling recovery action taken 5 h after LOOP occurrence is too late to prevent core heatup as already mentioned. As the mass lost through the breaks is the largest for ‘SL_LOSS_5’ scenario, the heatup occurs approximately half an hour earlier than in other loss types, in which the most RCS mass was discharged through the pressurizer relief valves due to inadequate decay heat removal through the steam generators.

In Table 10 the results of the quantitative assessment of sensitivity to varying loss flow type are shown for the three selected scenarios. Only the AA_m sensitivity measure and its total value are shown. For brevity, sensitivity measure VA_m is not given in Table 10. Nevertheless, these values could be determined multiplying AA_m with weights taken from Table 9 and N_{var}, following Eq. (5). Nevertheless, the total sensitivity $AA_{m\text{-}tot}$ for selected scenarios show that scenarios in general are rather similar and that selected loss types are not extremely influential to the extended SBO scenario progression. The reason for this is compensating effect. In the case of larger RCS inventory loss the pressure drops more and delays the pressure increase to the value of pressurizer safety relief valve opening setpoint, resulting form the core heatup (see Fig. 10(f)).

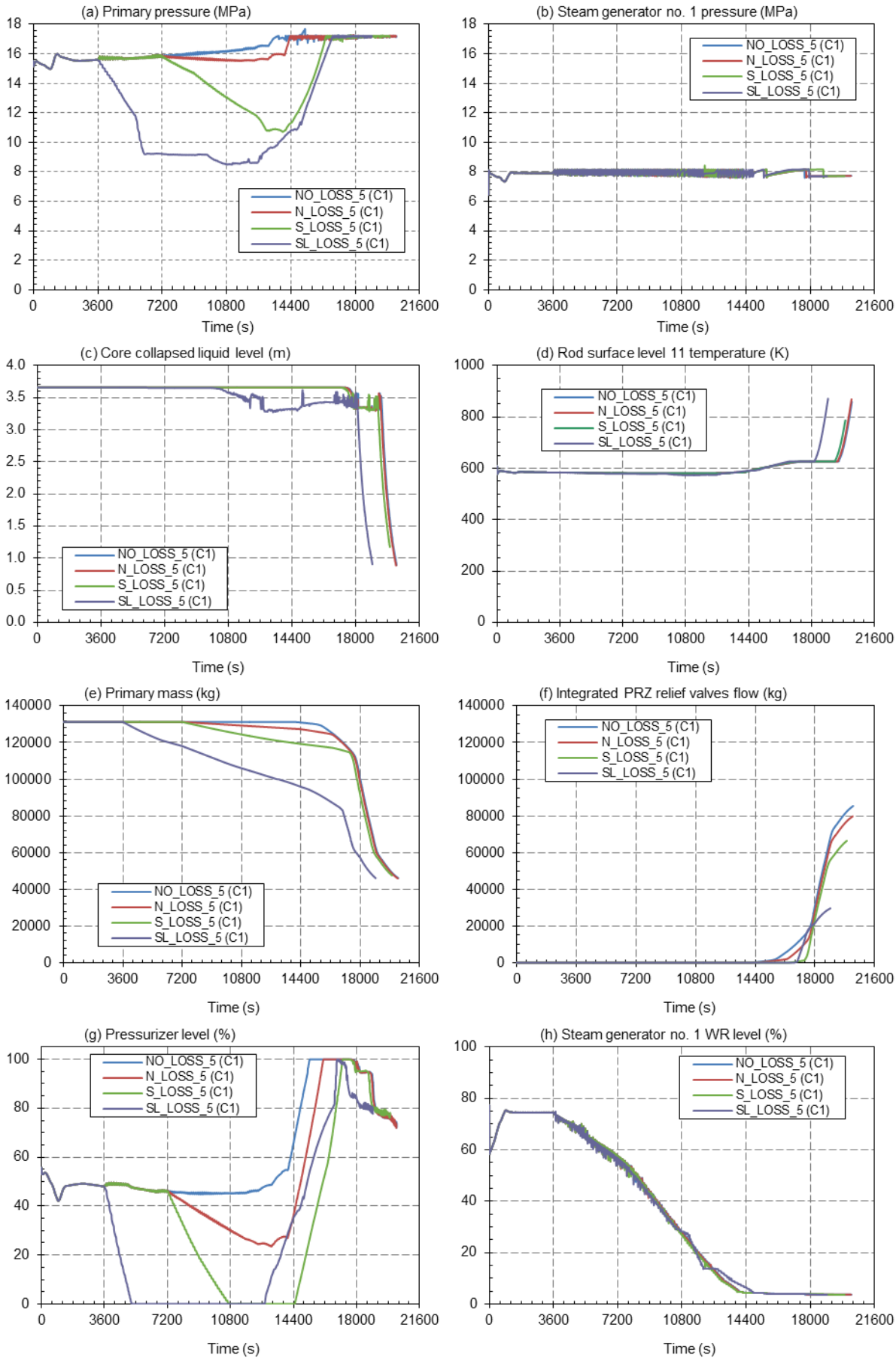

Fig. 10: Time trends of important variables for scenario with 5 h operator action delay to recover cooling

By this the release of RCS inventory through the pressurizer safety relief valves is delayed. This can be seen, when looking the value of AA_m for variable no. 6 (integrated pressurizer relief valves flow). The change of mass discharged for scenario with larger loss flow ('SL_LOSS_5 (C1)') is different from the one in the normal loss scenario ('N_LOSS_5 (C1)'), in which discharged mass is smaller because of delayed pressurizer relief valve opening (see pressure in Fig. 10(a)). Fig. 10(e) shows that there is qualitative difference between the seal and letdown RCS loss type. For the reactor coolant pumps seals the damage is assumed one hour after SBO initiation. For RCS loss type the primary pressure should drop below 4.2 MPa.

The second step of the FFTBM methodology is qualitative analysis with the visual observation of variables and requirement to understand all discrepancies. The AA_m sensitivity measure cannot show the sign of the sensitive parameter influence (for example, for variable no. 6 the largest discrepancy for 'SL_LOSS_5 (C1)' is due to the smaller discharge comparing to the reference case what is beneficial for mass inventory and core cooling). The heatup in the time interval 0 – 18900 s occurs only for 'SL_LOSS_5 (C1)', indicated as discrepancy in the calculated AA_m for rod surface temperature. Fig. 10(d) shows that the heatup occurs with some small delay also in the 'N_LOSS_5 (C1)' and 'S_LOSS_5 (C1)' scenarios. This means that all three scenarios are qualitatively similar, ultimately resulting in the core damage.

Fig. 11 shows how total $AA_{m\text{-}tot}$ changes over time, starting at zero time. The first influence of RCS loss type is in the 'SL_LOSS_5' scenario at 3600 s when the letdown loss type is assumed. At 7200 s the reactor coolant pump (RCP) seal damage is assumed, therefore also 'N_LOSS_5' and 'S_LOSS_5' scenarios are influenced by RCP seal loss flow. Another significant change in the $AA_{m\text{-}tot}$ is when pressurizer relief valves start to discharge the RCS inventory (i.e. primary mass). The last significant change is in the 'SL_LOSS_5' scenario, when the core heatup occurred. The measure total average amplitude $AA_{m\text{-}tot}$ is such that it accumulates the discrepancies during time. The trends of total average amplitude $AA_{m\text{-}tot}$ are rather similar after 7200 s from the start of the LOOP event.

Table 10: Sensitivity of whole transient to loss flow type (restoration of cooling after 5 h)

No.	Variable	AA_m for time interval 0 - 18900 s		
		N_LOSS_5	S_LOSS_5	SL_LOSS_5
1	Primary pressure	0.227	0.580	0.806
2	Core collapsed liquid level	0.120	0.182	0.807
3	Primary mass	0.045	0.130	0.350
4	Steam generator no. 1 mass	0.046	0.057	0.131
5	Steam generator no. 2 mass	0.023	0.048	0.111
6	Integrated pressurizer relief valves flow	0.126	0.313	0.608
7	Integrated accumulator flow	0.000	0.000	0.000
8	Rod surface level 11 temperature	0.007	0.014	0.345
9	Steam generator no. 1 pressure	0.333	0.357	0.471
10	Steam generator no. 1 wide range level	0.104	0.141	0.265
11	Steam generator no. 2 pressure	0.201	0.346	0.469
12	Steam generator no. 2 wide range level	0.065	0.113	0.264
13	Steam generator no. 1 valves discharge	0.049	0.059	0.131
14	Steam generator no. 2 valves discharge	0.025	0.050	0.109
15	Cold leg no. 1 liquid temperature	0.012	0.020	0.153
16	Cold leg no. 2 liquid temperature	0.007	0.018	0.126
17	Hot leg no. 1 liquid temperature	0.006	0.012	0.033
18	Hot leg no. 2 liquid temperature	0.006	0.012	0.034
19	Cold leg no. 1 flow	0.081	0.107	0.262
20	Cold leg no. 2 flow	0.126	0.124	0.296
21	Pressurizer level	0.454	0.962	0.892
	Total	0.466		

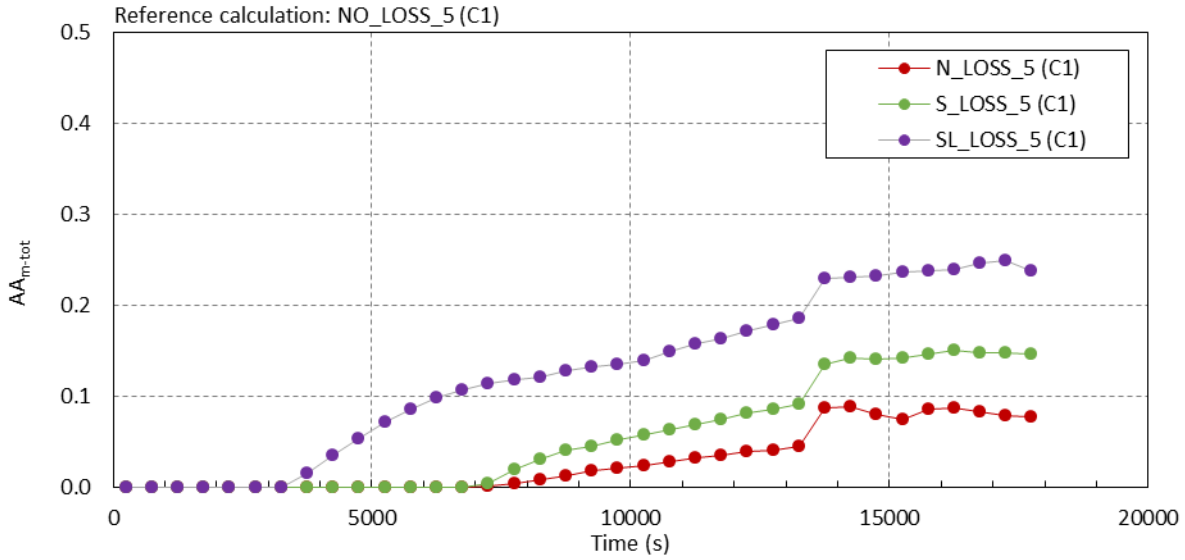

Fig. 11: Code calculation sensitivity (total average amplitude $AA_{m\text{-}tot}$) as a function of increasing time intervals starting at 0 s till 18900 s for scenario with no operator action

5.4.2 Sensitivity of SBO to RCS inventory loss type – restoration of cooling after 3 h

In the sensitivity case no. 3 (see Table 7) the RCS inventory loss types influence was studied, when restoration of cooling with 3 h delay is assumed. If RCS inventory is sufficient for natural circulation in the primary system, the heat transfer from the primary to secondary side is established in the case of filled steam generators and available steam generator relief valves, which provides heat sink for core decay heat removal. For further explanation of physical phenomena, refer to Section 5.4.1.

The calculated results of scenarios used for visual observation are shown in Fig. 12. Again as in the Section 5.4.1 only important variables are shown for simulated extended SBO with varying loss type for scenario with restoration of cooling after 3 h after SBO initiation - this means time 14400 s (4 h after LOOP initiation and 3 h after SBO initiation). Results show that before the SBO start, when EDG is running, there is no RCS inventory loss and the plant variables are stable. The primary pressure shown in Fig. 12(a) started to drop in the case of larger RCS mass loses (see Fig. 12(e), first in the scenario 'SL_LOSS_3' and then in the scenario 'S_LOSS_3'). In case of normal leakage the loss is smaller, therefore primary pressure because of heatup starts to increase before 14400 s, resulting in short opening of pressurizer relief valves. At 14400 s the cooling is restored by feeding steam generations (see Fig. 12(h)), resulting in the primary and secondary pressure drop (see Fig. 12(a) and Fig. 12(b)). Once steam generators are filled, the saturation pressure in the steam generators is established. The SG pressure oscillating between the opening and closure SG relief valve setpoint values is the indication that the heat (by releasing the steam during the valve opening period) is transferred to the heat sink (environment air). Once RCS inventory is depleted sufficiently in the 'SL_LOSS-3' scenario due to primary mass discharged through the breaks (see Fig. 12(e)), the core starts to uncover (see Fig. 12(e), oscillations occur because the steam produces a back-pressure opposing the driving head of coolant in the annulus and thereby slowing or even reversing the water level rise in the core) and when sufficiently uncovered, the core heatup occurs (Fig. 12(d)). The mass discharged through the pressurizer relief valves is small and occurred at the SBO initiation only (see (Fig. 12(f)). As can be seen from pressurizer level in Fig. 12(g), the pressurizer has not been filled, indicating that no liquid discharge occurred.

In Table 11 the results of the quantitative assessment of SBO scenario sensitivity to varying RCS inventory loss type are shown for the three selected cases with 3 h operator action delay to recover cooling. The sensitivity measures showed that in such scenario the SBO is very sensitive to RCS inventory loss type. The quantitative assessment of sensitivity has been done until 54000 s due to the core heatup resulting in the code calculation termination (no models

for core melt) in the 'SL_LOSS_3' scenario. The 'SL_LOSS_3' scenario is the most influential on RCS inventory loss type. Prolonging sensitivity calculations until the end of 24 h would even increase the differences (see Fig. 12).

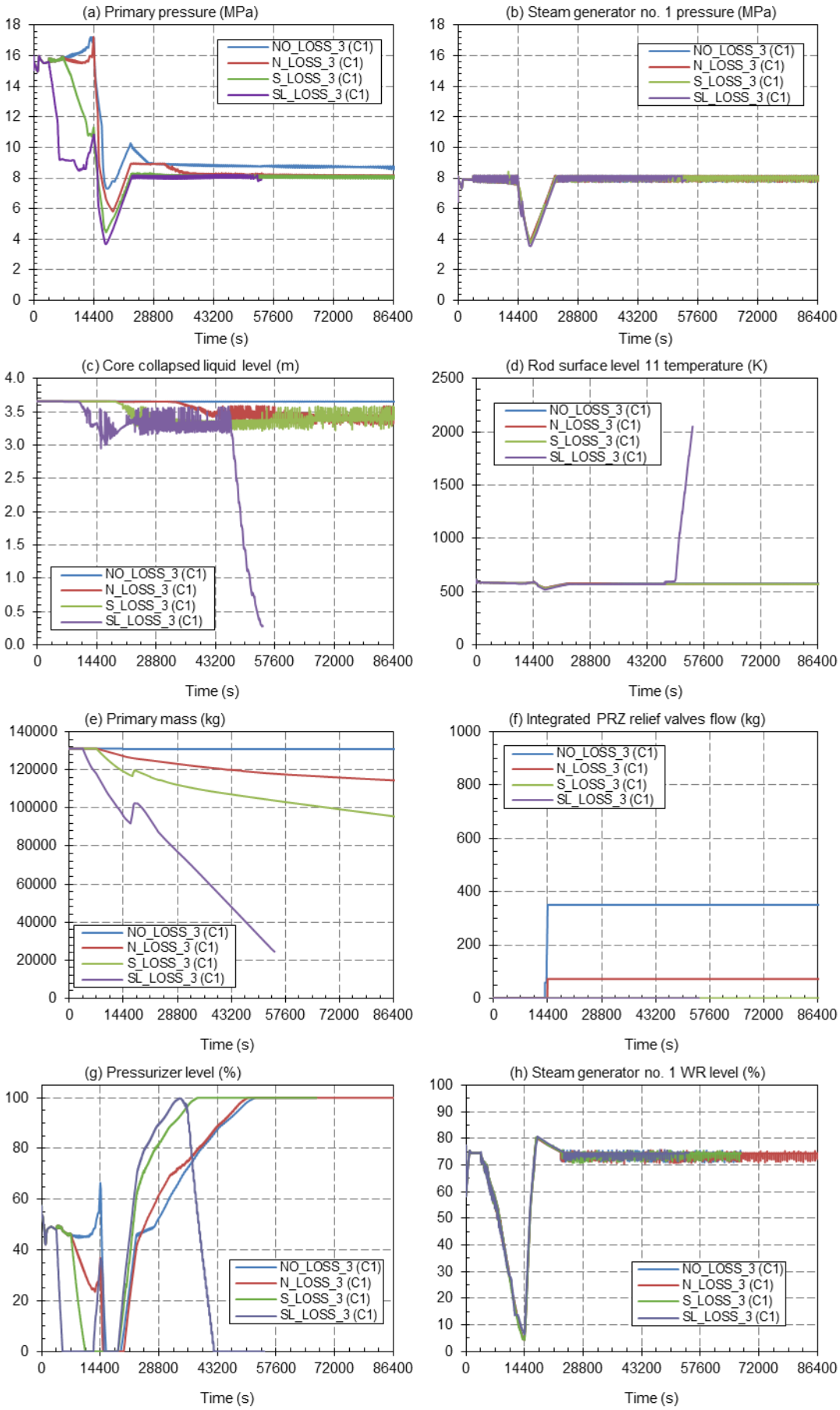

Fig. 12: Time trends of important variables for scenario with 3 h operator action delay to recover cooling

Table 11: Sensitivity of whole transient to RCS inventory loss type (restoration of cooling after 3 h)

No.	Variable	AA_m for time interval (0 – 54000 s)		
		N_LOSS_3	S_LOSS_3	SL_LOSS_3
1	Primary pressure	0.298	0.427	0.644
2	Core collapsed liquid level	0.382	0.516	1.674
3	Primary mass	0.116	0.298	0.917
4	Steam generator no. 1 mass	0.079	0.096	0.131
5	Steam generator no. 2 mass	0.085	0.093	0.119
6	Integrated pressurizer relief valves flow	0.830	1.000	1.000
7	Integrated accumulator flow	0.000	1.000	1.000
8	Rod surface level 11 temperature	0.036	0.053	2.016
9	Steam generator no. 1 pressure	0.331	0.350	0.467
10	Steam generator no. 1 wide range level	0.151	0.165	0.213
11	Steam generator no. 2 pressure	0.279	0.364	0.444
12	Steam generator no. 2 wide range level	0.161	0.161	0.217
13	Steam generator no. 1 valves discharge	0.198	0.111	0.156
14	Steam generator no. 2 valves discharge	0.200	0.090	0.142
15	Cold leg no. 1 liquid temperature	0.035	0.053	0.445
16	Cold leg no. 2 liquid temperature	0.033	0.057	0.244
17	Hot leg no. 1 liquid temperature	0.037	0.052	0.091
18	Hot leg no. 2 liquid temperature	0.035	0.052	0.092
19	Cold leg no. 1 flow	0.576	0.622	0.353
20	Cold leg no. 2 flow	0.629	0.576	0.367
21	Pressurizer level	0.301	0.686	1.104
	Total	0.160	0.242	0.527

Fig. 13 shows how total average amplitude $AA_{m\text{-}tot}$ changes with increasing time intervals from the beginning of simulation. The sensitivity measure total average amplitude $AA_{m\text{-}tot}$ is such that it accumulates the discrepancies during time. First discrepancies start when RCS inventory loss occurred (first in the 'SL_LOSS_3' scenario at 3600 s, then in the 'N_LOSS_3' and 'S_LOSS_3' scenarios at 7200 s). Fig. 13 shows that the influence of RCS inventory loss is smaller in the 'N_LOSS_3' than in the 'S_LOSS_3' scenario. The influences on RCS inventory loss types decrease when at 14400 s the core cooling is established. The last significant change in the sensitivity measure for 'SL_LOSS_3' scenario is the core uncovery and heatup slightly before the 50000 s.

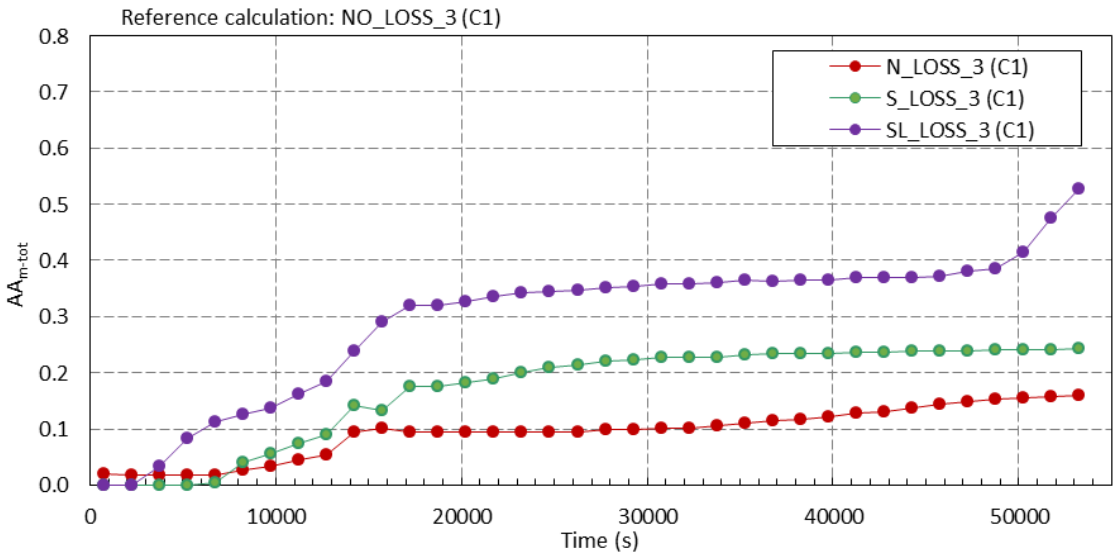

Fig. 13: Code calculation sensitivity (total average amplitude $AA_{m\text{-}tot}$) as a function of increasing time intervals starting at 0 s till 54000 s for scenario with operator action

5.5 Sensitivity of SBO to depressurization strategy

In sensitivity case no. 4 (see Table 7) the depressurization strategy assumed has been studied for 'SL_LOSS_5 (C1)' scenario, in which the core heatup could not be prevented due to large RCS inventory (primary mass) loss. In the 'SLD_LOSS_5 (C1)' scenario an operator action to start the steam generator depressurization after 0.5 h after SBO initiation has been assumed, while the other assumptions and initial and boundary conditions were the same as for 'SL_LOSS_5 (C1)' scenario. This means that EDG was running 1 h after LOOP initiation followed by SBO and restoration of cooling after 5 h after SBO initiation.

The time trends of main variables used for visual observation are shown in Fig. 14. Fig. 14(a) shows that the depressurization of the RCS through the secondary side was initially efficient for 'SLD_LOSS_5 (C1)' scenario (see also steam generator pressure in Fig. 14(b)). The pressure drops below accumulator's setpoint injection value, resulting in the coolant injection into the primary system, causing the primary mass increase (see Fig. 14(e)). However, due to the secondary side relief valve opening the steam generator inventory is lost faster (see Fig. 14(g)), therefore the heat sink is lost earlier for 'SLD_LOSS_5 (C1)' scenario than for 'SL_LOSS_5 (C1)' scenario. When steam generators have been boiled off around 10000 s for 'SLD_LOSS_5 (C1)' scenario, the primary system starts to repressurize due to the decay heat. When the pressurizer relief valves open, the primary mass decreases faster due to the additional mass discharge through pressurizer relief valves (see Fig. 14(f)), especially when liquid is discharged (pressurizer level at 100% - see Fig. 14(f)). Finally, the core uncovers as shown in Fig. 14(c), shortly followed by the core heatup (see Fig. 14(d)). To prevent the core heatup the cooling of the core through the secondary side should be restored in approximately 4 h or earlier after LOOP occurrence by delivering makeup water to the steam generators. Namely, with depletion of the steam generators the primary and secondary side pressures are decoupled, therefore primary side could not follow the secondary side pressure. Both analysed scenarios ended with the core heatup due to the RCS inventory (primary mass) discharged through the pressurizer relief valves.

Table 12 shows the results of quantitative assessment of sensitivity. The selected SBO scenario is rather sensitive to the operator action of depressurizing the RCS. Nevertheless, due to the large loss of RCS inventory and emptied steam generators the core melt is unavoidable without liquid injection into the RCS. The only source for temporarily RCS injection are the accumulators, when the primary pressure drops below 4.9 MPa. Early steam generator water makeup would provide cooling of the core, and prevent repressurization of RCS. This would at the same time terminate the letdown loss (when RCS pressure is below 4.2 MPa) and by this significantly reduce the RCS inventory loss. More detailed description of deterministic analysis is given in (Prošek and Volkanovski, 2015a). When looking values of AA_m for selected variables, the steam generator pressures seem to be the most influential (this is confirmed by VA_m). This is partly due to the peculiarity of the fast Fourier transform (FFT) transform, in which oscillations cause several harmonics and therefore the sum of amplitudes is larger. For information on how to reduce such effects, one can refer to Prošek and Leskovar (2009). The SBO 'SLD_LOSS' scenario is also very much influenced by integrated pressurizer relief valves flow and primary pressure.

Fig. 15 shows how total average amplitude $AA_{m\text{-}tot}$ changes with increasing time intervals from the beginning of simulation. First discrepancies start when RCS depressurization started at 5400 s in the 'SLD_LOSS_5' scenario. The depressurization strategy influences the transient till the end of simulation at 18700 s.

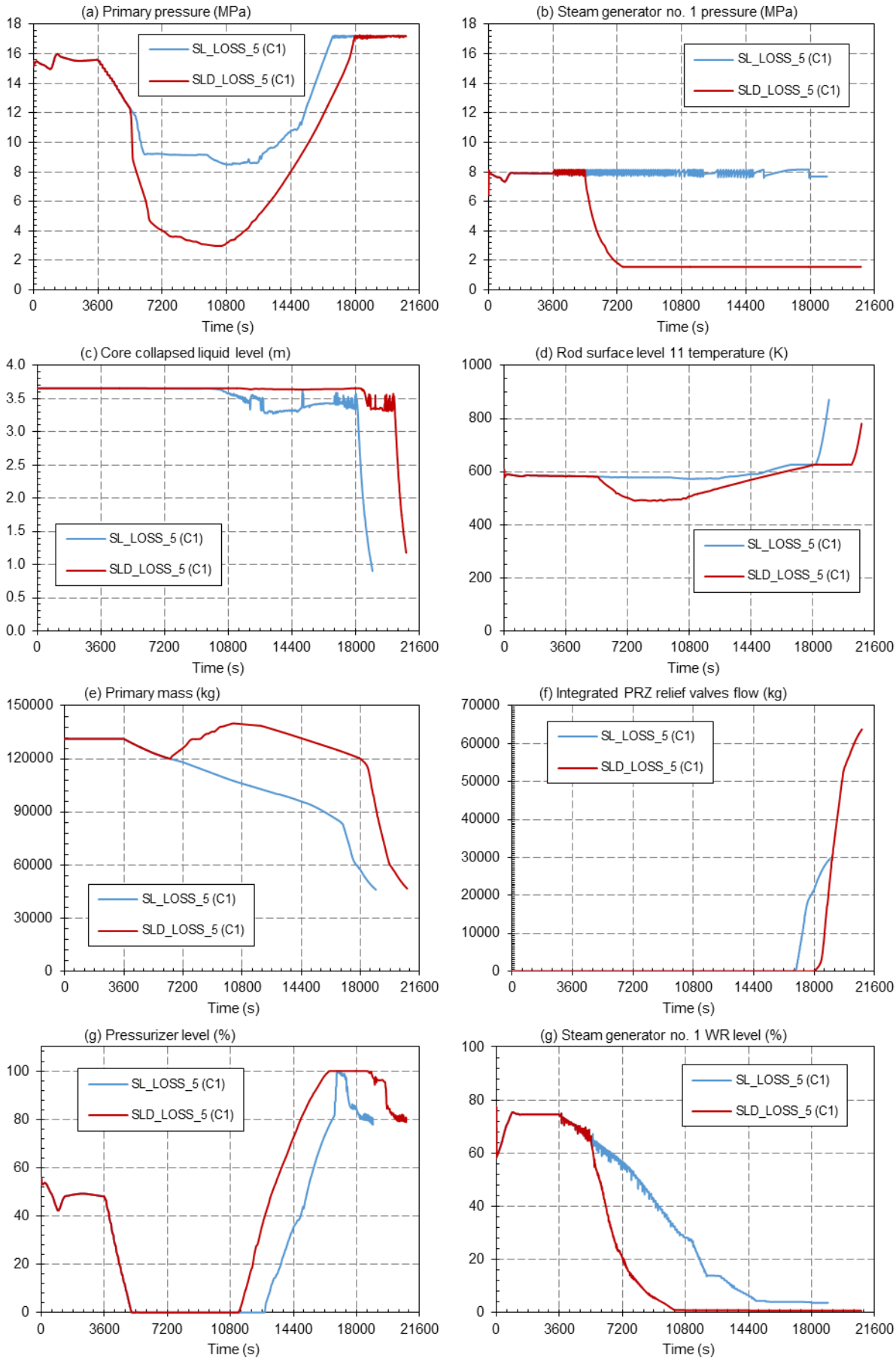

Fig. 14: Time trends of important variables for scenario with the depressurization strategy used 0.5 hour after SBO initiation and with 5 h operator action delay to recover cooling

Table 12: Sensitivity of whole transient to depressurization strategy (0.5 h delay, 'SLD_LOSS_5' scenario)

No.	Variable	time interval 0 – 8600 s	
		AA_m	VA_m
1	Primary pressure	0.619	0.802
2	Core collapsed liquid level	0.518	0.290
3	Primary mass	0.471	0.396
4	Steam generator no. 1 mass	0.529	0.444
5	Steam generator no. 2 mass	0.526	0.442
6	Integrated pressurizer relief valves flow	1.049	0.881
7	Integrated accumulator flow	0.355	0.298
8	Rod surface level 11 temperature	0.342	0.478
9	Steam generator no. 1 pressure	1.354	1.158
10	Steam generator no. 1 wide range level	0.630	0.353
11	Steam generator no. 2 pressure	1.369	1.171
12	Steam generator no. 2 wide range level	0.613	0.343
13	Steam generator no. 1 valves discharge	0.533	0.448
14	Steam generator no. 2 valves discharge	0.528	0.443
15	Cold leg no. 1 liquid temperature	0.290	0.577
16	Cold leg no. 2 liquid temperature	0.300	0.597
17	Hot leg no. 1 liquid temperature	0.214	0.427
18	Hot leg no.2 liquid temperature	0.215	0.427
19	Cold leg no. 1 flow	0.270	0.070
20	Cold leg no. 2 flow	0.295	0.077
21	Pressurizer level	0.642	0.359
	Total	0.499	

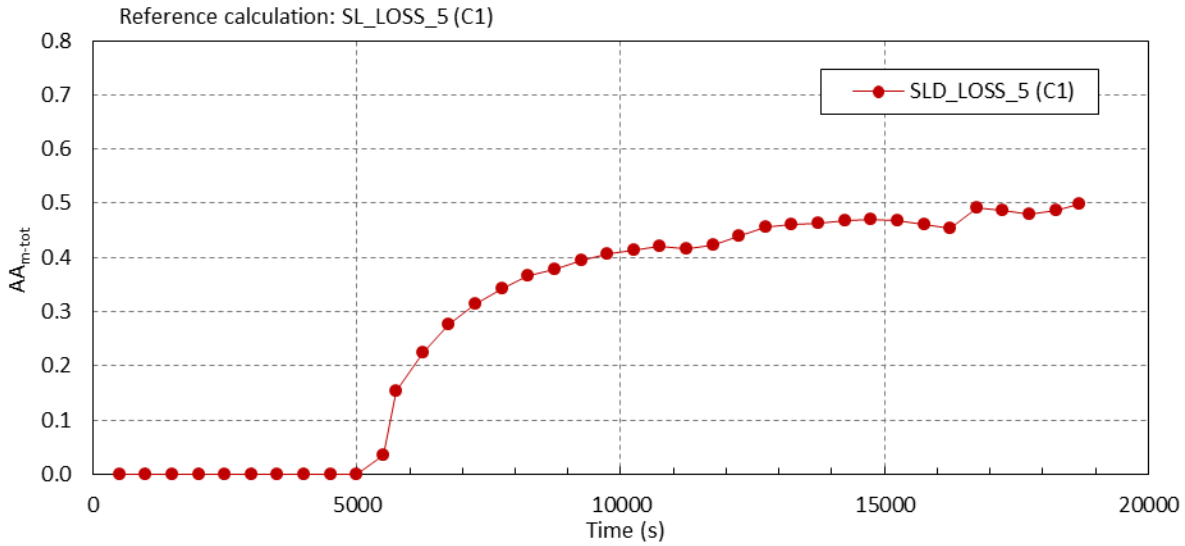

Fig. 15: Code calculation sensitivity (total average amplitude $AA_{m\text{-}tot}$) as a function of increasing time intervals starting at 0 s till 18700 s for scenario with depressurization after 0.5 hour after SBO initiation and with 5 h operator action delay to recover cooling

5.6 Sensitivity to delayed restoration of cooling

In the following two subsections the results of sensitivity cases no. 5 to 10 shown in Table 7 are described, dealing with delayed restoration of cooling influence for scenarios with EDG running 1 h after LOOP initiation (sensitivity cases no. 5, 6 and 7 - C1 case) and for scenarios

with no EDG running (sensitivity cases no. 8, 9 and 10 – C2 case). In the study by Prošek and Volkanovski (2015a) it was found that the reference calculation performed for 24 hours shows that maximum delay of the cooling start, which prevents the core damage, is 4 hours for Case 1 (C1) and 2 hours for Case 2 (C2). Therefore delay times 0.5 hour, 1 hour, 2 hours, 3 hours and 4 hours were considered in the sensitivity cases no. 5, 6 and 7, and delay times 0.5 hour, 1 hour, 2 hours in the sensitivity cases no. 8, 9 and 10, respectively. In the study the calculations prolonged to 72 hours have been used (Prošek and Volkanovski, 2015b), which showed that in the 'S_LOSS_4 (C1)' and 'S_LOSS-2 (C2)' scenarios the core heatup could not be prevented for 72 hours. Regarding 'SL_LOSS' RCS loss type it has been already explained that the core heatup could not be prevented in the first 24 hours without implementing the depressurization strategy.

5.6.1 Scenarios with EDG running 1 h

Sensitivity cases no. 5, 6 and 7 to determine the influence to the delayed restoration of cooling with EDG running 1 h considered three loss types: 'S_LOSS', 'SL_LOSS' and 'SLD_LOSS' (the influence of loss types has already been studied in Section 5.4). In each sensitivity case the reference calculation was the SBO scenario with cooling working all the time (i.e. by feeding the steam generators by passive or mobile equipment to enable heat removal from the primary to the secondary side and by using the steam generator relief valves to transport the heat to the heat sink – the atmosphere), what can be considered also as scenario with no delay (i.e. 0 h) of restoration of cooling. Compared scenarios have time delays in the range of 0.5 h to 4 h. The delay of 5 h has been excluded, as by this time the core is already partially uncovered and further heatup could not be prevented (see above). In the following, for each RCS inventory loss type the results of qualitative (visual observation) and quantitative assessment of sensitivity are presented.

The time trends of main variables for 72 h used for visual observation are shown in Figs. 16, 20 and 22. The main observation from the long term variable trends is that 'SL_LOSS' scenarios progress approximately six times faster than 'S_LOSS' scenarios (proportional to primary mass lost; see also Table 3 – at nominal conditions the letdown leakage is four times larger than RCP seal leakage what means that 'SL_LOSS' scenarios flow is five times larger than 'S_LOSS' scenario flows), but qualitatively are similar. On the other hand, 'SLD_LOSS' scenarios are qualitatively different especially for primary and secondary pressure progression due to the depressurization strategy used, but there are also some similarities. The results of visual observation also showed that in approximately 7 h in all scenarios the variables more or less stabilize, what means that after this time the sensitivity measures will not change much. For this reason, the short term time trends have been also used in the visual observation, when needed (see Figs. 18 and 24).

Sensitivity case no. 5 ('S_LOSS' scenarios for C1)

Sensitivity case no. 5 results of visual observation are shown in Figs. 16 and 18, respectively. The sensitivity measures are shown in Figs. 17 and 19, respectively.

Fig. 16 shows the long term response for 'S_LOSS' scenarios. It can be seen that the primary mass (see Fig. 16(e)) is steadily decreasing and that in the 'S_LOSS_4 (C1)' scenario this caused core uncovery (see Fig. 16(c)) and start of core heatup around 3 h later (see Fig. 16(d)). This time the reason is the primary mass lost in spite of the fact that the heat sink is available (with sufficient steam generator level as shown in Fig. 16(h) and the SG pressure high enough to open the relief valves, releasing the steam which transfer heat to environment – when the SG relief valve is opened the steam is released to the environment, resulting in the pressure drop, which causes valve closure; due to closed valve the generated steam starts again to increase the pressure until the relief valve open and this cycle is repeated and it is seen in Fig. 16(b) as oscillating pressure between the relief valve opening and closure setpoint value – in the following we will call this "oscillating behaviour" of pressure).

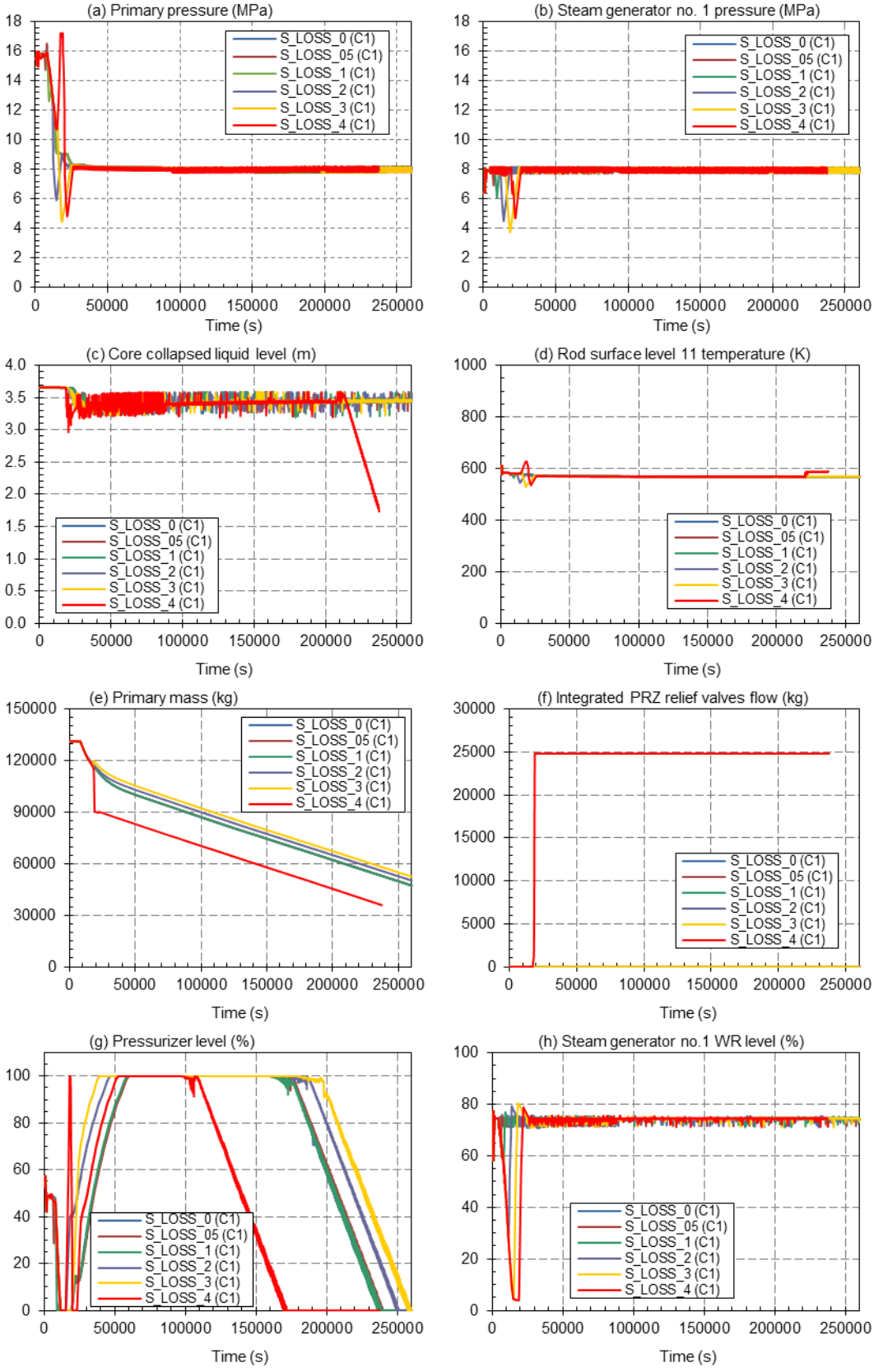

Fig. 16: Time trends of important variables for scenario S_LOSS with EDG running 1 h and varying operator action delay to recover cooling – (interval 0 – 260200 s)

Cooling of the core from the secondary side is important, as it delays the time of the core uncovery, but it cannot prevent the RCS inventory loss, when leaks and breaks are present (injection into primary system would be needed). The available RCS injections are accumulators, but to enable injection, the primary pressure should be below 4.9 MPa.

Fig. 17 shows the sensitivity measures. The change for 'S_LOSS_4 (C1)' scenario at the time of core uncovery start is seen as slight increase after 220000 s until the calculation is not aborted. The core heatup would probably cause further increase of sensitivity measure value as this is the case for the 'SL_LOSS_3 (C1)' scenario in Fig. 13.

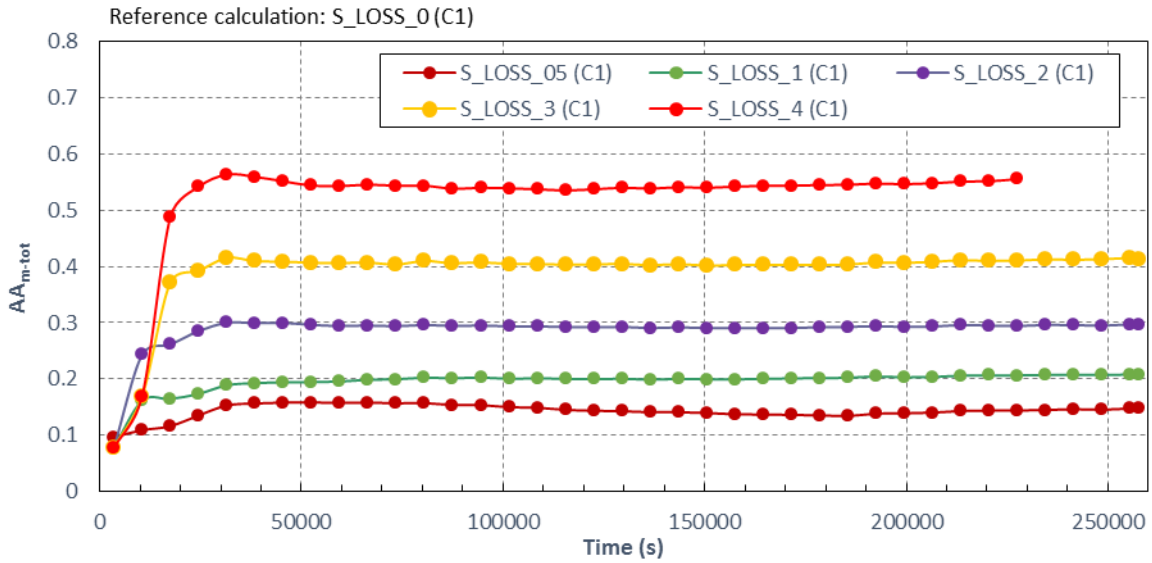

Fig. 17: Code calculation sensitivity (total average amplitude $AA_{m\text{-}tot}$) as a function of increasing time intervals starting at 0 s till 260200 s for scenario S_LOSS with EDG running 1 h – (interval 0 – 260200 s)

The differences in the beginning of the simulated scenarios are better seen from the plots for short term response of 30000 s. Fig. 18 shows that until 5400 s (0.5 h after SBO occurrence) all the time trends are the same. Once the restoration of the cooling (i.e. feeding steam generators) is established at 0.5 h, 1 h, 2 h, 3 h and 4 h after SBO initiation for compared calculations 'S_LOSS_05 (C1)', 'S_LOSS_1 (C1)', 'S_LOSS_2 (C1)', 'S_LOSS_3 (C1)' and 'S_LOSS_4 (C1)', respectively, the primary and secondary pressures shown in Figs. 18(a) and 18(b) started to decrease, when steam generator decreases (and vice versa, when increases). When the steam generator level stabilizes, the secondary pressure also stabilizes at saturation conditions, while primary pressure is steadily decreasing due to losing RCS inventory through the reactor coolant pump seals (see Fig. 18(e)). In case of 'S_LOSS_4 (C1)' scenario the sudden large drop in the primary mass is due to primary mass discharged through the pressurizer relief valves (see Fig. 18(f)). The pressurizer level also increased to 100% during discharging phase (Fig. 18(g)). When steam generator is almost empty in the 'S_LOSS_4 (C1)' scenario, the rod temperature started slowly to rise (see Fig. 18(d)).

The short term quantitative sensitivity results are shown in Fig. 19. Some significant differences started at around 4600 s (i.e. 1 h after LOOP power – SBO start, while first 1000 s are steady state calculations). It can be concluded that each additional delay of cooling restoration further contribute to the sensitivity measure value increase. After 22000 s the sensitivity measure trends more or less stabilize.

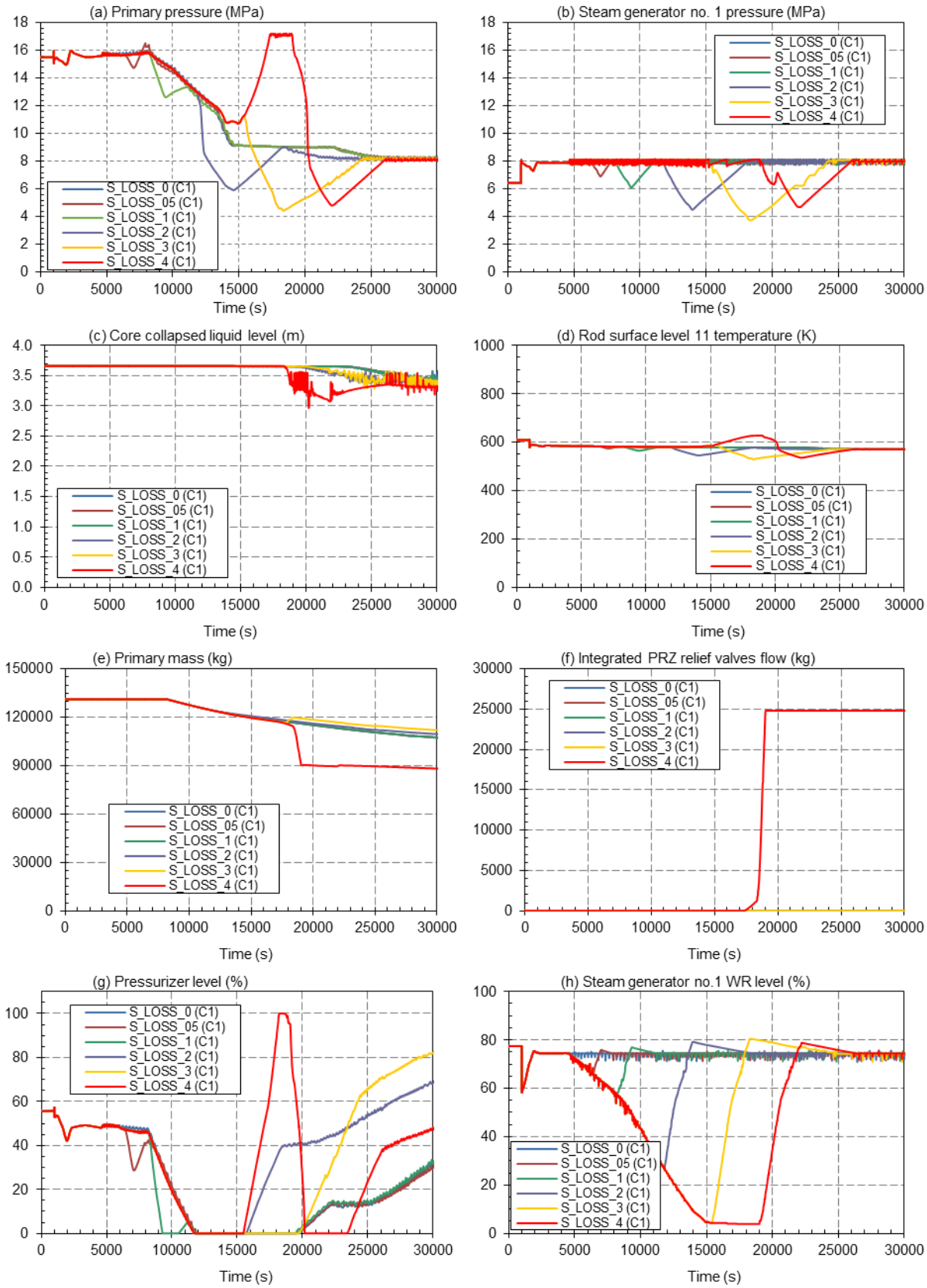

Fig. 18: Time trends of important variables for scenario S_LOSS with EDG running 1 h and varying operator action delay to recover cooling – (interval 0 – 30000 s)

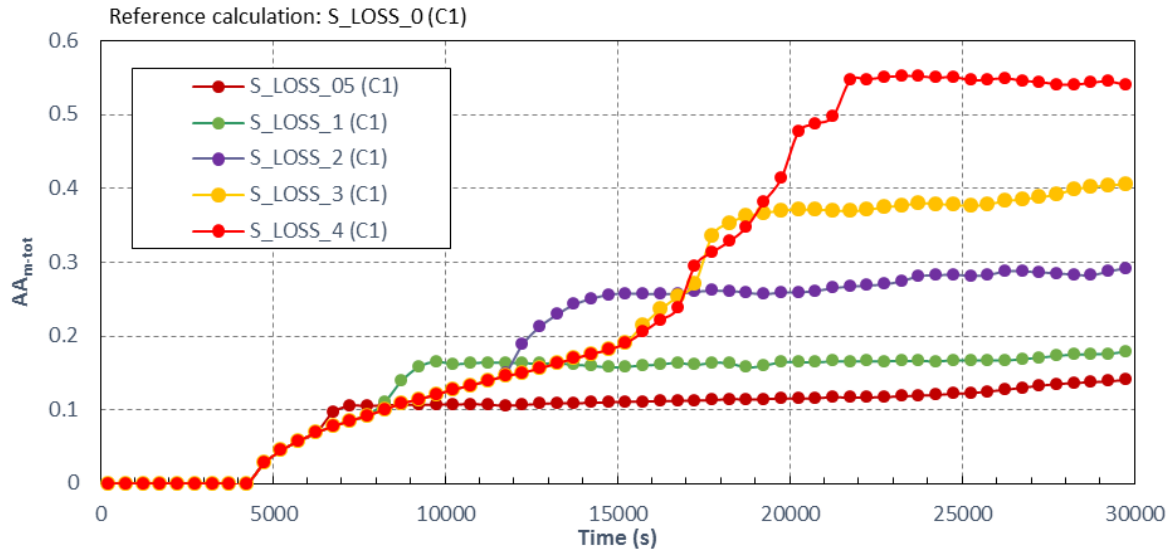

Fig. 19: Code calculation sensitivity (total average amplitude $AA_{m\text{-}tot}$) as a function of increasing time intervals starting at 0 s till 260200 s for scenario S_LOSS with EDG running 1 h – (interval 0 – 30000 s)

Sensitivity case no. 6 ('SL_LOSS' scenarios for C1)

Sensitivity case no. 6 results of visual observation and sensitivity measures are shown in Figs. 20 and 21, respectively.

Fig. 20 shows the response for 'SL_LOSS' scenarios. The plant response is different compared to 'S_LOSS' scenarios due to the faster primary mass discharge, resulting in faster core uncovery and also in the larger pressure drop, resulting in the accumulator injection into the primary system for 'SL_LOSS_2 (C1)', 'SL_LOSS_3 (C1)' and 'SL_LOSS_4 (C1)' scenarios. Besides this, the transient progression is qualitatively similar in the short term. On the secondary side the plant response is practically the same for 'SL_LOSS' and 'S_LOSS' scenarios (see the steam generator pressure in Fig. 12(b) and steam generator wide range levels in Fig. 12(h) comparing different RCS loss types). Once the restoration of cooling (i.e. feeding steam generators) is established at 0.5 h, 1 h, 2 h, 3 h and 4 h after SBO initiation for compared calculations 'SL_LOSS_05 (C1)', 'SL_LOSS_1 (C1)', 'SL_LOSS_2 (C1)', 'SL_LOSS_3 (C1)' and 'SL_LOSS_4 (C1)', respectively, the primary and secondary pressures shown in Figs. 20(a) and 20(b) started to decrease, when steam generator decreases (and vice versa, when increases). When the primary pressure is below 4.9 MPa, the accumulators are injected. When the steam generator level stabilizes, the secondary pressure stabilizes at saturation conditions (having "oscillating behaviour") and the RCS is also at saturation conditions. After accumulator injection the primary mass is steadily decreasing due to losing the RCS inventory through the reactor coolant pump seals and open letdown relief valve (see Fig. 20(e)). In the case of 'S_LOSS_4 (C1)' scenario the drop of the primary mass is due to the mass discharged through the pressurizer relief valves (see Fig. 20(f)). The pressurizer level is at 100% during discharging phase (Fig. 20(g)). When steam generator is almost empty for 'SL_LOSS_4 (C1)' scenario, the rod temperature started slowly to rise (see Fig. 20(d)). The plant stabilizes at 30000 s, except steadily losing the primary mass. This resulted in the core uncovery start at 36000 s and subsequent core heat at around 38500 s. Also in other scenarios due to the continuous mass discharge core uncovery is unavoidable.

The quantitative sensitivity results in Fig. 21 show that some significant influences of delayed restoration of cooling started at SBO start at 4600 s. It can be concluded that each delay additionally contributes to the sensitivity measure value increase. After 23000 s the sensitivity measure trends more or less stabilize. The sensitivity results are very similar to 'S_LOSS' scenarios, except that for 'SL_LOSS_3 (C1)' and 'SL_LOSS_4 (C1)' scenarios the sensitivity measures are a bit higher than for 'S_LOSS_3 (C1)' and 'S_LOSS_4 (C1)' scenarios.

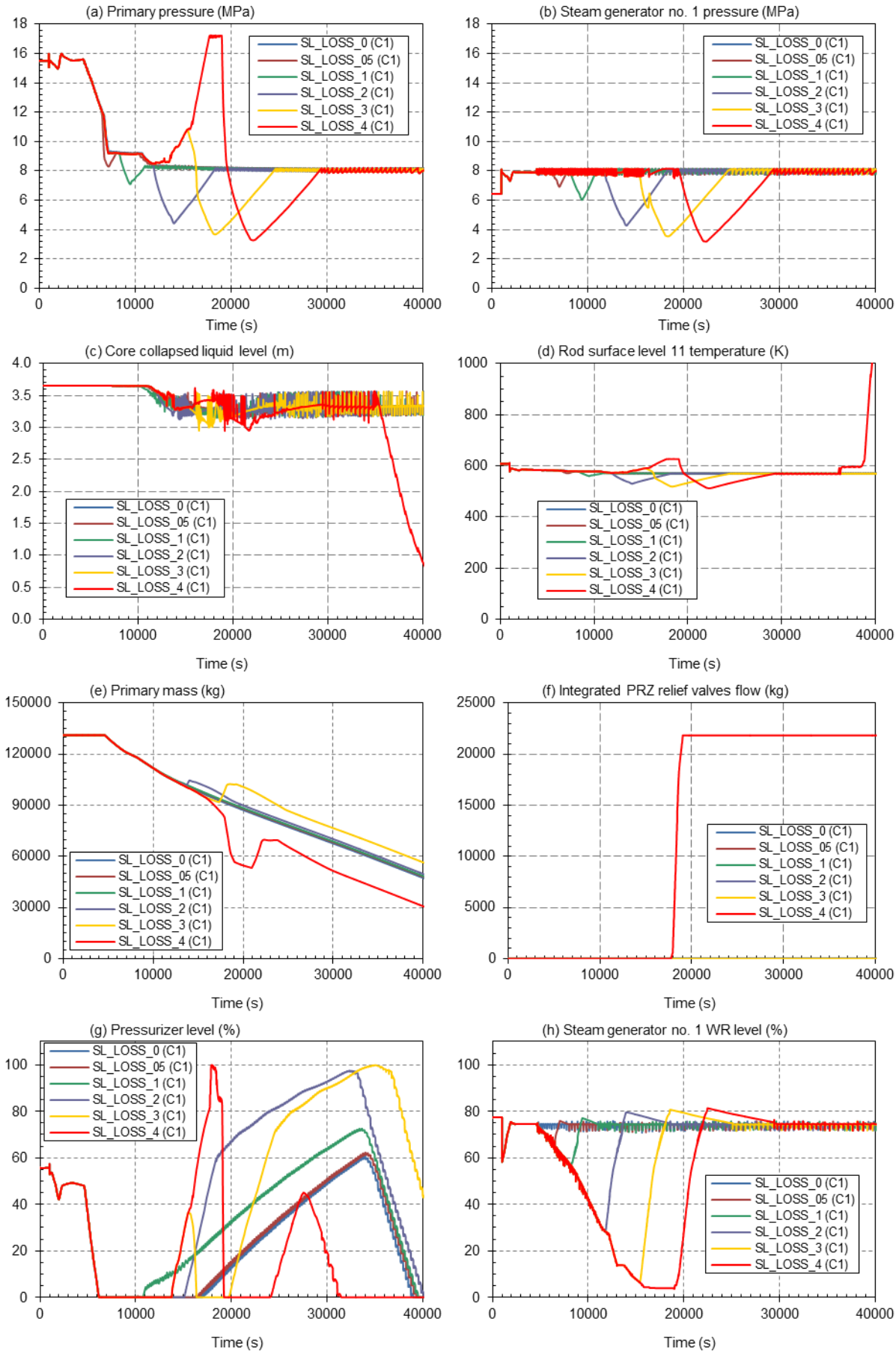

Fig. 20: Time trends of important variables for scenario SL_LOSS with EDG running 1 h and varying operator action delay to recover cooling

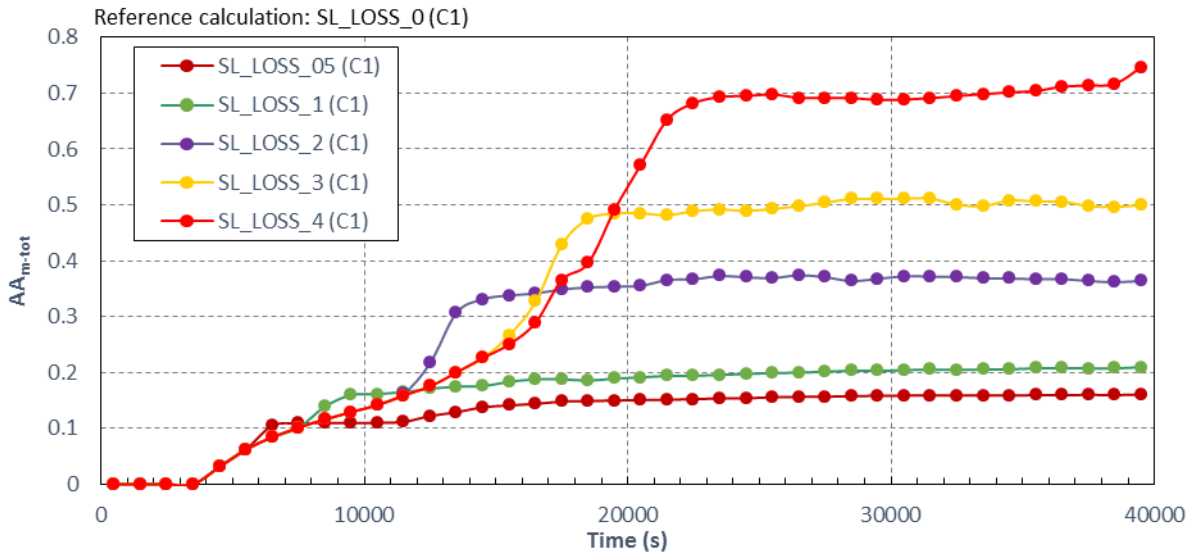

Fig. 21: Code calculation sensitivity (total average amplitude $AA_{m\text{-}tot}$) as a function of increasing time intervals starting at 0 s till 40000 s for scenario SL_LOSS with EDG running 1 h

Sensitivity case no. 7 ('SLD_LOSS' scenarios for C1)

Sensitivity case no. 7 results of visual observation are shown in Figs. 22 and 24, respectively. The sensitivity measures are shown in Figs. 23 and 25, respectively.

Fig. 22 shows the plots for visual observation of 'SLD_LOSS' scenarios. The plant response is different compared to 'SL_LOSS' scenarios due to depressurization of the primary system through secondary side depressurization. By depressurizing the primary system below the letdown relief valves opening setpoint, the valve closed and the discharge through the valve is terminated, the mass loss through the reactor coolant pumps is reduced too and the accumulator injection is enabled. Two accumulators store 70 m^3 of water, what represents slightly more than half of the primary mass. Therefore, all 'SLD_LOSS' scenarios survive 72 h period with core heating. Because of depressurization the secondary pressure drops (see Fig. 22(b)), causing primary pressure decrease shown in Fig. 22(a). The pressure increase in 'SLD_LOSS_5' scenario is due to the loss of heat sink (see Fig. 22(h)), the core partially uncover (see Fig. 22(c)) and the core heated up in that period (see Fig. 22(e)). When heat sink is established by feeding steam generators, the pressure drops again. After 50000 s most of variables are more or less stable, except decreasing primary mass (see Fig. 22(e)).

The sensitivity of SBO scenario calculations is shown in Fig. 23. After 20000 s the sensitivity measures stabilize. The larger is the time delay of cooling restoration, the larger is the sensitivity measure.

To see more in the detail the difference between scenarios with varied delay of cooling restoration, visual observation of variables has been done in the time interval 0 - 25000 s (see Fig. 24). The primary pressure starts to increase at 12000 s (see Fig. 24(a)), because the steam generator level shown in Fig. 24(h) is so low that heat transfer from primary to secondary side is terminated. The primary pressure increases until 19000 s, when the heat sink was restored by feeding steam generator. The core temperature decreased again.

The quantitative sensitivity results for short term are shown in Fig. 25. After 12000 s there are significant deviations of 'SLD_LOSS_4' and 'SLD_LOSS_5' scenarios results from reference 'SLD_LOSS_0' scenario due to significantly delayed restoration of cooling. After 21000 s all sensitivity measures stabilize.

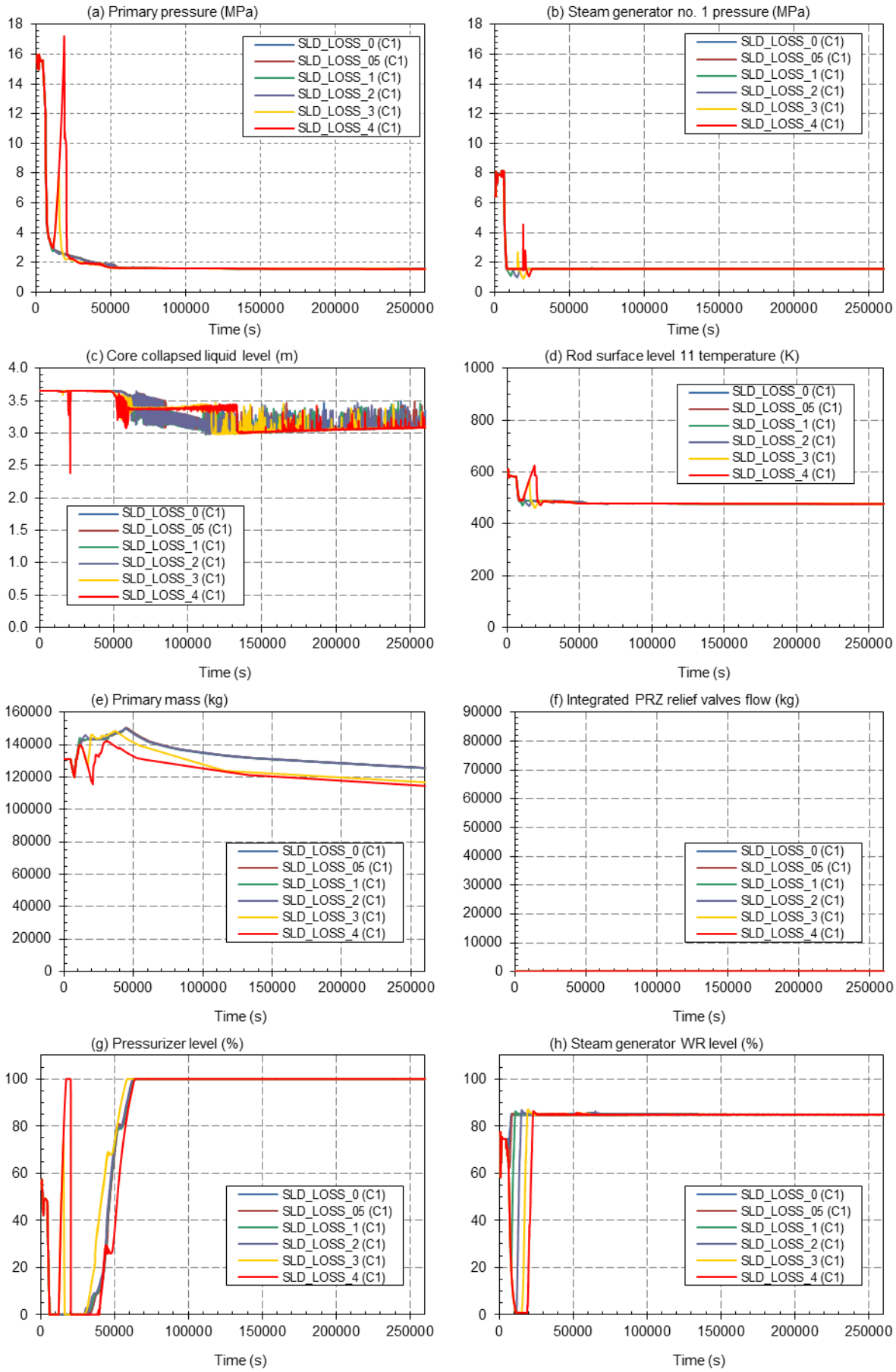

Fig. 22: Time trends of important variables for scenario SLD_LOSS with EDG running 1 h and varying operator action delay to recover cooling

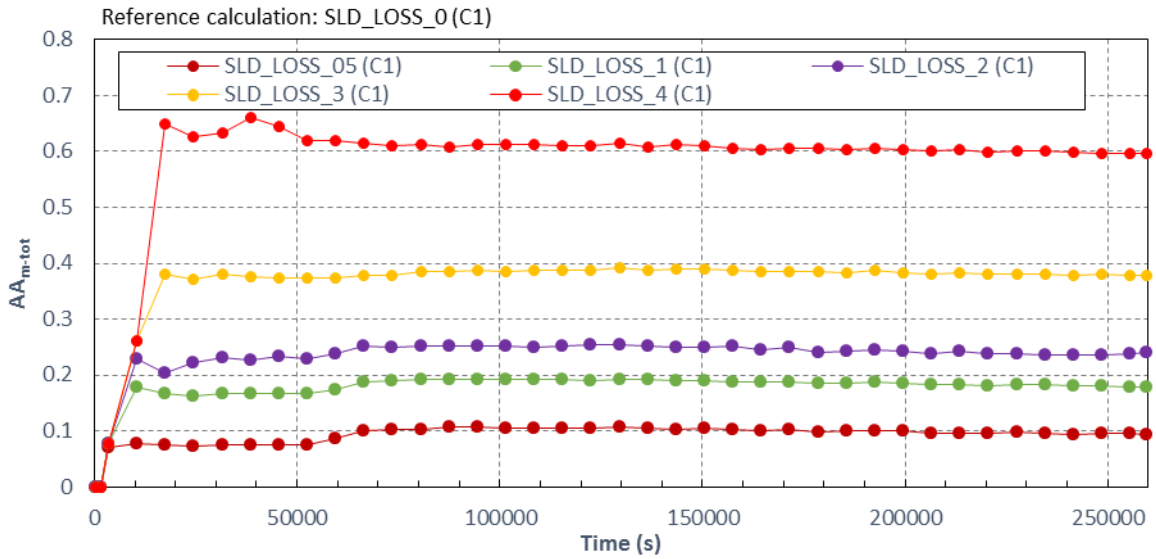

Fig. 23: Code calculation sensitivity (total average amplitude $AA_{m\text{-}tot}$) as a function of increasing time intervals starting at 0 s till 260200 s for scenario SLD_LOSS with EDG running 1 h

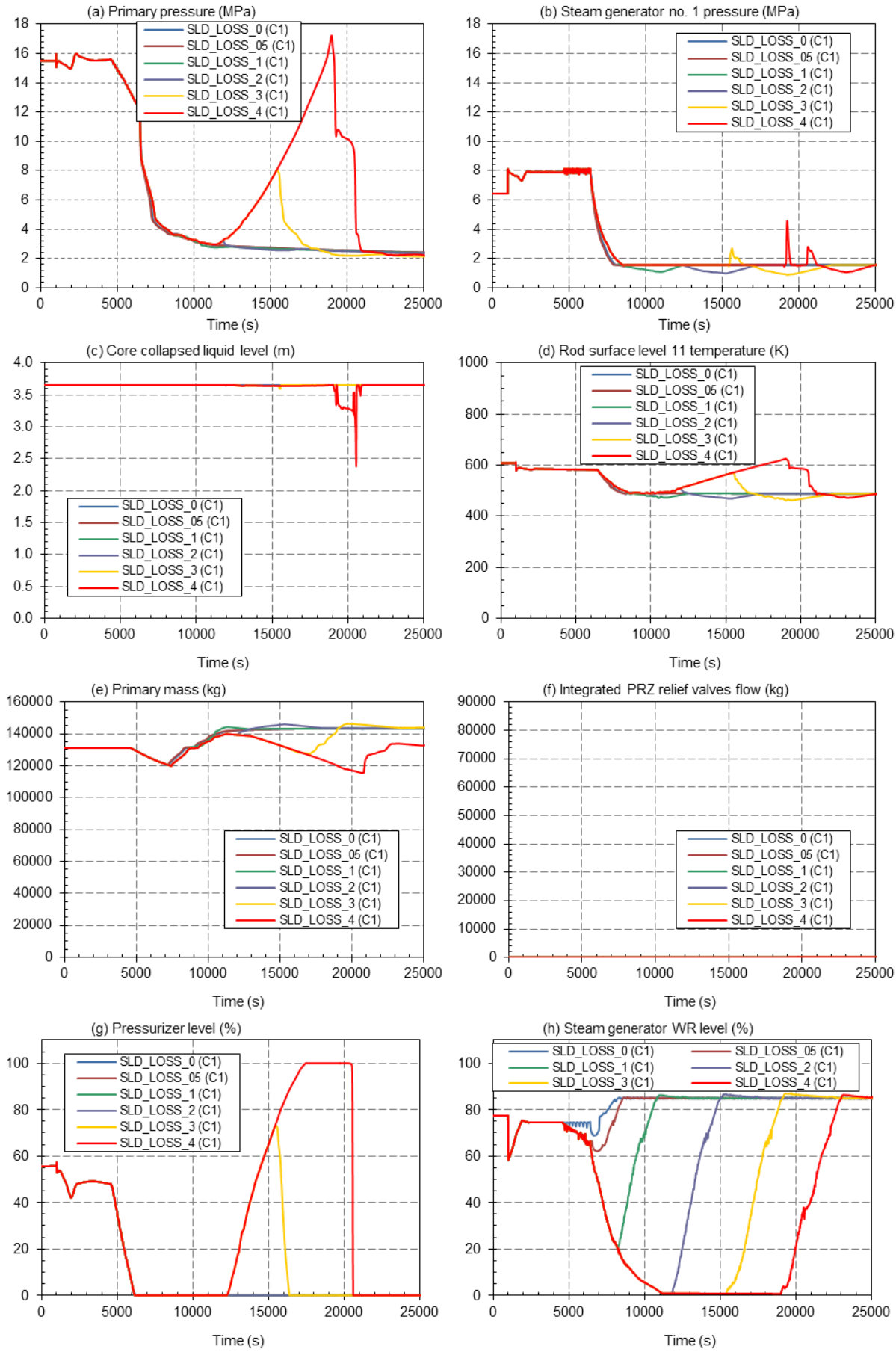

Fig. 24: Time trends of important variables for scenario SLD_LOSS with EDG running 1 h and varying operator action delay to recover cooling – (interval 0-25000 s)

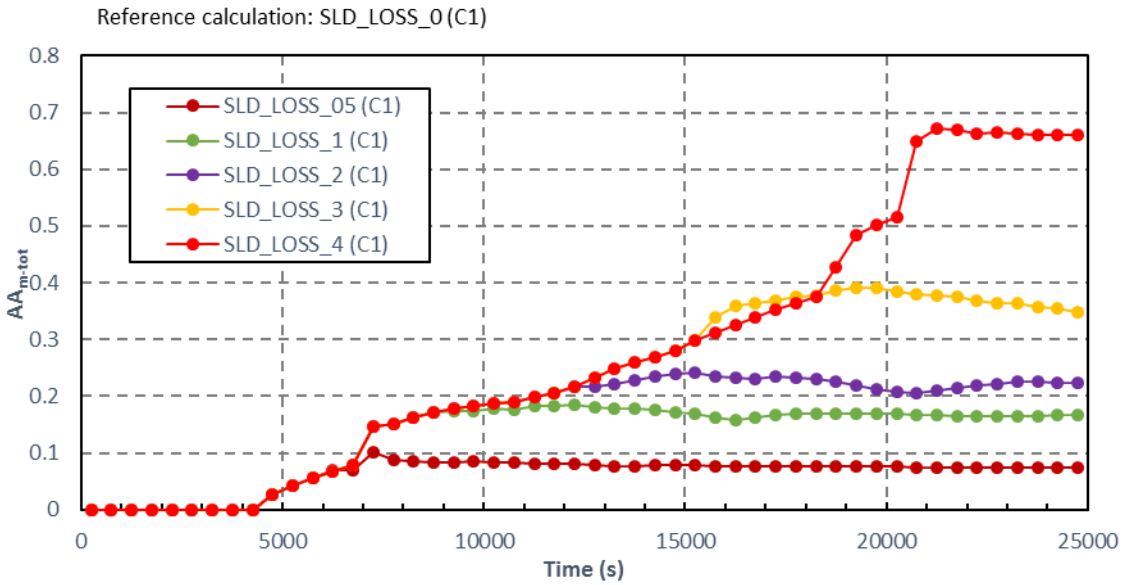

Fig. 25: Code calculation sensitivity (total average amplitude $AA_{m\text{-}tot}$) as a function of increasing time intervals starting at 0 s till 25000 s for scenario SLD_LOSS with EDG running 1 h

5.6.2 Scenarios with EDG not running

Sensitivity cases to determine the influence to the delayed restoration of cooling with EDG not running considered three loss types: 'S_LOSS', 'SL_LOSS' and 'SLD_LOSS'. In each sensitivity case the reference calculation is the SBO scenario with cooling working all the time (can be considered also as scenario with 0 h delay of restoration of cooling). Compared calculations have time delays in the range of 0.5 h to 2 h. The delay of 3 h has been excluded, as at this time the core is already partially uncovered and further heatup could not be prevented as explained in Section 5.6. In the following, for each loss type the results of visual observation and quantitative assessment of sensitivity are presented.

Sensitivity case no. 8 ('S_LOSS' scenarios for C2)

Sensitivity case no. 8 results of long and short term visual observation are shown in Figs. 26 and 28, respectively. Sensitivity measures are shown in Figs. 27 and 29.

Visual observation based on Fig. 26 showed that all scenarios except 'S_LOSS_2 (C2)' survive the SBO without core heatup in the first 72 h, that primary mass is steadily decreasing and that after 20000 s all shown variables are more or less stable. The primary pressure drops to saturation pressure (see Fig. 26(a)) and is slightly above the steam generator no. 1 pressure, having "oscillating behaviour" (see Fig. 26(b)). For more details the visual observation in shorter time interval is needed.

The sensitivity measures are shown in Fig. 27. All the changes occurred in the beginning of transient lasting 72 hours, as after 10000 s the sensitivity measures are practically constant. This means that delayed time of cooling restoration had an influence in the first hours of SBO scenario.

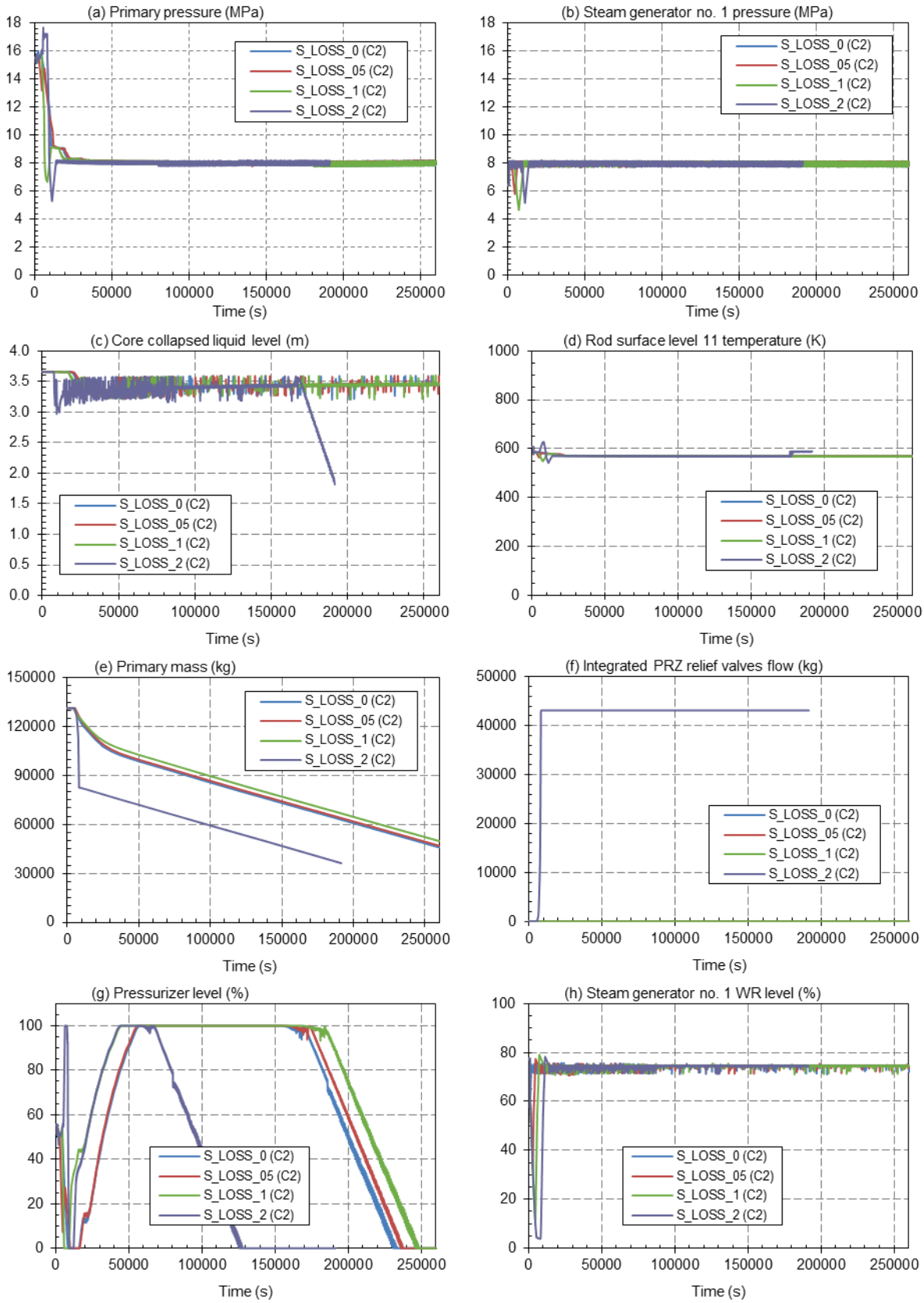

Fig. 26: Time trends of important variables for scenario S_LOSS with EDG not running and varying operator action delay to recover cooling – (interval 0 – 260200 s)

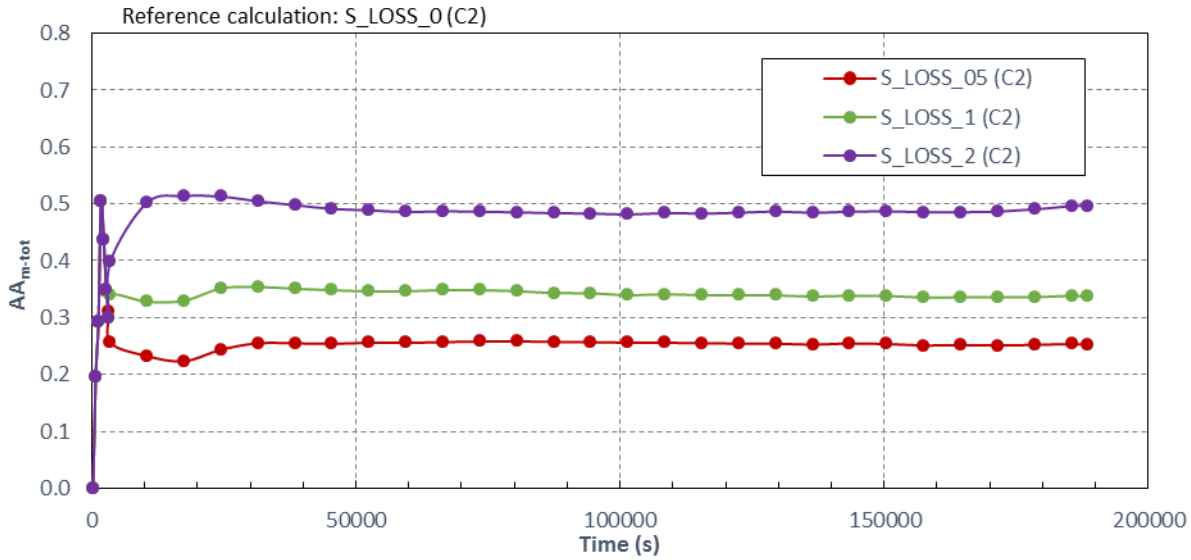

Fig. 27: Code calculation sensitivity (total average amplitude $AA_{m\text{-}tot}$) as a function of increasing time intervals starting at 0 s till 260200 s for scenario S_LOSS with EDG not running

Short term visual observation (based on Fig. 28) in the time interval 0 – 20000 s showed that in all but 'S_LOSS_2 (C2)' scenario the heat sink is available (see steam generator no. 1 level in Fig. 28(h)). The primary and secondary pressure shown in Figs. 28(a) and 28(b) started to decrease, when steam generator level decreases (and vice versa, when increases). When the steam generator levels stabilize, the secondary pressures also stabilize at saturation conditions (having "oscillating behaviour"), while primary system masses are steadily decreasing due to losing RCS inventory through the reactor coolant pump seals (see Fig. 28(e)). In the 'S_LOSS_2 (C2)' scenario due to loss of heat sink the primary system heats up, causing pressure increase until pressurizer relief valve opening setpoint is reached, causing valve opening. Much of primary mass was discharged through the valve, causing slight core heatup. After the cooling was restored, the heatup was terminated. Nevertheless, as shown in Fig. 26(c)), after 170000 s the core starts to uncover again due to the low content of primary mass.

The sensitivity measures are shown in Fig. 29. All the changes occurred between 4000 s and 9000 s, and after 10000 s the sensitivity measures are almost constant. This means that delayed times of cooling restoration have an influence in the first 3 hours of SBO scenario. The influence of delayed restoration time in the 'S_LOSS' scenarios with EDG not running is larger than in the 'S_LOSS' scenarios with EDG running 1 h.

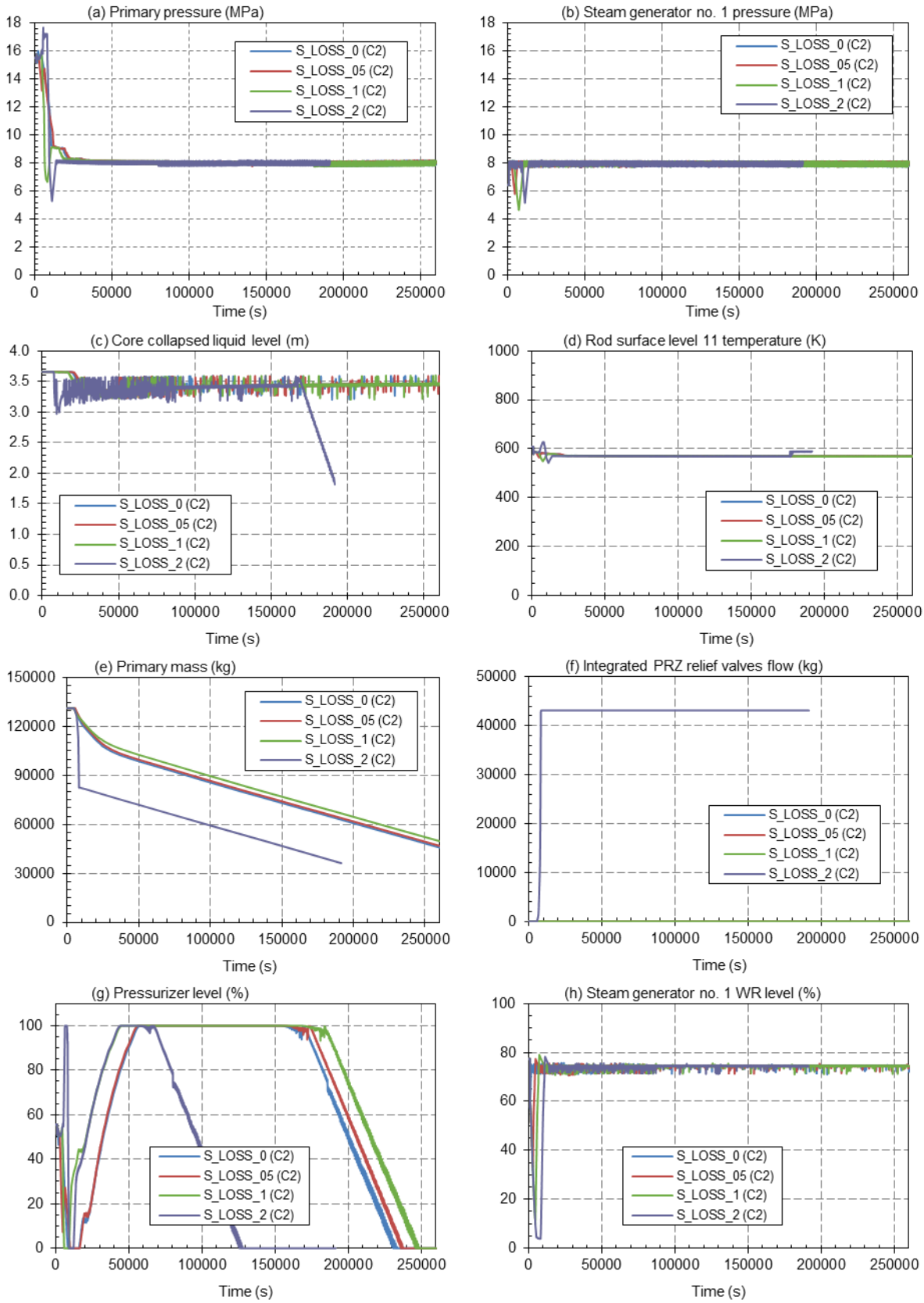

Fig. 28: Time trends of important variables for scenario S_LOSS with EDG not running and varying operator action delay to recover cooling – (interval 0 – 20000 s)

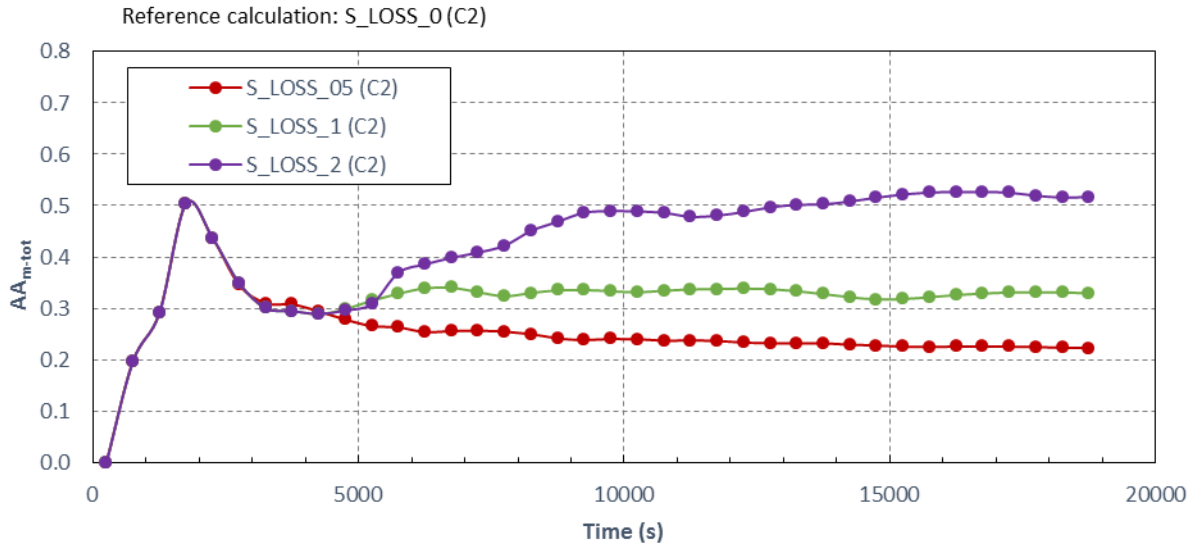

Fig. 29: Code calculation sensitivity (total average amplitude $AA_{m\text{-}tot}$) as a function of increasing time intervals starting at 0 s till 20000 s for scenario S_LOSS with EDG not running

Sensitivity case no. 9 ('SL_LOSS' scenarios for C2)

Sensitivity case no. 9 results of visual observation and sensitivity measures are shown in Figs. 30 and 31, respectively. Visual observation based on Fig. 30 showed that none of the scenarios could survive the SBO without core heatup for 72 h. The primary system mass in the 'SL_LOSS' scenarios is decreasing fast comparing to 'S_LOSS' scenarios due to additional letdown relief valve loss flow. In the case of the 'SL_LOSS_2 (C2)' scenario the heat sink is lost (see Fig. 30(h)) at around 5000 s, therefore primary side starts to heat up what resulted in the primary pressure increase (see Fig. 30(a)). When the primary pressure reached the pressurizer relief valve opening setpoint, the relief valve opens, resulting in the primary mass discharge (see Fig. 30(f)). At the time of discharging the pressurizer level increases too (this is an indication of release and not filling the primary system). When heat sink is established, the primary pressure dropped and the pressurizer relief valve closed at around 8000 s. The primary and secondary side pressures shown in Figs. 30(a) and 30(b) started to decrease, when the steam generator level decreases (and vice versa, when increases). When the steam generator level stabilizes, the primary and secondary pressures (having "oscillating behaviour") also stabilize at saturation conditions, while the primary system mass is steadily decreasing due to losing RCS inventory through the reactor coolant pump seals and letdown relief valve (see Fig. 30(e)). The core uncovers first in the 'SL_LOSS_2 (C2)' scenario due to the loss of the primary mass through the pressurizer relief valves, while in other scenarios this occurred around 5 hours later. This means that 35000 kg of primary mass would be sufficient to prolong the SBO coping time for approximately another 5 hours.

The sensitivity measures are shown in Fig. 31. All the significant changes in the sensitivity values occurred between 3000 s and 15000 s, and after 15000 s the sensitivity measures are almost constant until the core heatup. This means that the delayed time of cooling restoration influences in the first 4 hours of 'SL_LOSS', Case 2 scenarios. Then the values of sensitivity measures started to rise, but the calculation of sensitivity measures is terminated due to not available data for reference calculation. The influence in the scenarios with EDG not running is larger and happen faster than in the 'S_LOSS' scenarios with EDG running 1 h (see Fig. 19).

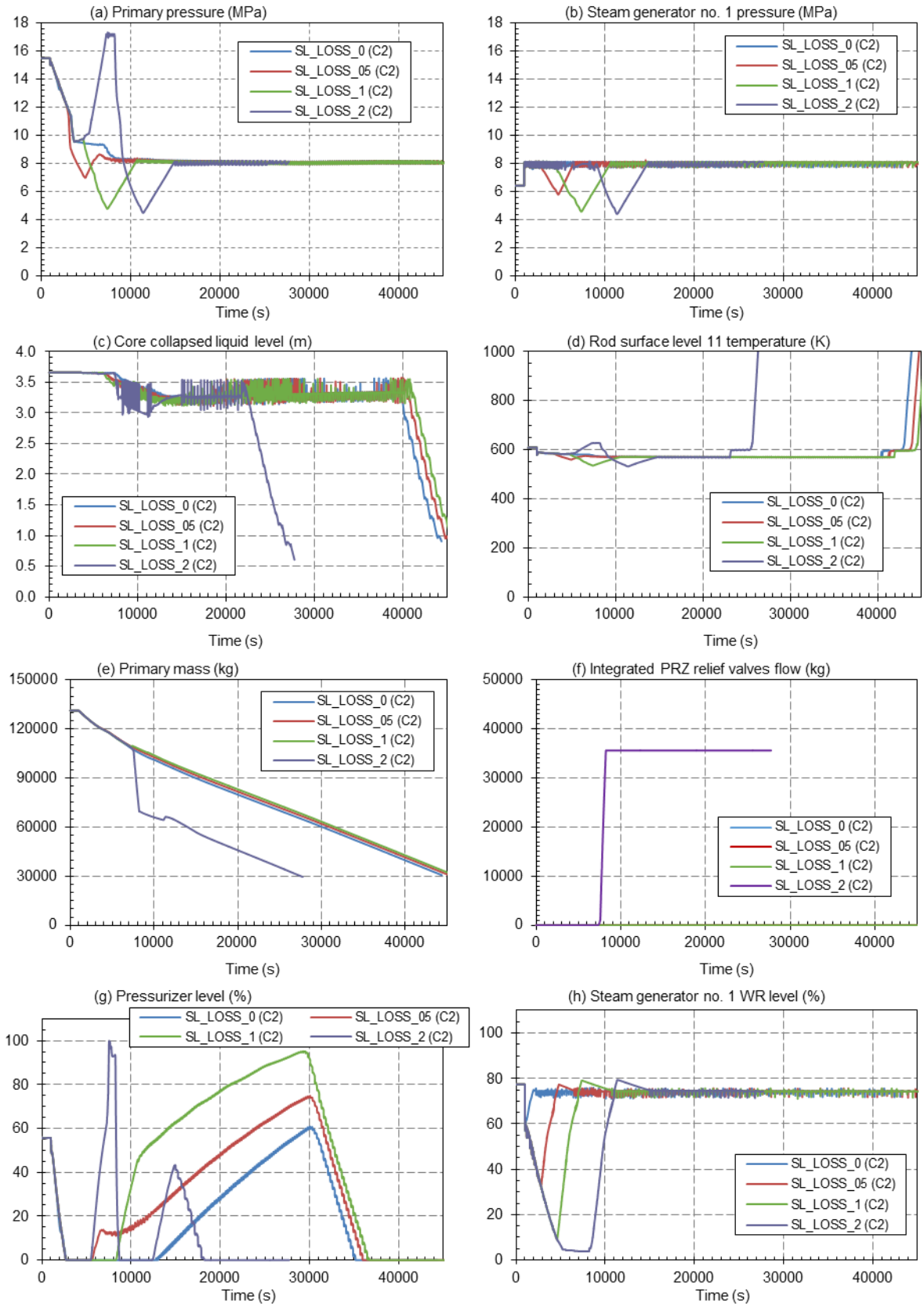

Fig. 30: Time trends of important variables for scenario SL_LOSS with EDG not running and varying operator action delay to recover cooling

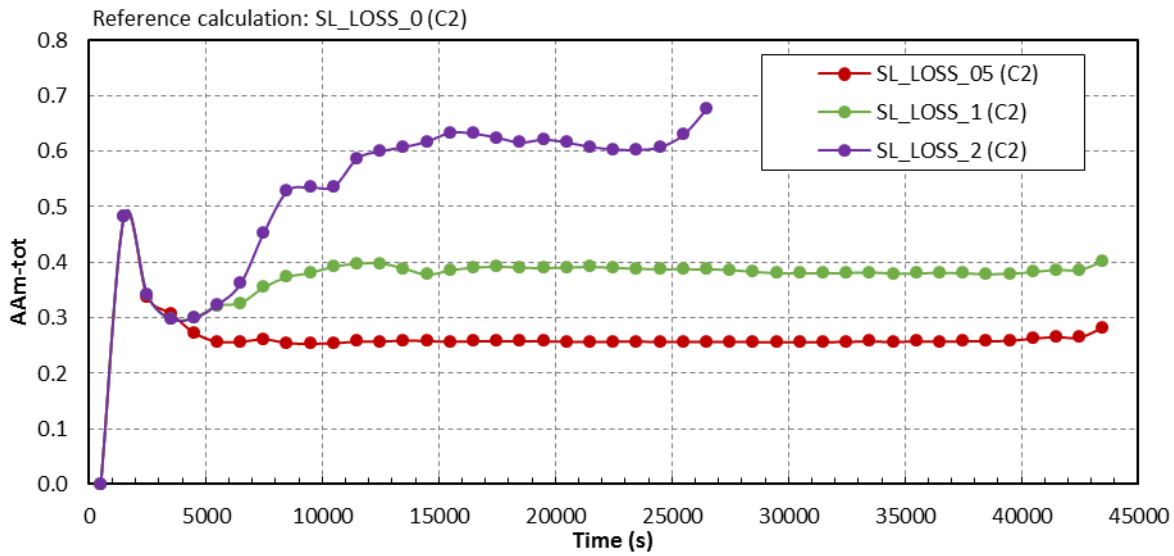

Fig. 31: Code calculation sensitivity (total average amplitude $AA_{m\text{-}tot}$) as a function of increasing time intervals starting at 0 s till 44000 s for scenario SL_LOSS with EDG not running

Sensitivity case no. 10 ('SLD_LOSS' scenarios for C2)

Sensitivity case no. 10 results of long and short term visual observation are shown in Figs. 32 and 34, respectively. Long and short term analysis results of sensitivity measures are shown in Figs. 33 and 35, respectively.

Visual observation based on Fig. 32 showed that all three scenarios with timely performed operator actions survive the SBO without the core heatup in the first 72 h. The primary system mass after accumulators are emptied, is steadily decreasing as shown in Fig. 32(e). In the 'SLD_LOSS_2 (C2)' scenario in the initial hours much of primary system mass was additionally lost through the pressurizer relief valves due to the increased primary pressure resulting from primary system heatup due to temporary lost heat sink. After 50000 s all shown variables are more or less stable. Also after 72 h the remaining primary system mass is sufficient for another few days in the 'SLD_LOSS_05 (C2)' and 'SLD_LOSS_1 (C2)' scenarios. This example clearly showed the importance of primary system depressurization strategy, which provides additional inventory injection by accumulators (when primary pressure below 4.9 MPa), at the same time it terminates the letdown loss (when primary pressure is below 4.2 MPa) and due to lower primary pressure also reactor coolant pump seal break flow reduces. All these contribute to significantly less primary mass lost.

The primary pressure (see Fig. 32(a)) dropped to the value slightly above the steam generator relief valves set pressure for opening, which is 1.57 MPa and maintains the steam generator no. 1 pressure at this value (see Fig. 32(b)). For other details visual observation in the shorter time interval has been performed.

Because the performed variation of delay time for cooling the most influences the first few hours of SBO scenarios, the visual observation and quantitative assessment of sensitivity has been performed for smaller time interval 0 – 20000 s. It should be noted, that the original FFTBM has been developed to evaluate phenomenological time windows only and its applications very rarely exceed five time windows (Prošek et al., 2002). Typical SBO analyses last few hours (for example, in the study by Saghafi et al., (2016), 15000 s have been considered and five time windows were selected for quantitative analysis by FFTBM). On the other hand, the FFTBM-SM has been improved in this respect to increase the number of time intervals to be considered, which are needed to calculate time dependent sensitivity measures.

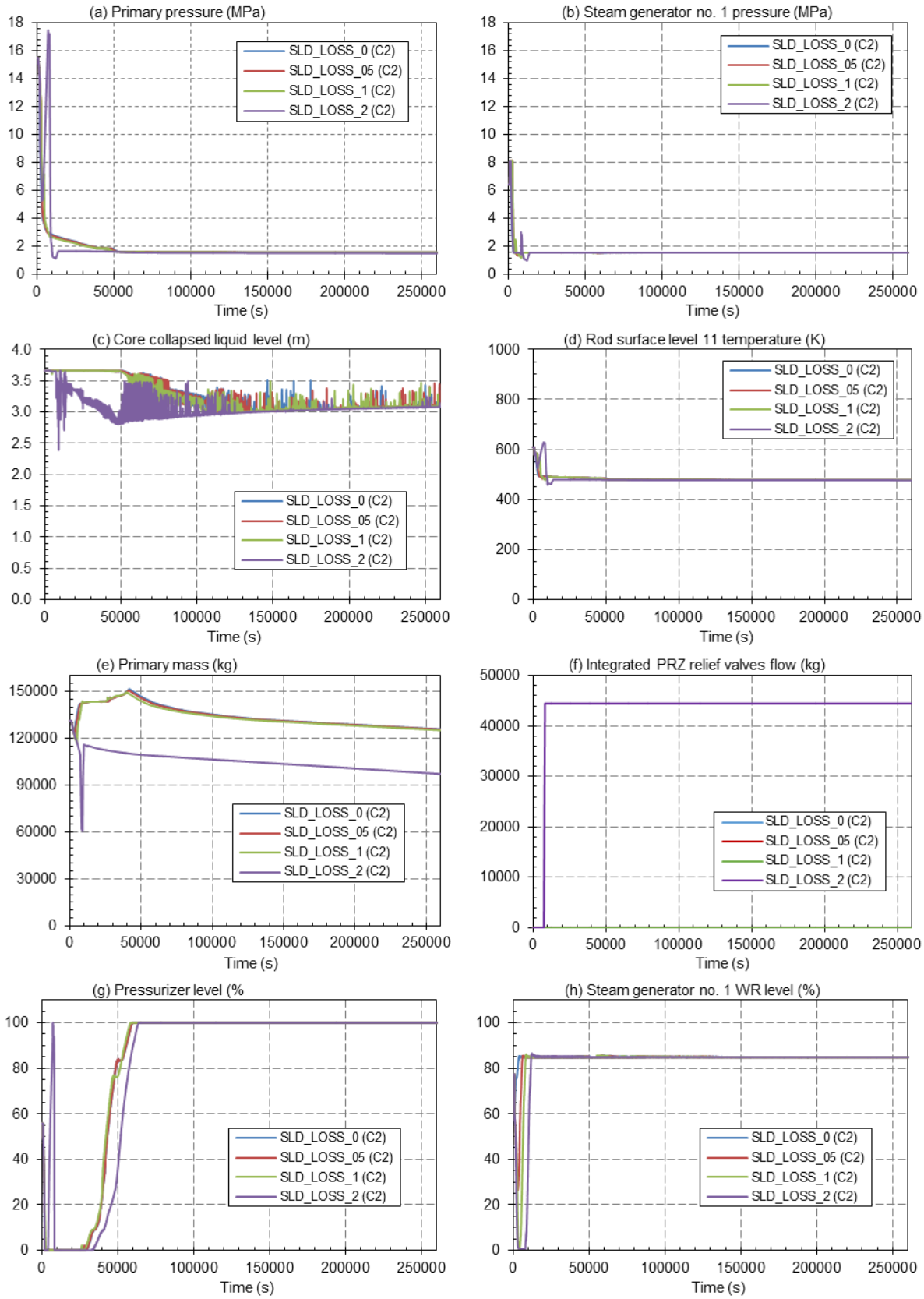

Fig. 32: Time trends of important variables for scenario SLD_LOSS with EDG not running and varying operator action delay to recover cooling – interval (0 – 260200 s)

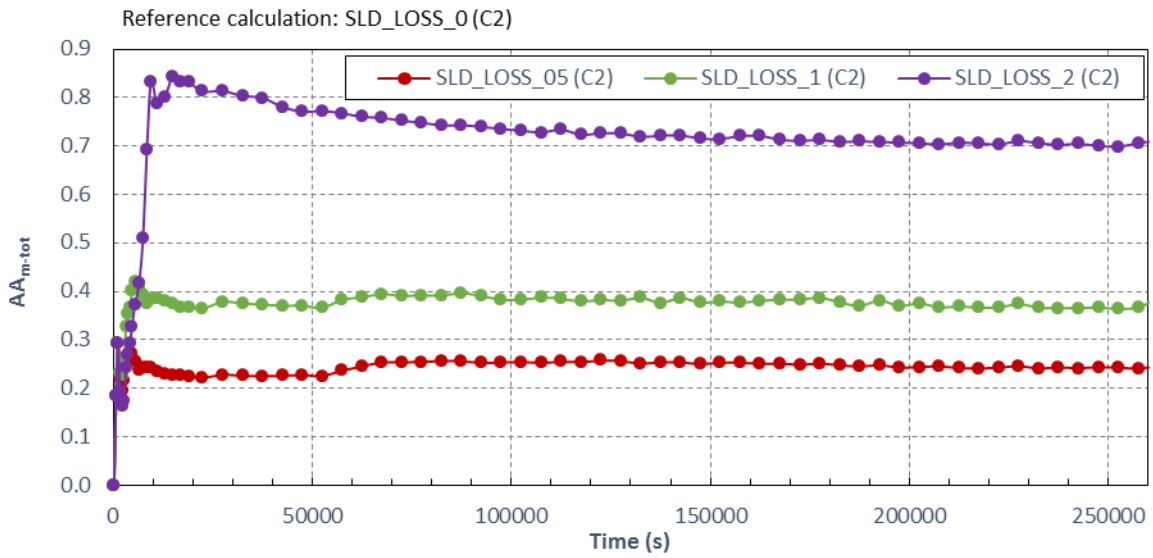

Fig. 33: Code calculation sensitivity (total average amplitude $AA_{m\text{-}tot}$) as a function of increasing time intervals starting at 0 s till 260200 s for scenario SLD_LOSS with EDG not running

Short term visual observation (based on Fig. 34) in the time interval 0 – 20000 s showed that in the 'SLD_LOSS_1 (C2)' and 'SLD_LOSS_2 (C2)' scenarios the heat sink is lost for some time (see steam generator wide range no. 1 level in Fig. 34(h)). The primary and secondary pressures shown in Figs. 34(a) and 34(b) started to decrease, when the steam generator level started to decrease and further drops 1800 s after the SBO start, when the depressurization is started. When the steam generator level stabilizes, the secondary pressure also stabilizes at saturation conditions, while primary pressure is steadily decreasing due to losing RCS inventory through the reactor coolant pump seals (see Fig. 34(e)). In 'SLD_LOSS_2 (C2)' due to loss of heat sink the primary system heats up, causing pressure increasing until pressurizer relief valve opens. Much of primary mass was discharged through the valve, causing slight core heatup. After the cooling was restored, the heatup was terminated. But as shown in Fig. 34(c)), after approximately 70000 s the core starts to uncover due to low primary mass, causing some rod surface temperature increase until the cooling has not been restored.

The sensitivity measures are shown in Fig. 35. All the changes occurred between 4000 s and 9000 s, and after 10000 s the sensitivity measures are almost constant. This means that the delayed time of restoration influences in the first 3 hours of SBO scenarios. The influence in the 'SLD_LOSS' scenarios with EDG not running is larger than in 'SLD_LOSS' scenarios with EDG running 1 h.

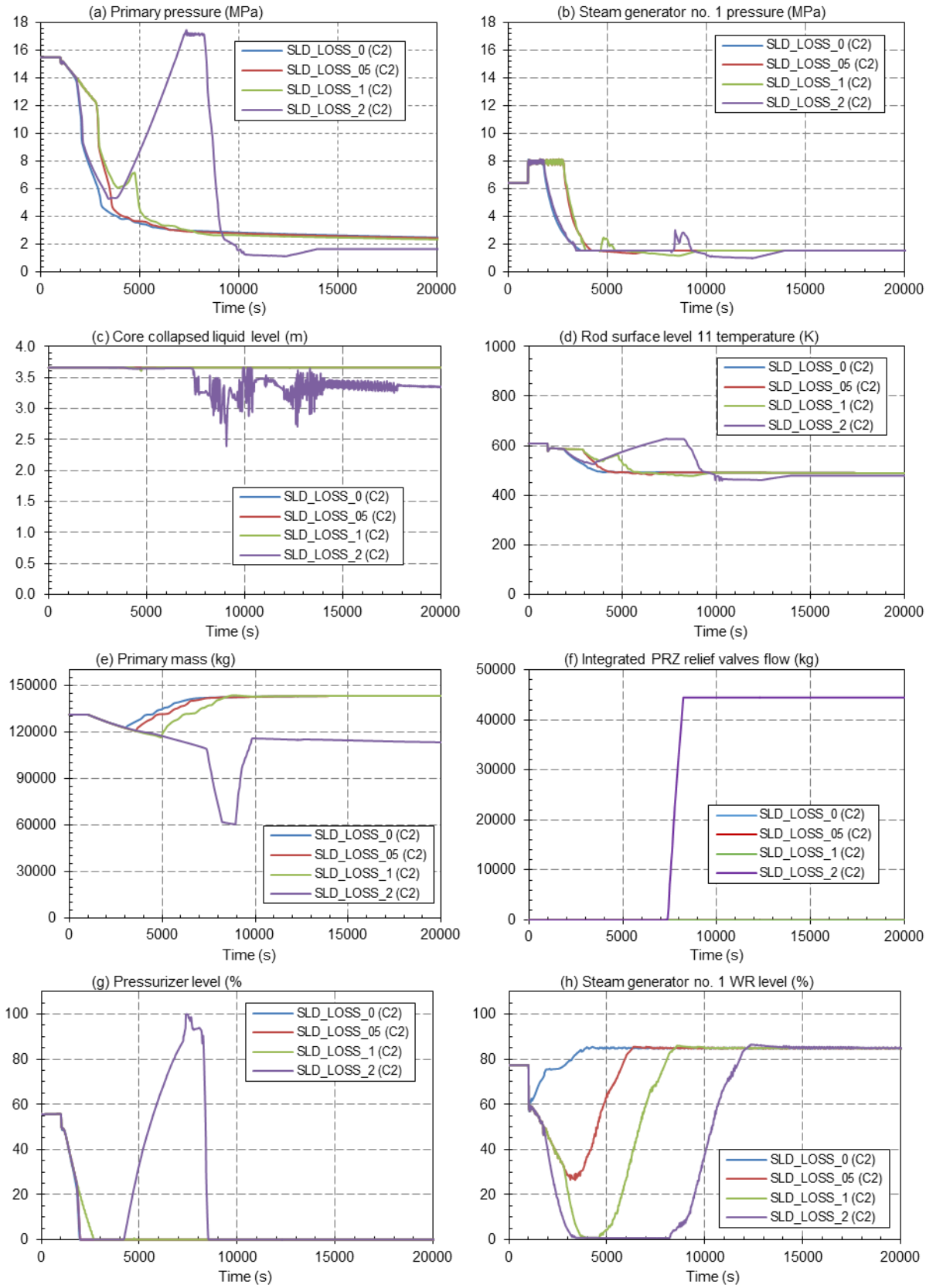

Fig. 34: Time trends of important variables for scenario SLD_LOSS with EDG not running and varying operator action delay to recover cooling – interval (0 – 20000 s)

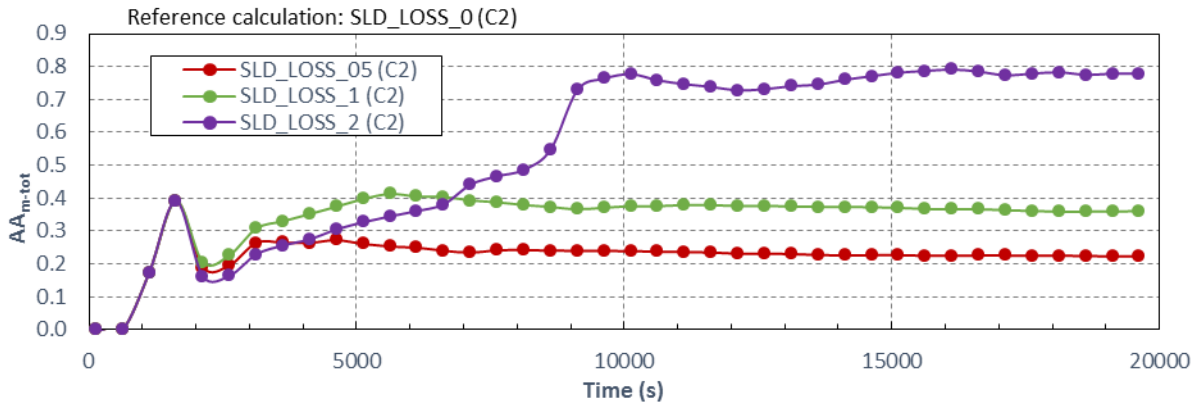

Fig. 35: Code calculation sensitivity (total average amplitude $AA_{m\text{-}tot}$) as a function of increasing time intervals starting at 0 s till 20000 s for scenario SLD_LOSS with EDG not running

5.7 Discussion of results obtained in the sensitivity study

The obtained results of $AA_{m\text{-}tot}$ for maximum time intervals for the selected sensitivity cases are shown in Table 13. The higher is the value of $AA_{m\text{-}tot}$, the larger is the influence of uncertain parameter variation as judged by FFTBM-SM. The quantitative sensitivity measures $AA_{m\text{-}tot}$ confirm the visual observation results in the following:

1. More severe is the loss type, larger is the influence as compared to no loss.
2. Larger is the delay time of cooling restoration, larger is its influence as compared to scenario with no delay of cooling restoration.
3. When emergency diesel generator is not running, the influence of delay time of cooling restoration is larger than when emergency diesel generator is running one hour after LOOP occurrence
4. Depressurization strategy significantly influences the obtained calculated plant results (as seen by visual observation it significantly prolongs the SBO coping time).

Based on the results of visual observations in this study it could be arbitrarily concluded that $AA_{m\text{-}tot}$ smaller than 0.3 indicates smaller change in the plant response, that $AA_{m\text{-}tot}$ between the 0.3 and 0.5 indicates significant change in plant response, while $AA_{m\text{-}tot}$ above 0.5 indicates qualitatively different plant response. The quantitative values do not tell the differences in the plant response but are rather a relative measure of how large the changes in plant response are, when parameter uncertainty is varied. In addition, it should be noted that the reader should always first look at the results of visual observation, which is a prerequisite to perform such quantitative assessment of sensitivity. Also, the reader should be aware that these values were obtained with respect to reference calculations, which are different for each sensitivity case (i.e. based on the quantitative number one could not judge the severity of scenario; for example, the 'SL_LOSS' scenarios all resulted in early core damage). Generally, it can be concluded, if loss type, delay time of restoration of cooling, the time of diesel generator running and availability of depressurization strategy are less uncertain, smaller are the differences in the plant response due to parameter uncertainty. In this way, the input uncertainties for probabilistic safety assessment could be constrained.

Table 13: Main results of sensitivity study

ID	Uncertain parameter varied	Reference calculation	Compared calculation	$AA_{m\text{-}tot}$
1	EDG operation time	S_LOSS_3 (C1)	S_LOSS_3 (C2)	0.464
2	RCS inventory loss type (delayed cooling for 5 h)	NO_LOSS_5 (C1)	N_LOSS_5 (C1)	0.074
			S_LOSS_5 (C1)	0.137
			SL_LOSS_5 (C1)	0.268
3	RCS inventory loss type (delayed cooling for 3 h)	NO_LOSS_3 (C1)	N_LOSS_3 (C1)	0.160
			S_LOSS_3 (C1)	0.242
			SL_LOSS_3 (C1)	0.527
4	Depressurization with 30 min. delay	SL_LOSS_5 (C1)	SLD_LOSS_5 (C1)	0.499
5	Delayed cooling restoration (loss type S_LOSS and EDG running 1 hour after LOOP)	S_LOSS_0 (C1)	S_LOSS_05 (C1)	0.147
			S_LOSS_1 (C1)	0.207
			S_LOSS_2 (C1)	0.297
			S_LOSS_3 (C1)	0.414
			S_LOSS_4 (C1)	0.555
6	Delayed restoration of cooling (loss type SL_LOSS and EDG running 1 hour after LOOP)	SL_LOSS_0 (C1)	SL_LOSS_05 (C1)	0.161
			SL_LOSS_1 (C1)	0.209
			SL_LOSS_2 (C1)	0.364
			SL_LOSS_3 (C1)	0.500
			SL_LOSS_4 (C1)	0.746
7	Delayed restoration of cooling (loss type SLD_LOSS and EDG running 1 hour after LOOP)	SLD_LOSS_0 (C1)	SLD_LOSS_05 (C1)	0.074
			SLD_LOSS_1 (C1)	0.167
			SLD_LOSS_2 (C1)	0.223
			SLD_LOSS_3 (C1)	0.349
			SLD_LOSS_4 (C1)	0.661
8	Delayed restoration of cooling (loss type S_LOSS and EDG not running after LOOP)	S_LOSS_0 (C2)	S_LOSS_05 (C1)	0.252
			S_LOSS_1 (C1)	0.337
			S_LOSS_2 (C1)	0.496
9	Delayed restoration of cooling (loss type SL_LOSS and EDG not running after LOOP)	SL_LOSS_0 (C2)	SL_LOSS_05 (C1)	0.256
			SL_LOSS_1 (C1)	0.387
			SL_LOSS_2 (C1)	0.675
10	Delayed restoration of cooling (loss type SLD_LOSS and EDG not running after LOOP)	SLD_LOSS_0 (C2)	SLD_LOSS_05 (C1)	0.250
			SLD_LOSS_1 (C1)	0.381
			SLD_LOSS_2 (C1)	0.697

Legend for $AA_{m\text{-}tot}$ cell colours: $AA_{m\text{-}tot} < 0.3$ | $0.3 < AA_{m\text{-}tot} < 0.5$ | $AA_{m\text{-}tot} > 0.5$

6 Main findings of sensitivity study

The demonstration of FFTBM-SM for quantitative assessment of sensitivity and evaluation of scenarios similarities is presented. This method is proposed to constrain main external and internal parameters uncertainties. Application of method shows that observation of variables (qualitative part of FFTBM-SM methodology) is sufficient to assess qualitatively the sensitivity to selected parameters. Quantitative assessment of sensitivity gives measures, which can be used to evaluate uncertain parameters impact on the obtained variables, representative of the plant response to SBO scenarios.

Obtained results demonstrate that source of uncertainties are both external (i.e. operator actions) as internal parameters. The operator actions provide strategies to restore the electric power and with that the function of core cooling and by this preventing the core damage. Such strategies largely influence the accident progression, more than uncertainties in the initial and boundary conditions, and the code model uncertainties. In the context of deterministic calculations to support BBN the latter present smaller contribution to the results on one side and require huge effort on the other side.

Obtained results show that external parameters uncertainties for probabilistic safety assessment could be only partly constrained without support of deterministic calculations using the advanced best estimate codes. Therefore, the deterministic calculations should be performed in parallel to BBN build up to provide the information like possible operator actions and available time for restoring safety functions.

Fig. 36 shows, based on the findings of the analysis of plant response (visual observation of calculated scenarios), the progression of the SBO event scenario with the main events and operator actions that are expected to be included in the BBN.

First important element defining the progression of the SBO scenario is the EDG’s start. In case of successful start, the next important element is the operational time of the EDG’s. In case of EDG’s failures, the important event is availability and capacity of the batteries to power essential electrical systems and turbine-driven auxiliary feed water system.

All these events related to power system availability are directly dependant on operator’s actions to start and/or restore them.

The progression of the event also depends on the state and events in the reactor cooling system: presence and type of leakages, operator actions (depressurization) in the system etc.

Fig. 36 shows that first event following the loss of the offsite power is the start of the EDG’s in the NPP. If EDG’s started successfully, the next parameter is their operational time.

If EDG’s operate all the time until offsite power is restored then the nuclear power plant safety is expected to be assured (marked with green box on Fig. 36). If EDG’s start but operates only for one hour (because of some event for example tsunami) then the progression of the event depends on the availability of the essential instrumentation and control (essential I&C powered by plant batteries) and turbine-driven auxiliary feed water system (TD-AFW system powered by the steam from the steam generators).

If the essential I&C and TD-AFW system are available then isolation of the letdown leakage (through letdown relief valve) is required in order to obtain safe plant condition (green box 'Letdown isolation YES'). In case of unsuccessful isolation of the letdown leakage, the safe state can be obtained by successful depressurization of the primary system of the NPP below pressure set point for opening of the letdown relief valve (green box 'Depressurization YES'). Unsuccessful depressurization leads to core uncovery and ultimately core damage (red box 'Depressurization NO').

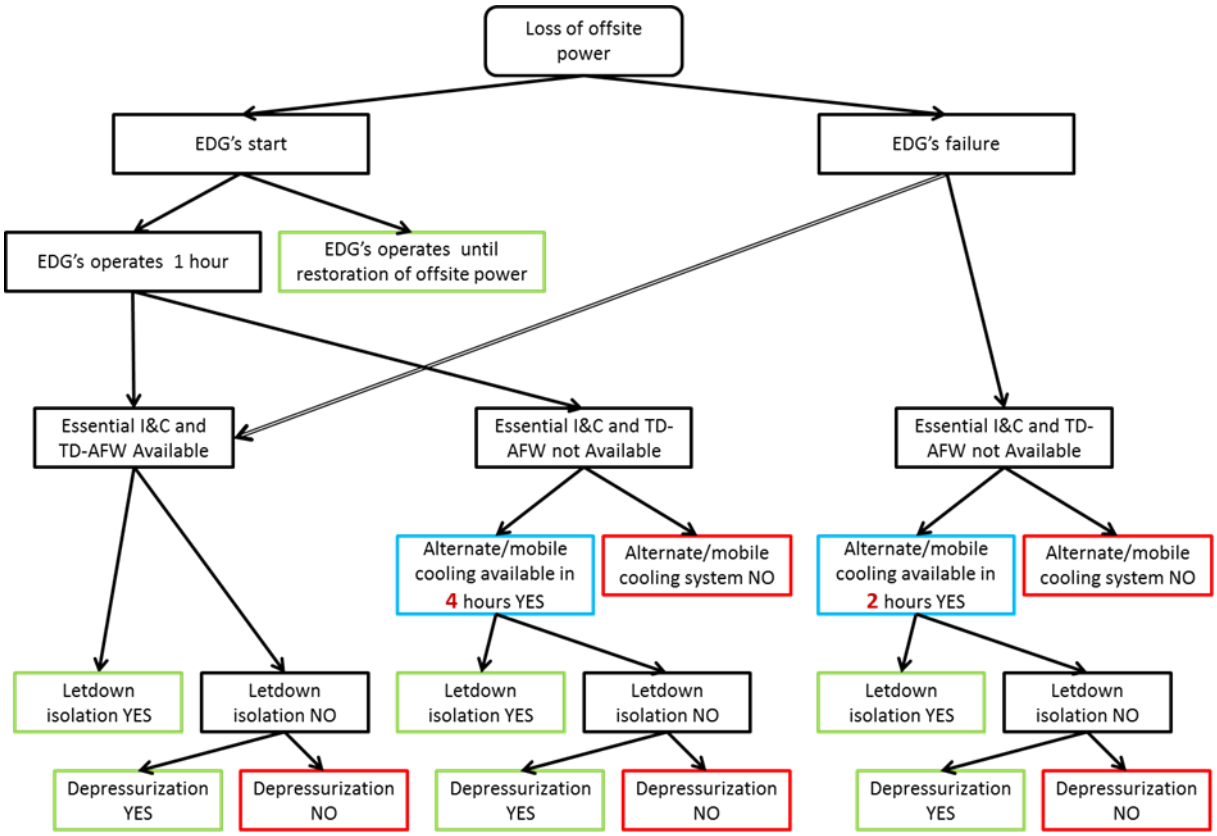

Fig. 36: SBO event progression tree

If essential I&C and TD-AFW are not available then progression of the event depends on the availability of the alternate/mobile system for the cooling of the plant. This system should be connected and started within limited timeframe, which is specific for each plant. Indicative value of 4 hours is given in Fig. 36 (blue box 'Alternate/mobile cooling available in 4 hours') obtained from the referenced studies (Volkanovski and Prošek, 2013; Prošek and Volkanovski, 2015a). If no cooling is restored within this period then core damage is inevitable (red box 'Alternate/mobile cooling system NO'). If alternate/mobile cooling system is activated within 4 hours then successful isolation of the letdown leakage results in safe plant state. In case of unsuccessful letdown isolation, the safe state can be obtained by successful depressurization of the primary system.

If EDG's fail concurrently with the loss of offsite power (which means that EDG's were lost immediately/together with the electrical grid resulting in station blackout) the progression of the scenario/event is similar to the scenario of EDG's failure after 1 hour. The main difference is that available time for utilization of alternate/mobile cooling system (when essential I&C and TD_AFW are not available) is shorter and now is 2 hours (blue box 'Alternate/mobile cooling available in **2** hours YES').

The events (and corresponding operator actions) given on Fig. 36 could be used besides static also for dynamic BBN corresponding to SBO event. The available time for restoration of the safety functions for given plant and design were assessed with the utilization of the deterministic code and corresponding calculations.

7 Conclusions

Based on the analysis presented in the previous sections the most important parameters that are affecting the development of the station blackout (SBO) event are identified. The parameters are classified into internal and external considering related type of the plant system.

The indicative values for the characterization of the uncertainties of those parameters are provided.

Obtained results demonstrate that both external (i.e. operator actions) and internal parameters may be source of large uncertainties.

The modelling of the station blackout event in other models/tools (for example Bayesian network as developed in NARSIS WP3) can include identified important parameters. In case of modelling of operator/human actions, the human failure probability for these actions can be assessed and included in the study.

8 References

Ambrosini, W., Bovalini, R., D'Auria, F. (1990), "Evaluation of accuracy of thermalhydraulic code calculations", *Energia Nucleare*, **7**: 5–16.

AREVA (2007), "U.S. EPR Safety Analysis Report" (https://www.nrc.gov/reactors/new-reactors/design-cert/epr/reports.html#fsar).

Bertucio, R.C. and Brown, S.R. (1990), "Analysis of core damage frequency: Sequoyah, Unit 1, internal events", NUREG/CR-4550, Vol.5, Rev.1.

Bertucio, R.C., Julius, J.A., Cramond, W.R. (1990), "Analysis of core damage frequency, Surry, Unit 1 internal events appendices", NUREG/CR-4550, Vol.3, Rev.1.

D'Auria, F., Leonardi, M., Pochard, R. (1994), "Methodology for the evaluation of thermalhydraulic codes accuracy", *Proc. Int. Conf. on New trends in Nuclear System Thermohydraulics*, Pisa, Italy, pp. 509-517.

Eide, S.A., Gentillon, C.D., Wierman, T.E., Rasmuson, D.M. (2005), "Reevaluation of Station Blackout Risk at Nuclear Power Plants", NUREG/CR-6890, Washington, D.C., USA.

Grabec, I. and Sachse, W. (1991), "Automatic modeling of physical phenomena: Application to ultrasonic data", *J. Appl. Phys.*, **69**: 6233-6244.

IEEE (2002), "IEEE Standard Criteria for Class 1E Power Systems for Nuclear Power Generating Stations", IEEE Std 308-2001 (Revision of IEEE Std 308-1991).

Kolaczkowski, A.M., Cramond, W.R., Sype, T.T., Maloney, K.J., Wheeler, T., Daniel, S.L., et al., (1989), "Analysis of core damage frequency: Peach Bottom, Unit 2 internal events appendices", NUREG/CR-4550, Vol.4, Rev.1.

Mavko B., Stritar, A., Prošek, A. (1993), "Application of code scaling, applicability and uncertainty methodology to large break LOCA analysis of two-loop PWR", *Nuclear Engineering and Design*, **143**: 95-109.

Mitsubishi Heavy Industries (MHI) (2013), "Design Control Document for the US-APWR", Mitsubishi Heavy Industries Ltd., MUAP-DC001, Rev. 1 (https://www.nrc.gov/reactors/new-reactors/design-cert/apwr/dcd.html).

Nishio, M. and Fujimoto, H. (2011), "Study on Seismic PSA for a BWR in shutdown state", *Proc. International Topical Meeting on Probabilistic Safety Assessment and Analysis (PSA 2011)*, Wilmington, NC, pp. 38.1-11.

Prošek, A. (2002), "Accuracy assessment of IAEA-SPE-4 predictions with improved FFTBM", *Presented at 2002 Winter Meeting of the American Nuclear Society, November 17-21, 2002, Washington, Transactions of the American Nuclear Society*, **87**: 199-201.

Prošek, A. and Leskovar, M. (2007), "Improved FFTBM by signal mirroring as a tool for code assessment", *Proceedings of the ICAPP, International congress on advances in nuclear power plants*, pp. 7121.1-7121.9.

Prošek, A. and Leskovar, M. (2009), "Extensions of the fast Fourier transform based method for quantitative assessment of code calculations", *Elektrotehniški vestnik*, **76**: 251-256.

Prošek, A. and Leskovar, M. (2015), "Use of FFTBM by signal mirroring for sensitivity study", *Annals of Nuclear Energy*, **76**: 253-262.

Prošek, A. and Mavko, B. (1999a), "Evaluating code uncertainty - I: Using the CSAU method for uncertainty analysis of a two-loop PWR SBLOCA", *Nuclear Technology*, **126**: 170-185.

Prošek, A. and Mavko, B. (1999b), "Evaluating code uncertainty - II: An optimal statistical estimator method to evaluate the uncertainties of calculated time trends", *Nuclear Technology*, **126**: 186-195.

Prošek, A. and Mavko, B. (2007), "The state-of-the-art theory and applications of best-estimate plus uncertainty methods", *Nuclear technology*, **158**: 69-79.

Prošek, A. and Volkanovski, A. (2015a), "Extended blackout mitigation strategy for PWR", *Nuclear Engineering and Design*, **295**: 360-373.

Prošek, A. and Volkanovski, A. (2015b), "RELAP5/MOD3.3 analyses for prevention strategy of extended station blackout", *Journal of nuclear engineering and radiation science*, **1**(4): 041016-1-041016-10.

Prošek, A., D'Auria, F., Mavko, B. (2002), "Review of quantitative accuracy assessments with fast Fourier transform based methods (FFTBM)", *Nuclear Engineering and Design* **217**: 179-206.

Prošek, A., Končar, B., Leskovar, M. (2016), "Uncertainty analysis of CFD benchmark case using optimal statistical estimator", *Nuclear Engineering and Design*, **321**: 132-143.

Prošek, A., Leskovar, M., Mavko, B. (2008), "Quantitative assessment with improved fast Fourier transform based method by signal mirroring", *Nuclear Engineering and Design*, **238**: 2668-2677.

Saghafi, M., Ghofrani, M.B., D'Auria, F. (2016), "Development and qualification of a thermal-hydraulic nodalization for modeling station blackout accident in PSB-VVER test facility", *Nuclear Engineering and Design*, **303**: 109-121.

Saltelli, A., Aleksankina, K., Becker, W., Fennell, P., Ferretti, F., Holst, N., Li, S., & Wu, Q. (2019). Why so many published sensitivity analyses are false: A systematic review of sensitivity analysis practices. Environmental modelling & software, 114, 29-39.

TEPCO (2011), "Overview of the Earthquake & Tsunami and Nuclear Accident: The Great East Japan Earthquake and Current Status of Nuclear Power Stations".

U.S. NRC (1988), "Station Blackout", Regulatory Guide 1.155, Washington, D.C., USA.

U.S. NRC (2011), "Tohoku-Taiheiyou-Oki Earthquake Effects on Japanese NPP", Information Notice IN-11-05 Washington, D.C., USA (https://www.nrc.gov/docs/ML1107/ML110760432.pdf).

USGS (2011), "The 03/11/2011 Mw9.0 Tohoku Japan Earthquake-Educational Slides", U.S. Geological Survey, National Earthquake Information Center.

Volkanovski A. and Cizelj, L. (2018), "Fukushima Daiichi Nuclear Power Plant Off-site Power System Analysis", *Proc. 27th International Conference Nuclear Energy For New Europe*, Portorož, Slovenia, pp. 507.1-507.8.

Volkanovski, A. and Čepin, M. (2011), "Implication of PSA uncertainties on risk-informed decision making", *Nuclear Engineering and Design*, **241(4)**: 1108-1113.

Volkanovski, A. and Prošek, A. (2013), "Extension of station blackout coping capability and implications on nuclear safety", *Nuclear Engineering and Design*, **255**: 16-27.